Second harmonic generation and ferroelectric phase transitions in thick and ultrathin $Pb_{0.35}Sr_{0.65}TiO_3$ films on (001) MgO substrates

S. W. Liu,[a] J. Chakhalian, and Min Xiao[b]
Department of Physics, University of Arkansas, Fayetteville, Arkansas 72701

C. L. Chen
Department of Physics and Astronomy, University of Texas at San Antonio, San Antonio, Texas 78249

(Received 12 June 2006; accepted 17 December 2006; published online 22 January 2007)

Second harmonic generation of a 16-nm-thick ultrathin $Pb_{0.35}Sr_{0.65}TiO_3$ film and a 243-nm-thick $Pb_{0.35}Sr_{0.65}TiO_3$ film grown on (001) MgO substrates by pulsed laser deposition is investigated. It is concluded that in the ultrathin film the ferroelectric phase is still present and the diffuse phase transition is absent. In contrast, the thick film exhibits a pronounced diffuse phase transition. Theoretical analysis based on the polarization diagrams shows that the compensated *c*-domain fraction is dominant in both films whereas the nonlinear susceptibility of the ultrathin film has a different tensor property from the thick film. © *2007 American Institute of Physics.*
[DOI: 10.1063/1.2433023]

Ferroelectric thin films have been considered to be very promising materials for a number of applications. These applications are usually related to their large nonlinear responses to the electromagnetic radiation from microwave to optical light. These effects include microwave tunability, electro-optic effect, nonlinear optical absorption and refraction, second harmonic generation (SHG), etc. Especially, SHG process has also been widely used as a highly sensitive probe to study the interfacial, surface, and thin film phenomena because the efficiency of SHG is highly dependent on the materials' structural symmetry.[1] For a typical perovskite ferroelectric material such as $PbTiO_3$ with a centrosymmetric cubic symmetry in the paraelectric state, the bulk contribution to SHG is absent in the electric-dipole approximation above the Curie temperature. Upon cooling $PbTiO_3$ undergoes a sharp structural phase transition to ferroelectric state by lowering its symmetry from centrosymmetric cubic to polar tetragonal. This symmetry breaking process produces a dramatic change in SHG efficiency.

Recently, ferroelectric $Pb_{0.35}Sr_{0.65}TiO_3$ (PST) thin films have been regarded as an important candidate for the room temperature tunable microwave devices such as microwave phase shifters because of its high dielectric constant and large tunability.[2–4] In this compound a partial substitution of Pb^{2+} by Sr^{2+} results in a pronounced diffuse phase transition observed in both ceramics and single-crystal specimens.[5,6] The diffuse phase transition in ferroelectrics is characterized by a broadened phase transition in a wide temperature interval (so called Curie range) around the temperature (T_m) where the dielectric permittivity assumes its maximum value and shows the most remarkable relaxor features such as small dielectric hysteresis or dielectric anhysteresis within the transition range. It is the suppression or lack of the dielectric hysteresis that makes the relaxor compounds useful in the tunable microwave devices with precise tunability. Similar phenomena have been observed in some other ferroelectrics via dielectric measurements including $(Ba,Sr)TiO_3$,[7,8] $Ba(Ti,Sn)O_3$,[9] $Pb(Mg_{1/3}Nb_{2/3})O_3$,[10] etc. Such thermally broadened phase transition has generally been attributed to the presence of the nanopolar clusters that may be detected by the method of SHG. In addition, the size effect in the ferroelectrics has currently attracted considerable experimental and theoretical attention and remains a challenging issue because the ferroelectricity is strongly influenced by the external effects such as composition, strain, and dislocation.[11–13] As a *noncontact* and highly sensitive technique, optical SHG is a more convenient probe of ferroelectricity because it avoids disturbing effects (such as "dead-layer" effects[14]) from electrodes compared to the conventional dielectric measurements. In this letter, we present the first SHG measurements of the novel PST films. The domain structures and the nonlinear susceptibility were analyzed by measuring the polarization diagrams of SHG for both thick and ultrathin $Pb_{0.35}Sr_{0.65}TiO_3$ thin films. We have investigated the ferroelectricity for both thick and ultrathin $Pb_{0.35}Sr_{0.65}TiO_3$ thin films by measuring SHG intensity in a wide temperature range of 78–380 K. We observed the

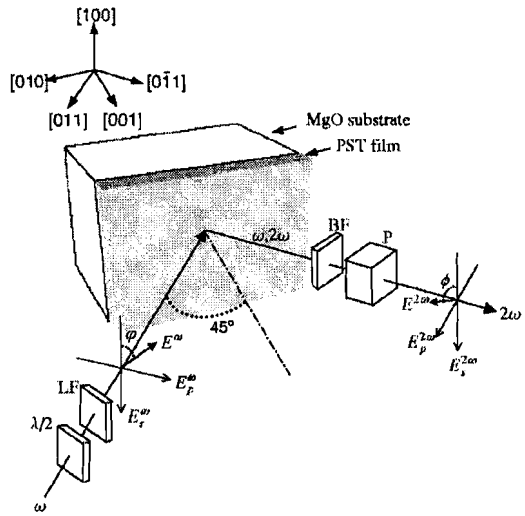

FIG. 1. Schematic diagram of the experimental configuration. The fundamental light of frequency ω (810 nm) is incident under 45° to the normal [001] of the PST/MgO sample (i.e., incident in the [0$\bar{1}$1] direction), and the SH radiation is observed under specular reflection (i.e., in the [0$\bar{1}$1] direction). Inset: The relevant crystallographic directions. LF, long-pass filter; $\lambda/2$, half-wave plate; BF, bandpass filter; and P, Glan polarizer.

[a]Electronic mail: sxl03@uark.edu
[b]Electronic mail: mxiao@uark.edu

Journal of Modern Optics
Vol. 54, Nos. 16–17, 10–20 November 2007, 2441–2450

Taylor & Francis
Taylor & Francis Group

Stochastic resonance with multiplicative noise in a three-level atomic bistable system

HAIBIN WU, AMITABH JOSHI and MIN XIAO*
Department of Physics, University of Arkansas,
Fayetteville, Arkansas 72701, USA

(*Received 22 February 2007; in final form 29 August 2007*)

We experimentally investigate stochastic resonance phenomenon with multiplicative noise in a Λ-type three-level atomic bistable system. The system perturbed by a periodic low frequency forcing term shows an improved signal-to-noise ratio at certain strength of the multiplicative noise applied onto the cavity frequency.

Stochastic resonance (SR) [1–3] has been the subject of intensive research interest in past decades. It has been explored in a wide variety of physical systems, such as bistable ring lasers [4], nanomechanical systems [5], electronic and magnetic systems [6], and biological and neuronal systems [7–10]. With an external periodic perturbation applied to such two-state nonlinear systems, an addition of noise to the input of the system can induce synchronized jumps between the two stable states, showing a resonance-like peak behaviour in the signal-to-noise ratio (SNR) for certain noise strength when the noise level is scanned. Under certain conditions increasing the disorder of the input noise in a two-state nonlinear system can actually lead to an increase in the order of the output (i.e. improved SNR). It is well established that for three-level atoms, the Kerr nonlinear refractive index can be greatly enhanced due to the induced atomic coherence accompanying with reduced linear absorption [11], which can substantially modify the thresholds of the atomic optical bistability (AOB) and switching time between the bistable steady states, and control the width and height of the double-well potential (the shape of the bistable curves) [12]. These features, together with the high stability and reproducibility in the experimental setup, make the system an ideal candidate to study the detail characteristics of the SR. Studying SR in such multi-level atomic systems can help our understanding of the noise properties in these systems, and hopefully lead to new techniques to improve small signal detection and information processing in such coherent atomic systems. We have experimentally demonstrated the SR

*Corresponding author. Email: mxiao@uark.edu

Journal of Modern Optics
ISSN 0950-0340 print/ISSN 1362-3044 online © 2007 Taylor & Francis
http://www.tandf.co.uk/journals
DOI: 10.1080/09500340701656296

Controlling four-wave and six-wave mixing processes in multilevel atomic systems

Yanpeng Zhang,[a] Utsab Khadka, Blake Anderson, and Min Xiao[b]
Department of Physics, University of Arkansas, Fayetteville, Arkansas 72701, USA

(Received 10 September 2007; accepted 4 November 2007; published online 29 November 2007)

We experimentally demonstrate that four-wave mixing (FWM) and six-wave mixing (SWM) processes can be selectively turned on and off in a close-cycled four-level atomic system. Under certain laser beam configuration, the FWM and SWM processes can be made to coexist with similar signal amplitudes and transmit through the same electromagnetically induced transparency window in such folded four-level atomic system. By introducing an additional pumping laser beam connecting to the fifth energy level, both FWM and SWM signals can be greatly enhanced.
 [DOI: 10.1063/1.2817744]

Although four-wave mixing (FWM) and six-wave mixing (SWM) processes have been individually observed in close-cycled (folded) multilevel atomic systems in the past few years,[1–4] the coexisting FWM and SWM have, so far, only been observed in open-cycled multilevel (such as Y-type[5] and inverted Y-type[6]) atomic systems. In these open-cycled multilevel atomic systems, the FWM and SWM signals can be simultaneously generated via transitions in different branches associated with different electromagnetically induced transparency[7,8] (EIT) indows, which can be separated (or placed together to overlap) in frequency by adjusting the frequency detunings of various coupling laser beams.[5,6] The atomic coherence effect is the key to enhance the magnitude of the higher-order SWM signal to be comparable to the FWM signal (which is suppressed at the same time), so the interference between the FWM and SWM signals can be experimentally observed.

In the close-cycled (or folded) four-level atomic system, as shown in Fig. 1(a), the SWM process (via the path $|0\rangle \xrightarrow{\omega_1} |1\rangle \xrightarrow{\omega_2} |2\rangle \xrightarrow{-\omega_3} |3\rangle \xrightarrow{\omega_3} |2\rangle \xrightarrow{-\omega_2} |1\rangle \xrightarrow{-\omega_1} |0\rangle$) will have to go through the FWM path ($|0\rangle \xrightarrow{\omega_1} |1\rangle \xrightarrow{\omega_2} |2\rangle \xrightarrow{-\omega_2} |1\rangle \xrightarrow{-\omega_1} |0\rangle$).[9] So when an efficient FWM process with one weak probe beam E_1 (ω_1, $\mathbf{k}_1$, and Rabi frequency G_1, connecting transition $|0\rangle$ and $|1\rangle$) and two coupling laser beams (E_2 with ω_2, $\mathbf{k}_2$, and Rabi frequency G_2 and E_2' with ω_2, $\mathbf{k}_2'$, and Rabi frequency G_2', connecting upper transition $|1\rangle$ and $|2\rangle$) exists, it will dominate the wave-mixing processes since the SWM process will be several orders of magnitude smaller than the FWM signal in such case even when the strong fields E_3 (ω_3, $\mathbf{k}_3$, and Rabi frequency G_3) and E_3' (ω_3, $\mathbf{k}_3'$, and Rabi frequency G_3') (connecting transition $|2\rangle$ to $|3\rangle$) are present. However, one can turn off the dominant FWM process by blocking either E_2 or E_2' beam, in which case the system will promote and only generate the SWM processes $[\rho_{00}^{(0)} \xrightarrow{\omega_1} \rho_{10}^{(1)} \xrightarrow{\omega_2} \rho_{20}^{(2)} \xrightarrow{-\omega_3} \rho_{30}^{(3)} \xrightarrow{\omega_3} \rho_{20}^{(4)} \xrightarrow{-\omega_2} \rho_{10}^{(5)}]$, as demonstrated in Refs. 4.

In this letter, we show that by using a strong E_2 and a weaker E_2' ($E_2' \ll E_2$) for the upper transition $|1\rangle$ and $|2\rangle$, together with E_3 and E_3' (for transition $|2\rangle$ and $|3\rangle$), both FWM and SWM processes can be generated simultaneously and, with appropriate conditions, made to be in similar magnitudes. To experimentally demonstrate different wave-mixing processes, such as pure FWM, pure SWM, coexisting FWM and SWM, as well as dressed FWM, different coupling laser beams will be blocked during the experiments. Also, when an additional pumping laser beam E_4 (ω_4, connecting transition $|4\rangle$ to $|3\rangle$) is turned on, as shown in Fig. 1(b), the dressed-FWM and SWM signals can be greatly enhanced, indicating optical pumping, as well as dressed-SWM effect. One ladder-type EIT subsystem will form between transitions $|0\rangle \rightarrow |1\rangle \rightarrow |2\rangle$ and an EIT window appears [bottom curve of Fig. 2(a), labeled as P],[8] which depends on the frequency detuning Δ_2 ($\Delta_i = \Omega_i - \omega_i$ with atomic resonant frequency Ω_i for the corresponding transition). The generated multiwave mixing (MWM) signals at frequency ω_1 all fall into this EIT window and can pass through the medium with reduced absorption. To spatially separate these generated MWM signals from the probe beam E_1 and satisfy the phase-matching conditions and two-photon Doppler-free configurations,[5,8] the laser beams are aligned spatially in the square-box pattern shown in Fig. 1(c), with five laser beams ($E_2, E_2', E_3, E_3', E_4$) propagating through the atomic medium in the same direction with small angles ($\sim 0.3°$) between them. The probe beam E_1 propagates in the opposite direction. The generated MWM signals are then all propagating in one direction labeled as E_M in Fig. 1(c).

The experimental demonstration of coexisting MWM processes through one EIT window was carried out in atomic vapor of ^{85}Rb. The energy levels of $5s_{1/2}(F=3)$, $5p_{3/2}$, $5d_{3/2}$,

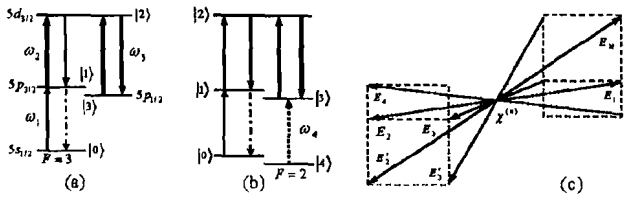

FIG. 1. (a) Folded four-level atomic system for generating FWM and SWM processes ($E_2' \ll E_2$). (b) The folded five-level atomic system with an additional pumping beam E_4 (the dashed arrow). (c) Square box-pattern beam geometry used in the experiment. The dash-dotted arrows are the generated MWM signals.

[a]Electronic mail: ypzhang@mail.xjtu.edu.cn.
[b]Electronic mail: mxiao@uark.edu.

PRAMANA
— journal of
physics

Vol. 69, No. 2
August 2007
pp. 219–228

Single-photon all-optical switching using coupled microring resonators

WENGE YANG*, AMITABH JOSHI and MIN XIAO
Department of Physics, University of Arkansas, Fayetteville, AR 72701, USA
*Current address: School of Engineering, University of CA, Santa Cruz, 1156 High Street, Santa Cruz, CA, 95064, USA
E-mail: wyang@soe.ucsc.edu; ajoshi@uark.edu

MS received 21 January 2007; revised 18 April 2007; accepted 7 May 2007

Abstract. We study the nonlinear phase response of a microring resonator coupled to a bus waveguide and the use of this nonlinear phase shift to store information in the microring resonator and enhance the switching characteristics of a Mach–Zehnder interferometer (MZI). By introducing coupling between adjacent microring resonators, the switching characteristics of the MZI can be exponentially enhanced as a function of the number of microring resonators, when compared to the linear enhancement for uncoupled resonators. With only a few moderate-finesse microring resonators, the switching power can be reduced to attowatt level, allowing for photonic switching devices that operate at single-photon level in ordinary optical waveguides.

Keywords. Microring resonator; single-photon switching.

PACS Nos 42.65.Pc; 42.79.Gn; 42.82.Et

1. Introduction

The optical properties of a waveguide can be tailored using side-coupled microrings. Lossless microring resonators are generally used as phase equalizers or dispersion compensators in optical communication systems [1–4], add-drop filters for wavelength-division multiplexing [5], all-optical switching [6,7], wavelength-dependent delay lines [8], and to stop [9] and reverse [10] the light propagation using coherent effects. Lossy microring resonators, on the other hand, can be used for detecting biological pathogens sensitively [11] and for manipulating the speed of light propagation [12,13]. In this work, we discuss the applications of nonlinear microring resonators in information storage devices. We also demonstrate that the switching threshold power of a resonator-enhanced MZI can be exponentially reduced as a function of the number of coupled microrings. With only a few coupled microring resonators, the switching power can be reduced down to attowatt level, making the system to be an effective single-photon all-optical switching device.

Reflective second harmonic generation near resonance in the epitaxial Al-doped ZnO thin film

S.W. Liu[1*], J.L. Weerasinghe[1], J. Liu[2], J. Weaver[2], C.L. Chen[2], W. Donner[3], and Min Xiao[1*]

[1]*Department of Physics, University of Arkansas, Fayetteville, Arkansas 72701*
[2]*Department of Physics and Astronomy, University of Texas at San Antonio, San Antonio, Texas 78249*
[3]*Department of Physics, University of Houston, Houston, Texas 77204*
**Corresponding authors: sxl03@uark.edu, mxiao@uark.edu*

Abstract: The second harmonic (SH) generation from the highly epitaxial Al-doped ZnO film on sapphire was measured, using the femtosecond Ti:Sapphire laser at the near-resonant SH wavelength, in reflection geometry to avoid the sapphire's contribution in the conventional Maker fringes technique. By investigating SH intensities as a function of the azimuthal angle along the film's normal, we found that the sapphire substrate had a negligible contribution to the reflective SH signal and the film had a pure and well-aligned c-domain. We also developed a new method to calculate the component's ratios of the nonlinear susceptibility tensor by analyzing the polarization diagrams of SH intensities under the incidence with two different angles. The ratios indicate that Kleinman's symmetry is broken due to the absorption at SH wavelength and the dominant component of the nonlinear susceptibility tensor is d_{33}. Calibration using the Z-cut quartz shows a possible overestimate of the nonlinear response by Maker fringes technique.

OCIS codes: (190.4400) Nonlinear optics, materials; (310.6860) Thin films, optical properties; (999.9999) Zinc oxide.

References and links

1. S. H. Jeong, J. W. Lee, S. B. Lee, and J. H. Boo, "Deposition of aluminum-doped zinc oxide films by RF magnetron sputtering and study of their structural, electrical and optical properties," Thin Solid Films **435**, 78-82 (2003).
2. S. J. Henley, M. N. R. Ashfold, and D. Cherns, "The growth of transparent conducting ZnO films by pulsed laser ablation," Surf. Coat. Technol. **177-178**, 271-276 (2004).
3. B. Wacogne, M. P. Roe, T. J. Pattinson, and C. N. Pannell, "Effective piezoelectric activity of zinc oxide films grown by radio-frequency planar magnetron sputtering," Appl. Phys. Lett. **67**, 1674-1676 (1995).
4. M. P. Roe, B. Wacogne, and C. N. Pannell, "High-efficiency all-fiber phase modulator using an annular zinc oxide piezoelectric transducer," IEEE Photon. Technol. Lett. **8**, 1026-1028 (1996).
5. P. Fons, K. Iwata, A. Yamada, K. Matsubara, and S. Niki etc., "Uniaxial locked epitaxy of ZnO on the a face of sapphire," Appl. Phys. Lett. **77**, 1801-03 (2000).
6. C. R. Gorla, N. W. Emanetoglu, S. Liang, W. E. Mayo, and Y. Lu etc., "Structural, optical, and surface acoustic wave properties of epitaxial ZnO films grown on (01T 2) sapphire by metalorganic chemical vapor deposition," J. Appl. Phys. **85**, 2595-2602 (1999).
7. A. F. Aktaruzzaman, G. L. Sharma, and L. K. Malhotra, "Electrical, Optical And Annealing Characteristics Of Zno : Al Films Prepared By Spray Pyrolysis," Thin Solid Films **198**, 67-74 (1991).
8. Sang Il Park, Tae Sik Cho, Seok Joo Doh, Jong Lam Lee, and Jung Ho Je, "Structural evolution of ZnO/sapphire(001) heteroepitaxy studied by real time synchrotron X-ray scattering," Appl. Phys. Lett. **77**, 349-351 (2000).
9. M.C. Larciprete, D. Passeri, F. Michelotti, S. Paoloni, C. Sibilia, M. Bertolotti, A. Belardini, F. Sarto, F. Somma, and S. Lo Mastro, "Second order nonlinear optical properties of zinc oxide films deposited by low temperature dual ion beam sputtering," J. Appl. Phys. **97**, 023501-6 (2005).

#82037 - $15.00 USD Received 12 Apr 2007; revised 1 Jun 2007; accepted 7 Jun 2007; published 8 Aug 2007

Growth of and optical emission from GaMnAs thin films grown by molecular beam epitaxy

J. F. Xu, S. W. Liu, Min Xiao, and P. M. Thibado[a)]
Department of Physics, University of Arkansas, Fayetteville, Arkansas 72701

(Received 15 January 2007; accepted 24 February 2007; published 31 July 2007)

GaMnAs thin films with different Mn doping concentrations were grown via molecular beam epitaxy using a substrate temperature of 250 °C. The thin films were investigated using photoluminescence (PL) measurements from 8 to 300 K. Transitions involving Mn acceptors were identified and a binding energy of ~0.1 eV was found. A Mn doping concentration dependent PL spectrum was found to lend insight into the film quality at a local level. Temperature dependent PL studies show that the doping related emissions drop faster in energy than other peaks with increasing temperature, indicating that they are more sensitive to changes in the surrounding environment.
 [DOI: 10.1116/1.2746349]

I. INTRODUCTION

The incorporation of transition metal dopants with semiconductors may open up opportunities for utilizing a carrier's spin property in conventional electronic devices.[1,2] The Mn-doped GaAs (GaMnAs) system grown by molecular beam epitaxy (MBE) has attracted much attention in this area of study.[3,4] However, the Curie temperature T_C of GaMnAs has been limited to ~150 K at this moment.[5] The reason for suppression in T_C has been derived from the extremely low Mn solubility limit in GaAs (Ref. 6) and high defect density associated with the Mn doping. At present, some of the best samples of GaMnAs have been grown by MBE and using a low-substrate temperature.[7] The low-temperature MBE growth allows one to dope GaAs with Mn beyond its solubility limit, making it possible to realize a III-V-based diluted magnetic semiconductor. However, the low-temperature growth also induces more defects in GaMnAs. It is important to investigate and optimize the sample growth process so that the GaMnAs system has a relatively high Mn solubility and low defect concentration.

In GaMnAs, when Mn substitutes at Ga sites it will take on the dual role of acceptor and local magnetic moment.[8,9] In this article, we have grown GaMnAs thin films with different levels of Mn doping by MBE at a substrate temperature of 250 °C. The photoluminescence (PL) spectra of these GaMnAs films were investigated using a temperature range of 8–300 K. Mn concentration dependent PL spectra from GaMnAs thin films were also obtained, and these provide information about how the local film quality changes with doping concentration.

II. EXPERIMENTAL PROCEDURE

Samples were prepared in an ultrahigh vacuum (UHV) MBE growth chamber (Riber 32) having a base pressure of $\sim 2 \times 10^{-10}$ Torr. The MBE chamber includes Ga and Mn effusion cells together with a two-zone As valved-cracker cell. It is also equipped with a reflection high-energy electron diffraction (RHEED) system. The highest-quality commercially available, "epiready," semi-insulating 2 in. diameter GaAs(001)±0.1° wafers (AXT, Inc., etch pit density <5000 cm^{-2}, full width at half maximum=3.8 arc sec) were used in this study after being cleaved into quarters. One quarter was mounted on a 2 in. diameter standard MBE molybdenum block using indium as solder. The substrate was then loaded into the load-lock chamber without any chemical cleaning. Next, the substrate was transferred to the heating stage inside the MBE chamber, and the chamber was cooled down using liquid nitrogen. The substrate was heated to 580 °C while exposing the surface to As_4 to remove the surface oxide layer. A thin buffer layer of GaAs was grown on the substrate for 5 min. During this time RHEED oscillations were used to determine that the growth rate of the GaAs was 780 nm/h. Next, the substrate temperature (T_S) was set to the desired growth temperature of 250 °C. GaMnAs films were then grown for 1 h, while RHEED was used to monitor the surface reconstruction during and following the growth. After growth, the sample was cooled down and removed from the UHV system. Samples were cleaved into multiple smaller pieces (5×5 mm^2) for characterization measurements.

The PL measurements were performed in a variable temperature (8–300 K) closed-cycle helium cryostat. The 532 nm line from a double neodymium-doped yttrium aluminum garnet laser was used for continuous-wave PL excitation. The PL signal from the sample was dispersed by a monochromator (resolution ≈ 0.001 eV) and detected by a liquid-nitrogen-cooled charged-coupled device.

III. RESULTS

For Mn-doped GaMnAs films, the thickness range is between 0.6 and 1 μm. The Mn distribution within each sample is uniform as determined by Auger electron spectroscopy or secondary ion mass spectrometry depth profiling.[10] The Mn concentration in GaMnAs films depends on the Mn cell temperature. The relation between Mn concentration in GaMnAs and Mn cell temperature is shown in Fig. 1. The

[a)]Electronic mail: thibado@uark.edu

Measurement of laser-induced refractive index change of inverted ferroelectric domain $LiNbO_3$

Yunlin Chen,[1,*] S. W. Liu,[1] Dongdong Wang,[2] Tianlin Chen,[2] and Min Xiao[1]

[1]Department of Physics, University of Arkansas, Fayetteville, Arkansas 72701, USA
[2]Department of Physical Science, Nankai University, Tianjin 300071, People's Republic of China

*Corresponding author: ylchen@uark.edu

Received 24 July 2007; accepted 12 September 2007;
posted 13 September 2007 (Doc. ID 85632); published 25 October 2007

Optical nonlinearities of periodically poled $LiNbO_3$ crystals were investigated by the single beam Z-scan technique with a continuous wave (cw) laser beam at 532 nm. The nonlinear optical absorption coefficient and refractive index change are determined to be 8.1×10^{-6} cm/W and 2.6×10^{-4} at 0.5 MW/cm^2 light intensity, respectively. Both sign and magnitude of the measured refractive nonlinearity are considerably different from the Z-scan results in congruent $LiNbO_3$. The nonlinearities in the periodically poled $LiNbO_3$ induced by 532 nm continuous waves are believed to be mainly due to the photorefractive effect. © 2007 Optical Society of America

OCIS codes: 190.5330, 160.2260.

1. Introduction

Ferroelectric material, lithium niobate ($LiNbO_3$), is widely used for various applications, such as nonlinear frequency converters, photonic band-gap devices, electro-optic Bragg switches, and data storage [1–4]. Especially, the periodically poled $LiNbO_3$ (PPLN) has been successfully exploited in quasi-phase-matched (QPM) frequency conversion processes. QPM frequency conversion has been the subject of numerous investigations. Most of the research efforts have been focused on the second-order optical nonlinearity $\chi^{(2)}$ because of its applications in second harmonic generation and optical parametric oscillation. However, less effort has been made to study the third-order nonlinearity of ferroelectric domain inversion in $LiNbO_3$. Congruent $LiNbO_3$ (cLN) crystal possesses photorefractive properties that may cause a change in optical characteristics upon exposure to laser radiation. It was demonstrated that the photorefractive effect was strongly suppressed in periodic ferroelectric domain inversion structure crystals [5,6]. Therefore, it is essential to measure the nonlinear optical absorption and refraction of PPLN crystals.

Several techniques [7,8] were used to measure the nonlinear optical absorption and refraction of $LiNbO_3$ crystals, but they were performed at light intensities at least two orders of magnitude lower than those typically used for frequency conversion devices. The input intensity range of the measurements should be the same as that used in the frequency conversion processes since the nonlinear optical absorption and refraction depend on the intensity. The single-beam Z-scan is a well-established technique to measure the nonlinear absorption and refraction of solid and liquid samples [9]. Using the Z-scan technique, the nonlinear optical absorption and refraction of undoped and doped $LiNbO_3$ crystals have already been measured [10–12]. However, reported studies using this method to investigate the nonlinear optical absorption and refraction of PPLN crystals are scarce.

In this paper, we report an experimental investigation of nonlinear optical properties of PPLN crystal using a single-beam Z-scan technique with continuous wave (cw) laser beam at 532 nm. Using this technique we compared the nonlinear refractive index of both $LiNbO_3$ and ferroelectric domain inverted $LiNbO_3$ crystal. It has been found that both the refractive index change and the nonlinear absorption coefficient of ferroelectric domain inverted $LiNbO_3$ crystal are different from the results of the congruent

0003-6935/07/317693-04$15.00/0

Available online at www.sciencedirect.com
ScienceDirect
Physics Letters A 367 (2007) 415–419
PHYSICS LETTERS A
www.elsevier.com/locate/pla

Generation of a two-mode generalized coherent state in a cavity QED system

Amitabh Joshi [a,*], Shoukry S. Hassan [b], Min Xiao [a]

[a] Department of Physics, University of Arkansas, Fayetteville, AR 72701, USA
[b] Department of Mathematics, College of Science, University of Bahrain, PO Box 32038, Bahrain

Received 27 January 2007; received in revised form 15 March 2007; accepted 16 March 2007

Available online 23 March 2007

Communicated by P.R. Holland

Abstract

A collection of three-level atoms in Λ-configuration confined in a bimodal cavity and strongly driven by a classical field is considered and it is shown that under certain conditions cavity field can evolve in to a SU(2) generalized coherent state. The realization of SWAP gate operation is also demonstrated.

PACS: 42.50.Dv; 42.50.Pq

1. Introduction

In recent years the investigation of nonclassical states of electromagnetic field and their generation in various physical processes has been an exciting topic in the quantum optics literature [1]. Among other states, the two-mode squeezed state generated by the nonlinear interaction [2] of type: $H = \alpha a^{\dagger} b^{\dagger} + \text{H.c.}$ is found to be highly entangled state under certain conditions, which can be employed for verification of Bell's inequalities [3] and implementing quantum teleportation [4]. The two mode squeezed operator $S(\beta) = e^{(\beta a^{\dagger} b^{\dagger} + \beta^* ab)}$ is the generator of SU(1,1) generalized coherent state (GCS) [5,6]. The fault tolerant phase-gate operation using such states was recently demonstrated [7]. On the other hand the two mode operator of type $S(\chi) = e^{(\chi a^{\dagger} b + \chi^* ab^{\dagger})}$ is a generator of SU(2) GCS. The SU(2) GCS exhibits sub-Poissonian statistics and anti-correlations [8]. Generation of such states in parametric process and interaction of collection of two-level atoms with a single mode radiation field has been reported [5,6,8]. Our aim in this work is how to realize this generator of SU(2) GCS in a cavity quantum electrodynamics (CQED) system.

A large number of proposals for quantum state engineering, entanglement generation for quantum information processing were given [9,10] in the realm of cavity QED [11]. Here we propose a scheme of deterministic generation of SU(2) GCS for the bimodal cavity field. We consider a collection of three-level atoms which interacts with the quantum fields sustained in the bimodal cavity and also strongly driven by a classical field. We will show that under the suitable choice of initial atomic state and interaction time the cavity field can evolve in to the SU(2) state.

The rest of the Letter is organized as follows. In Section 2, we give the model to generate SU(2) GCS. The implementation of SWAP gate operation is discussed in Section 3. In Section 4, some concluding remarks are given.

* Corresponding author.
E-mail addresses: ajoshi@uark.edu (A. Joshi), shoukryhassan@hotmail.com (S.S. Hassan), mxiao@uark.edu (M. Xiao).

0375-9601/$ – see front matter
doi:10.1016/j.physleta.2007.03.035

Cavity linewidth narrowing and broadening due to competing linear and nonlinear dispersions

Haibin Wu and Min Xiao*

Department of Physics, University of Arkansas, Fayetteville, Arkansas 72701, USA
**Corresponding author: mxiao@uark.edu*

Received July 2, 2007; revised August 31, 2007; accepted September 14, 2007;
posted September 24, 2007 (Doc. ID 84702); published October 22, 2007

We experimentally demonstrate cavity linewidth control by manipulating dispersion of the intracavity medium. By making use of the dramatic change of Kerr nonlinearity near electromagnetically induced transparency resonance in a three-level atomic system, the cavity transmission linewidth can be greatly modified. As the cavity input intensity increases, the cavity linewidth changes from below to above empty cavity linewidth, corresponding to subluminal and superluminal photon propagation in the cavity, respectively.

OCIS codes: 190.3270, 020.1670, 140.4480, 260.2030, 300.3700, 270.1670.

Cavity transmission linewidth depends on cavity mirror transmissions, as well as on the interaction and coupling between the cavity field and the intracavity medium. Many factors can influence the cavity transmission linewidth, such as intracavity absorption and dispersion properties. It is well-known that intracavity absorption broadens the cavity linewidth and steep normal dispersion reduces the cavity linewidth [1]. For a strong coupling atom-cavity system, the cavity transmission linewidth is the mean value of the empty cavity decay rate and the atomic decay rate [2,3]. A recent experiment [4] has demonstrated that the sharp linear normal dispersion slope accompanying the electromagnetically induced transparency (EIT) in a three-level atomic system can substantially reduce the cavity linewidth. Such cavity linewidth narrowing can be considered as due to the reduced photon group velocity, and therefore increased photon effective lifetime, in the cavity caused by the sharp normal dispersion slope of the EIT system [5–7].

The group index of the intracavity dispersion medium can be written as

$$n_g = n + \omega_p(\partial n/\partial\omega_p), \tag{1}$$

where n is the index of refraction of the medium and ω_p is the probe laser beam frequency. For a three-level EIT medium, one can easily calculate and measure such a dispersion slope [5,6]. In all previous works on reducing group velocity of light pulses, the probe intensity has always been kept low to avoid nonlinear distortion. Also, the nonlinear dispersion associated with the Kerr nonlinearity in such an EIT medium has been shown to have an opposite sign (anomalous dispersion) from the linear dispersion [8,9], therefore it will be an obstacle for reducing group velocity and will set a lower limit of how much the light pulses can be slowed down. For $n = n_1 + n_2 I_p$, the group index can be written as

$$n_g = (n_1 + n_2 I_p) + \omega_p\left(\frac{\partial n_1}{\partial\omega_p} + \frac{\partial n_2}{\partial\omega_p} I_p\right), \tag{2}$$

where I_p is the probe beam intensity and n_1 and n_2 are the linear and Kerr nonlinear refractive indices, respectively. Since $(\partial n_2/\partial\omega_p)$ is usually always much smaller than $(\partial n_1/\partial\omega_p)$ and has an opposite sign, the nonlinear term is normally considered as a small correction, which only has an effect at either very high probe intensity or very slow group velocity. Therefore, such nonlinear dispersion contribution has always been neglected in previous works of slowing light pulses [7].

In this Letter, we demonstrate that due to the greatly enhanced nonlinear dispersion near three-level EIT resonance [8], such sharp changing nonlinear dispersion can actually be used to balance the linear dispersion [5] and to control the cavity linewidth. To illustrate the basic idea, the linear and nonlinear refractive indices, n_1 and n_2, as well as their derivatives over probe beam frequency detuning ($\Delta_p = \omega_p - \omega_{12}$, where ω_{12} is the frequency of the probe transition) are plotted in Fig. 1 for certain parameters relevant to our experiment [5,8,9]. As shown in Figs. 1(a) and 1(c), linear index has a normal dispersion and nonlinear index (n_2) has an anomalous dispersion near the EIT condition ($\Delta_p = 0$). Their derivatives over Δ_p are shown in Figs. 1(b) and 1(d). Since $(\partial n_1/\partial\omega_p)$ and $(\partial n_2/\partial\omega_p)$, as well as n_1 and n_2, can have opposite signs and change dramatically near the EIT resonance, one can easily find certain detuning value Δ_p, at which the condition $n_g = 1$ is satisfied for a particular I_p value, as indicated by the dotted line in Figs. 1(b) and 1(d). As I_p is further increased, n_g will be less than 1 and even become negative [$\partial n_2/\partial\omega_p < 0$ at such frequency detuning], which corresponds to the superluminal phenomenon [10], shows a linewidth broadening since photons will hit the mirrors more often and have more chance to escape the cavity per unit time. The modified cavity linewidth due to such intracavity medium can be written as [4,11]

$$(\Delta\nu) = \frac{(\Delta\nu)_0(1 - R\kappa)}{\sqrt{\kappa}(1 - R)} \frac{1}{1 + \frac{l}{L}(n_g - 1)}, \tag{3}$$

where $(\Delta\nu)_0$ is the empty cavity linewidth; R is the reflectivity of both the input and output mirrors;

Violation of Bell's inequality for two coupled quantum dots confined in a cavity

Amitabh Joshi,* Blake Anderson, and Min Xiao†
Department of Physics, University of Arkansas, Fayetteville, Arkansas 72701, USA
(Received 9 October 2006; revised manuscript received 20 December 2006; published 5 March 2007)

A system of two coupled quantum dots entangled through their interaction with a cavity mode, including Förster and exciton-phonon interactions, exhibits violation of Bell's inequality at certain interaction times of these dots with the field mode. The effects of relative positions of these dots in the cavity and exciton-phonon and Förster interaction strengths on the violation of Bell's inequality are discussed.

DOI: 10.1103/PhysRevB.75.125304 PACS number(s): 73.21.La, 03.67.Mn, 42.55.Sa

I. INTRODUCTION

In recent years, considerable progress has been made in the areas of quantum computation and information,[1–3] which have the potential for doing any computation task exponentially faster than their classical counterparts. The entanglement due to superposition of states in qubits plays the central role in speeding up the performing tasks. The entanglement is quite fragile and could be lost easily due to interaction with environment or the other noise sources. One of the attracting physical systems for quantum information processing in recent years is to have a semiconductor quantum dot (QD) embedded in a semiconductor microcavity.[4–7] In QDs, the exciton constitutes an alternate two-level system, which replaces the usual two-level atomic system. However, QDs are very much affected by exciton-phonon interaction[8–10] during their interaction with photons. The excitons in the QDs have many advantages for the implementation of quantum computations. In order to have some more advantages one can employ cavity-QED techniques for the QDs.[11–14] For the cavity-QED based QD system, the role of both exciton-phonon interaction[11,12] and exciton-exciton interaction[13] is very important. For the system having more than one QD in the cavity, the coupling and the interactions between QDs become equally important, e.g., the static exciton-exciton dipole coupling that exists when both QDs are excited. Such interactions are capable of producing entangled few-exciton states via ultrafast laser-pulse sequences.[4] Another prominent interaction between two QDs, which is responsible for the transfer of an exciton from one QD to another, is called Förster interaction, which can be used to generate maximally entangled Bell states, GHZ states,[15] quantum teleportation, and optical switching.[16] The effect of exciton-exciton interaction in QD cavity-QED system leading to decoherence (which causes spoiling of entanglement) becomes very significant for studying the above-mentioned quantum phenomena. The cavity-QED system with two QDs becomes entangled through the cavity mode and exciton interaction. Entanglement is a characteristic of the quantum system, which plays a major role in quantum information processing, quantum communications, and quantum cryptography. Violation of Bell's inequality is a tool to demonstrate entanglement in a quantum system,[17,18] and here we utilize this tool to observe the evolution of entanglement in the system of coupled QDs. During the interaction, two excitons and the cavity field become correlated and at a later time become separated (and vice versa) in such a way that it could provide a test of quantum entanglement (and local hidden variable theories), leading to the violation of the Bell's inequality, which is the motivation of this work.

The rest of the paper is organized as follows. In Sec. II, we give the physical model with theoretical description, where two coupled QDs interact with the quantized cavity-field mode. Section III is devoted to describe the violation of Bell's inequality in the above system. In Sec. IV, calculation of entanglement measure is presented. Some concluding remarks are given in Sec. V.

II. THE MODEL

We consider two coupled QDs (situated at some distance from each other) resonantly interacting with a single mode cavity field in a high-Q cavity and coupled to common phonon fields. We keep the position of one QD fixed at the peak of the cavity-field mode (i.e., at antinode) and allow the position of the second dot to be changed. Thus, the separation between QDs is a variable parameter, which determines the coupling strength of the second dot with the electromagnetic field mode of the cavity. Each QD has ground state $|l\rangle$ and first excited state $|u\rangle$ (the two dots are nearly the same size). The Hamiltonian for this system is[11–13]

$$
\begin{aligned}
H = {} & \omega_c a^\dagger a + \omega_{d1}\left(S_z^{(1)} + \frac{1}{2}\right) + \omega_{d2}\left(S_z^{(2)} + \frac{1}{2}\right) + 2F_z\left(S_z^{(1)} + \frac{1}{2}\right) \\
& \times \left(S_z^{(2)} + \frac{1}{2}\right) + g_{d1}[a^\dagger S_-^{(1)} + a S_+^{(1)}] + g_{d2}[a^\dagger S_-^{(2)} + a S_+^{(2)}] \\
& + W[S_+^{(1)} S_-^{(2)} + S_-^{(1)} S_+^{(2)}] + \sum_k \omega_k\left(b_k^\dagger b_k + \frac{1}{2}\right) \\
& + \left(S_z^{(1)} + \frac{1}{2}\right)\sum_k (\zeta_k^{(1)} b_k^\dagger + \zeta_k^{(1)*} b_k) \\
& + \left(S_z^{(2)} + \frac{1}{2}\right)\sum_k (\zeta_k^{(2)} b_k^\dagger + \zeta_k^{(2)*} b_k),
\end{aligned} \tag{1}
$$

in which the ladder operators $S_\pm^{(j)}$ and operators $S_z^{(j)}$ corresponding to two QDs are defined as

$$
S_+^{(j)} = |u\rangle_{jj}\langle l|, \quad S_-^{(j)} = |l\rangle_{jj}\langle u|,
$$

Domain microstructures and ferroelectric phase transition in $Pb_{0.35}Sr_{0.65}TiO_3$ films studied by second harmonic generation in reflection geometry

S. W. Liu,[a] S. Jolly,[b] and Min Xiao[c]
Department of Physics, University of Arkansas, Fayetteville, Arkansas 72701

Z. Yuan, J. Liu, and C. L. Chen
Department of Physics and Astronomy, University of Texas at San Antonio, San Antonio, Texas 78249, Texas Center for Superconductivity, University of Houston, Houston, Texas 77204, and Department of Physics, University of Houston, Houston, Texas 77204

Wenkai Zhu
Department of Physics, University of Houston, Houston, Texas 77204

(Received 18 October 2006; accepted 25 March 2007; published online 31 May 2007)

Second harmonic generation (SHG) measurements were performed in the reflection geometry using the femtosecond Ti:sapphire laser at the wavelength of 810 nm for $Pb_{0.35}Sr_{0.65}TiO_3$ films, which were epitaxially deposited on (001) MgO substrates by pulsed laser ablation under different oxygen pressures. We formulated the procedures to measure the ratios of the compensated fractions of both *c* domains and in-plane domains and the ratios of the components of the nonlinear susceptibility tensor under only a non-normal incidence of the fundamental beam. We applied this technique to characterize the domain microstructures of the $Pb_{0.35}Sr_{0.65}TiO_3$ films at three typical temperatures (78, 150, and 300 K) and found these films to exhibit a larger compensated fraction of *c* domains. The ratios of the components of the nonlinear susceptibility tensor were calculated to be relatively constant regardless of the temperature and the oxygen pressure. On the other hand, their SHG intensities were found to increase as the oxygen pressure goes lower, which is attributed to the higher density of the oxygen vacancies in the films. These films also exhibit the diffuselike phase transition in a very wide temperature range, which is attributed to the structural inhomogeneity and the nonuniform distribution of Pb^{2+} and Sr^{2+} in the $Pb_{0.35}Sr_{0.65}TiO_3$ films. © *2007 American Institute of Physics*. [DOI: 10.1063/1.2735406]

I. INTRODUCTION

Thin films of ferroelectric lead strontium titanate $(Pb,Sr)TiO_3$ (PST) have recently been regarded as an important candidate for applications in various tunable microwave devices (for example, phase shifter and high-Q resonators)[1,2] and also have the potential applications in the high-density dynamic random access memories (DRAMs). They exhibit bistable polarization states, high relative dielectric constant (ε_r) values, and also tunable ε_r by applying an electric field. Both applications are related to the polarization states of the ferroelectric films. In the case of the tunable microwave device, an in-plane bias field is usually applied to the coplanar electrodes on the top of the films to tune laterally the microwave dielectric constants, where the tunability is obviously dependent on the behaviors of the in-plane domains (*a*/*b* domains). In the case of the DRAM, a normal electric field can reverse the orientation of the out-of-plane domains (*c* domains) in the ferroelectric film. The efficiency and speed of DRAM depend on the fraction of *c* domains and their dynamics.[3]

On the other hand, ferroelectric thin films have received much attention for fabricating novel functional devices for optical applications. The typical perovskite ferroelectric materials have excellent linear optical properties such as a wide energy band gap (>3 eV), low absorption coefficient, and high refraction index (>2.0). Also, they often exhibit the large nonlinear responses to the optical electromagnetic wave such as electro-optic (E-O) effect, nonlinear optical absorption and refraction, and second harmonic generation (SHG), etc. Especially, the SHG process may be used as a highly sensitive probe to study the domain structures of the ferroelectric films because the efficiency of SHG is highly dependent on both the domains' structural symmetry and their orientations. Since $(Pb,Sr)TiO_3$ films are the materials which can only be epitaxially grown recently, their optical characterizations are basically absent. Our manuscript systematically studied their linear and second-order optical properties that are basis for their potential applications in optical devices.

Several groups (such as Gopalan and Raj [4] Barad *et al.*,[5] and Mishina *et al.*[3]) have investigated the domain structures of the ferroelectric $KNbO_3$, $Bi_4Ti_3O_{12}$, and $(Ba,Sr)TiO_3$ films, etc., by coherent and incoherent optical SHGs in the transmission geometry. However, the *c* domains do not contribute to SHG under the normal incidence in the transmission geometry. To probe the *c* domains, additional measurements under the non-normal incidence have to be performed. Mishina *et al.*[3] investigated the *c* domains of the $(Ba,Sr)TiO_3$ film under the non-normal incidence in the

[a]Electronic mail: sxl03@uark.edu
[b]Permanent address: School of Electrical and Computer Engineering and School of Physics, Georgia Institute of Technology, Atlanta, GA 30332.
[c]Electronic mail: mxiao@uark.edu

Competition between two four-wave mixing channels via atomic coherence

Yanpeng Zhang,[a] Blake Anderson, Andy W. Brown, and Min Xiao[b]
Department of Physics, University of Arkansas, Fayetteville, Arkansas 72701

(Received 10 June 2007; accepted 13 July 2007; published online 8 August 2007)

Two four-wave-mixing (FWM) processes can coexist in a four-level Y-type atomic system with carefully arranged coupling laser beams. The generated two FWM signal beams fall into two simultaneously opened dual electromagnetically induced transparency (EIT) windows, which can be tuned to overlap or separate by various frequency detunings. The authors report our experimental observation of competing FWM processes, especially mutual suppression of the two FWM signals when the two EIT windows merge in frequency. Controlling FWM processes can have important applications in wavelength conversion for optical communication. © *2007 American Institute of Physics*. [DOI: 10.1063/1.2768872]

Efficient four-wave-mixing (FWM) processes enhanced by atomic coherence in multilevel atomic systems[1–4] are of great current interest. With enhanced higher-order nonlinearity and reduced linear absorption for the generated signal beams using electromagnetically induced transparency (EIT),[5] efficient six-wave mixing (SWM) has been generated experimentally.[6,7] Recently, interference between two FWM processes in two-level atomic system has been studied,[8] which can generate biphotons and entangled photon pairs. By suppressing the FWM processes with atomic coherence and multiphoton interference in a multilevel open-cycled atomic system, higher-order SWM or eight-wave mixing[9] can be made to be comparable and coexist with the lower-order FWM processes, and, therefore, to observe interference between these two different wave-mixing processes.[7]

In this letter, we report an experimental demonstration of generating two highly efficient and competing FWM processes simultaneously in an open-cycled Y-type atomic system in which the dual-EIT windows are used to transmit the two generated FWM signal beams, respectively. The Y-type four-level atomic system is shown in Fig. 1(a). If we consider the lower transition ($|0\rangle$ to $|1\rangle$) together with only one upper branch (either $|1\rangle$ to $|2\rangle$ or $|1\rangle$ to $|3\rangle$), it is a simple ladder-type three-level atomic system. If only one coupling beam is used in the upper transition, the three-level ladder system has a simple EIT peak.[5] If two coupling beams (with one each) interact with the two upper branches, respectively, double EIT peaks will appear in such four-level atomic system.[10] However, if two coupling beams (with same frequency) are used at one upper transition (for example, $|1\rangle$ to $|2\rangle$), a FWM signal (ω_{f1}) will be generated at the same frequency as ω_1,[7] which will fall into the EIT window in this ladder-type system ($|0\rangle-|1\rangle-|2\rangle$). Similarly, a FWM signal (ω_{f2}) will be generated If we only consider another upper transition ($|1\rangle$ to $|3\rangle$) with two coupling beams. The generated FWM signal ω_{f2} will fall into a different EIT window (due to ($|0\rangle-|1\rangle-|3\rangle$ ladder system). Now, when both upper branches are used with four coupling laser beams, as shown in Fig. 1(a), the two generated FWM signals (ω_{f1} and ω_{f2}) via the two different channels (or different upper branches) will compete with each other. These two FWM signals can be either distinguishable when the frequency detunings of the coupling beams are different (with two separate EIT windows) or "no distinguishable" when the two EIT windows are tuned to overlap with each other. We investigate the interplay and competition between these two FWM processes under different frequency detunings and coupling laser intensities.

The laser beams are aligned spatially in the square pattern, as shown in Fig. 1(b), with four coupling beams (E_2, E_2', E_3, and E_3') propagating through the atomic medium in the same direction with small angles (~0.3°) between them. For a simple four-level Y-type atomic system, as shown in Fig. 1(a), two strong coupling fields, E_2 (ω_2, $\mathbf{k}_2$, and Rabi frequency G_2) and E_2' (ω_2, $\mathbf{k}_2'$, and Rabi frequency G_2'), drive the upper transition $|1\rangle$ to $|2\rangle$ and the other two strong laser fields, E_3 (ω_3, $\mathbf{k}_3$, and Rabi frequency G_3) and E_3' (ω_3, $\mathbf{k}_3'$, and Rabi frequency G_3'), drive the transition $|1\rangle$ to $|3\rangle$. A weak laser field, E_1 (ω_1, $\mathbf{k}_1$, and Rabi frequency G_1), probes the lower transition ($|0\rangle$ to $|1\rangle$). With the phase-matching conditions $\mathbf{k}_{f1}=\mathbf{k}_1+\mathbf{k}_2-\mathbf{k}_2'$ [called FWM process (I) for the subsystem $|0\rangle-|1\rangle-|2\rangle$) and $\mathbf{k}_{f2}=\mathbf{k}_1+\mathbf{k}_3-\mathbf{k}_3'$ [called FWM process (II) for the subsystem $|0\rangle-|1\rangle-|3\rangle$], the two generated FWM signals are in the exactly same direction [as shown in the right lower corner in Fig. 1(b)]. This system also generates SWM signals,[11] which propagate in a different direction due to phase matching ($\mathbf{k}_s=\mathbf{k}_1+\mathbf{k}_2-\mathbf{k}_2'+\mathbf{k}_3-\mathbf{k}_3'$) when all four coupling beams are on. However, if one of the coupling beams (either E_2' or E_3') is blocked, one of the FWM processes will be turned off and a SWM signal will be generated in its place in the same direction as the FWM signal (deter-

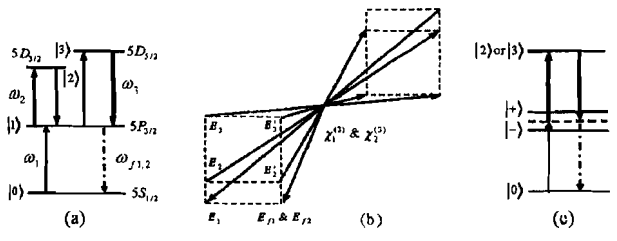

FIG. 1. (a) Four-level Y-type atomic system with four coupling laser beams and one probe beam. The dash-dotted lines are the two generated FWM ($\omega_{f1,2}$) signals. (b) Square box-pattern beam geometry used in the experiment. (c) Dressed-state picture for the Y-type atomic system.

[a]Electronic mail: ypzhang@mail.xjtu.edu.cn
[b]Electronic mail: mxiao@uark.edu

PHYSICAL REVIEW A 75, 051801(R) (2007)

Preparation and determination of spin-polarized states in multi-Zeeman-sublevel atoms

Bo Wang,[1] Yanxu Han,[1] Jintao Xiao,[1] Xudong Yang,[1] Chunhong Zhang,[1] Hai Wang,[1,*] Min Xiao,[1,2] and Kunchi Peng[1]
[1]*The State Key Laboratory of Quantum Optics and Quantum Optics Devices, Institute of Opto-Electronics, Shanxi University, Taiyuan, 030006, People's Republic of China*
[2]*Department of Physics, University of Arkansas, Fayetteville, Arkansas 72701, USA*
(Received 16 November 2006; published 2 May 2007)

We demonstrate a simple, all-optical technique to prepare and determine the desired internal quantum states in multi-Zeeman-sublevel atoms. By choosing appropriate coupling and pumping laser beams, atoms can be easily prepared in a desired Zeeman sublevel with high purity or in any chosen ground-state population distributions (spin-polarized quantum-state engineering). The population distributions or state purities of such prepared atomic states can be determined by using a weak, circularly polarized probe beam due to differences in transition strengths among different Zeeman sublevels. This technique will have potential impact on quantum-information processing in multilevel atomic systems.

DOI: 10.1103/PhysRevA.75.051801 PACS number(s): 42.50.Gy, 03.65.Wj, 32.80.Pj

Preparing atoms into one specified internal quantum state and determining the population distribution in multi-Zeeman-sublevel atomic systems are very important in studying atom-field interactions, especially interesting schemes for quantum-information processing (QIP) such as light storage [1], quantum phase gate [2–5], and entanglement between atomic assemble and photons [6] or between a single trapped ion and a single photon [7]. Demonstrations of these effects require more than two atomic energy levels and a well-defined initial internal quantum state for the atoms, which cannot be accomplished by simple optical pumping as in the case for a two-level atomic system. Although in most cases interesting effects can be experimentally demonstrated by simply considering degenerate Zeeman levels, so no specific ground-state population preparations are needed [as in the cases of electromagnetically induced transparency (EIT) [8–10] and photon storage [11,12]], there are many effects that demand better quantum-state preparation and determination in the multi-Zeeman-sublevel atomic systems. For example, in order to demonstrate a quantum phase gate in multilevel atomic systems, such as the five-level M-type [3] and five-level combined M and tripod-type [5] systems, initial ground-state populations have to be prepared in specific Zeeman sublevels. Another example is the synthesis of arbitrary quantum states with atoms [13]. Several techniques were developed previously to prepare and determine the ground-state populations in multi-Zeeman-level atomic systems by using a magnetic field [14–17] or microwave field [18–20], or light-induced momentum transfer [21,22]. These experiments were all done in atomic beams or in atomic vapor cells, and they are too cumbersome to be used for QIP experiments, especially since they are strong measurements which erase the prepared original quantum state [23]. More importantly, most of these techniques cannot be used for cold atoms trapped by a magneto-optical trap (MOT), in which the magnetic field has to be near zero at the center and it could be difficult to apply a strong microwave field. Reference [23] demonstrated a method to estimate the prepared quantum state in cold atoms with weak measurement by probing the Lamor procession and Wigner function reconstruction, which is an indirect way with complicated data processing. Since many recent experiments on QIP were done in cold atoms in a MOT (such as [6,11,12]), it is necessary to develop a new technique that can prepare and directly determine the spin-polarized states in multi-Zeeman-level systems without employing a magnetic field or microwave field, and without destroying the prepared spin-polarization states in the measurements.

In this Rapid Communication, we present a simple procedure to prepare any desired internal quantum states at various Zeeman sublevels, and more importantly, we demonstrate an all-optical technique to determine the ground-state population distributions simply by applying a weak, circularly polarized probe laser beam. The preparation of a desired quantum state is achieved by combining optical pumping from two polarized laser beams. The basic mechanism for detecting and determining the prepared internal quantum state is to make use of the differences in transition strengths among different Zeeman sublevels (different Clebsch-Gordan coefficients), as shown in Fig. 1(b), and the changes in the corresponding multi-dark-state resonances (MDSR) [as shown in Fig. 1(c)] [24]. By combining the measured probe spectrum with the theoretical calculation, one can easily determine the ground-state population distribution and the purity of the prepared quantum state with high precision. This technique of determining the prepared spin-polarized states has several advantages over the previously demonstrated ones since it is all-optical with direct measurement and fast response, and it does not destroy the prepared spin-polarized states, which is ideal for QIP experiments using cold atoms in a MOT.

The experiment was performed with the D1 line of ^{87}Rb atoms, as shown in Fig. 1(b), in a vapor cell magneto-optical trap (MOT) which is the same as in Ref. [24]. A strong coupling beam with linear polarization in the z direction [as shown in Fig. 1(a)] propagates along the x axis through the cold atoms while a weak, left-circularly polarized probe beam propagates along the z axis through the atoms. The diameters of the coupling and probe beams are 2.6 and

*Corresponding author. Email address: wanghai@sxu.edu.cn

Resonance Fluorescence from a Coherently Driven Semiconductor Quantum Dot in a Cavity

A. Muller,[1] E. B. Flagg,[1] P. Bianucci,[1] X. Y. Wang,[1] D. G. Deppe,[2] W. Ma,[3] J. Zhang,[3] G. J. Salamo,[3] M. Xiao,[3] and C. K. Shih[1,*]

[1]*Department of Physics, The University of Texas at Austin, Austin, Texas 78712, USA*
[2]*College of Optics and Photonics (CREOL), University of Central Florida, Orlando, Florida 32816, USA*
[3]*Department of Physics, University of Arkansas, Fayetteville, Arkansas 72701, USA*
(Received 11 April 2007; published 1 November 2007)

We show that resonance fluorescence, i.e., the *resonant* emission of a *coherently* driven two-level system, can be realized with a semiconductor quantum dot. The dot is embedded in a planar optical microcavity and excited in a waveguide mode so as to discriminate its emission from residual laser scattering. The transition from the weak to the strong excitation regime is characterized by the emergence of oscillations in the first-order correlation function of the fluorescence, $g(\tau)$, as measured by interferometry. The measurements correspond to a Mollow triplet with a Rabi splitting of up to 13.3 μeV. Second-order correlation measurements further confirm nonclassical light emission.

DOI: 10.1103/PhysRevLett.99.187402 PACS numbers: 78.67.Hc, 42.50.Pq, 78.47.+p, 78.55.−m

Semiconductor quantum dots (QDs) [1] have offered unique opportunities to investigate sophisticated quantum optical effects in a solid-state system. These include quantum interference [2], Rabi oscillations [3–6], as well as photon antibunching [7], and were previously only observable in isolated atoms or ions. In addition, QDs can be readily integrated into optical microcavities, making them attractive for a number of applications, particularly quantum information processing and high efficiency light sources. For example, QDs could be used to realize deterministic solid-state single photon sources [8] and qubit-photon interfaces [9]. Advances in high-Q cavities have shown that not only can the spontaneous emission rate be dramatically increased by the Purcell effect [10], but emission can be reversed in the strong coupling regime [11]. Despite these efforts, however, quantum dot-based cavity quantum electrodynamics (QED) lacks an ingredient essential to the success of atomic cavity QED, namely, the ability to truly resonantly manipulate the two-level system [8]. Current approaches can at best populate the dot in one of its excited states, which subsequently relaxes in some way to the emitting ground state. This incoherent relaxation has been addressed theoretically [12], and experimentally [13] but direct resonant excitation and collection in the ground state has so far not been reported as it is very challenging to differentiate the fluorescence from same frequency laser scattering off defects, contaminants, etc., In quantum dots without cavities, coherent manipulation of ground state excitons has nonetheless been achieved with a number of techniques including differential transmission [5], differential reflectivity [14], four-wave mixing [15], photodiode spectroscopy [6], and Stark-shift modulation absorption spectroscopy [16]. However, none of these is able to collect and use the actual photon emission which limits their use in many potential applications of QDs.

This Letter presents the first measurement of resonance fluorescence in a single self-assembled quantum dot. Described by Mollow in 1969 [17], the resonant emission of a two-state quantum system under strong coherent excitation is distinguished by an oscillatory first-order correlation function, $g(\tau)$, that we observe with interferometry. We use a planar optical microcavity to guide the excitation laser between the cavity mirrors and simultaneously enhance the single photon emission in the orthogonal direction. Overcoming previous limitations associated with incoherent excitation, our approach enables, for the first time, true resonant excitation of a single dot in a cavity.

Self-assembled InGaAs QDs were grown epitaxially between two distributed Bragg reflectors of moderate reflectivity (Fig. 1). While the sample is maintained at low temperature in a He flow cryostat, a single mode optical fiber, mounted on a three-axis inertial walker at room temperature, is brought within a few microns of the cleaved sample edge. An in-plane polarized tunable continuous-wave Ti:Sapphire laser is introduced through the fiber to excite the dots; it couples efficiently into the high index semiconductor and propagates deeply before diverging appreciably. The QD emission is then collected by a conventional micro-PL setup equipped with a two-dimensional

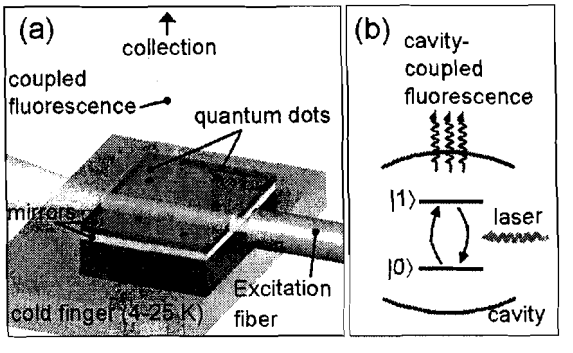

FIG. 1 (color online). (a) Apparatus for orthogonal excitation and detection. (b) Energy level diagram for two-level quantum dot. The two arcs represent the microcavity in which the dots are embedded.

IOP PUBLISHING JOURNAL OF PHYSICS B: ATOMIC, MOLECULAR AND OPTICAL PHYSICS

J. Phys. B: At. Mol. Opt. Phys. **40** (2007) 3319–3329 doi:10.1088/0953-4075/40/17/001

Intermixing between four-wave mixing and six-wave mixing in a four-level atomic system

Yanpeng Zhang, Andy W Brown, Chenli Gan and Min Xiao

Department of Physics, University of Arkansas, Fayetteville, AR 72701, USA

E-mail: ypzhang@mail.xjtu.edu.cn

Received 4 May 2007, in final form 29 June 2007
Published 15 August 2007
Online at stacks.iop.org/JPhysB/40/3319

Abstract

We investigate the interplay between six-wave mixing (SWM) and four-wave mixing (FWM) resulting from atomic coherence and polarization beat in a four-level atomic system. The dressed FWM evolution and competition pathways can be controlled by the coupling field to exhibit two FWM and SWM turning points, FWM+SWM, and FWM+FWM interference regions. Quantum interference between two FWM or one FWM and one SWM channels leads to nonlinear signal enhancement and suppression under different conditions. The fifth-order nonlinear response can be obtained by the phase control of the polarization beat between the FWM and SWM signals.

1. Introduction

Multiwave mixing due to atomic coherence and polarization beat (PB) in multi-level atomic systems has attracted a lot of attention recently [1–5]. PB originates from the interference between the macroscopic polarizations that are excited simultaneously in the medium [3–5]. An important application of electromagnetically induced transparency (EIT) [1] is its ability to enhance the efficiencies of nonlinear optical processes. Two of the interesting nonlinear optical processes are four-wave mixing (FWM) and six-wave mixing (SWM), which normally have high efficiencies in closely-cycled four-level systems such as double-Λ system [6–8]. Recently, SWM processes were observed in closed four-level atomic systems [7]. Such high-order SWM process is often obscured by sequential or parallel cascade third-order FWM processes that compete with the direct process and give similar time domain behaviour though they probe different overtone vibrational dynamics [9]. Garrett *et al* also explored the two-photon plus three-photon resonant FWM and SWM involving stimulated hyper Raman generation as opposed to pause cognate generation [10].

Although triple resonance spectroscopy has been reported previously by fluorescence detection [11], the current method is a coherence phenomenon, where atomic coherence is induced among different energy levels. Due to the parametric nature of this process, the signal

0953-4075/07/173319+11$30.00

Size dependence of nonlinear optical absorption and refraction of Mn-doped ZnSe nanocrystals

Chenli Gan and Min Xiao[a)]
Department of Physics, University of Arkansas, Fayetteville, Arkansas 72701, USA

David Battaglia, Narayan Pradhan, and Xiaogang Peng
Department of Chemistry and Biochemistry, University of Arkansas, Fayetteville, Arkansas 72701, USA

(Received 26 July 2007; accepted 23 October 2007; published online 13 November 2007)

Nonlinear refractive index and nonlinear absorption coefficient of high-quality Mn:ZnSe nanocrystals are measured by z-scan technique at 800 nm wavelength. The synthesized nanocrystals with nucleation doping have tunable wavelength (between 565–610 nm), high quantum yield (~50%), and high thermal as well as photochemical stabilities. The unique nanocrystal structure (with a MnSe core, $Zn_{1-x}Mn_xSe$ diffusion region, and an outer ZnSe layer) shows size-dependent nonlinear effects, which can be qualitatively explained by a simple model using crystal field. Studies of nonlinear optical properties are very important and necessary for high-power optical applications (such as light-emitting diodes and lasers) of such Mn-doped ZnSe nanocrystals. © *2007 American Institute of Physics*. [DOI: 10.1063/1.2811713]

Although doped semiconductor nanocrystals have been synthesized more than twenty years ago, the developments in the synthesis of high quality Mn- and Cu-doped ZnSe,[1–4] and Mn-doped CdS/ZnS core/shell[5] nanocrystals have stirred new excitement in this field of making colloidal nanocrystals. Such transition metal-doped nanocrystals (d-dots) have many superior properties compared to the traditional semiconductor quantum dots,[6–10] such as reduced self-quenching due to large Stokes shift, greatly suppressed host emission, and improved stabilities over thermal, chemical, and photochemical disturbances.[1] Such greatly improved optical properties of d-dots, specifically those not containing any heavy metal ions, can be used to advance practical applications in biomedical labels,[11] light-emitting diodes (LEDs),[12] beads-based bar coding,[13] and lasers.[14]

The traditional synthetic approaches for doping nanocrystals usually put both dopant ions and competitive host ions in the reaction systems, which result in large portion of nanocrystals without dopants. The recently developed technique is to decouple the doping from nucleation and/or growth through nucleation-doping and growth-doping strategies.[1,4,5,10] By using such synthetic technique to prepare Mn^{2+}:ZnSe d-dots, the resulting samples have very high dopant emission (>99% in intensity), tunable wavelength from 565 to 610 nm, and high photoluminescence (PL) quantum yield (QY) of about 40%–70%.[4]

With nucleation-doping procedure,[1,4] the dopant uniformity can be well controlled and the PL spectrum shows a sharp emission peak (mainly from Mn^{2+} dopant) near 580 nm, which is separated from the host (ZnSe) absorption band, as shown in Fig. 1(a).[1] Such large separation between host absorption band and dopant emission peak (Stokes shift) greatly reduces the reabsorption of the PL and is very important in certain applications. Since such d-dots can have potential high-power applications to improve next generation LEDs and nanocrystal lasers, the nonlinear optical properties of such d-dots can be very important and need to be investigated. In this work, we report our experimental measurements of nonlinear (two-photon) optical absorption and refraction of such Mn-doped ZnSe d-dots by using z-scan technique. Since the dot size and overcoating larger thickness can both greatly modify the QY and other optical properties,[4] we specially investigate the dependence of nonlinear optical coefficients of samples on the thickness of the ZnSe overcoating layer with the same doped core.

The nanocrystalline Mn-doped ZnSe samples with particle sizes of 3.5, 5.0, 6.0, 7.0, and 8.0 nm in diameter (according to transmission electron microscopy images) are prepared using the nucleation-doping procedure as described in Ref. 1. The resulting Mn: ZnSe nanocrystals have the structure shown in Fig. 1(b), with a fixed small MnSe nanocluster core (~1.5 nm) and a diffused interface region between the nanocluster core and the ZnSe overcoating layer. For the same core size, samples with different ZnSe coating layers

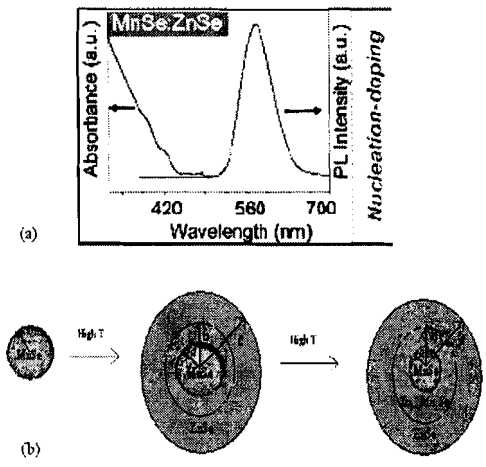

FIG. 1. (Color online) (a) The UV-Vis and PL spectra of the nucleation-doping Mn-doped ZnSe nanocrystals. Mn:Zn=1:22, T=280 °C for overcoating. (b) Theoretical structure model for Mn-doped ZnSe nanocrystal grown by nuclearation doping. Here, a is the radius of the MnSe core, b is the radius of MnSe core plus $Zn_{1-x}Mn_xSe$ diffusion region, and c is the radius of the total Mn-doped ZnSe nanocrystal sphere.

a)FAX: 479-5754580. Electronic mail: mxiao@uark.edu

Observation of interference between four-wave mixing and six-wave mixing

Yanpeng Zhang, Andy W. Brown, and Min Xiao

Department of Physics, University of Arkansas, Fayetteville, Arkansas 72701, USA

Received December 4, 2006; revised January 9, 2007; accepted January 29, 2007;
posted February 7, 2007 (Doc. ID 77736); published April 3, 2007

We report generation of four-wave mixing enhanced by electromagnetically induced transparency and optical pumping in a ladder-type atomic system. When two pumping laser beams are used to form a conjugate small-angle static grating, both four-wave and six-wave mixing processes are shown to exist at the same time. Interference between these two nonlinear wave-mixing signals is experimentally demonstrated.

OCIS codes: 190.4380, 270.4180, 300.2570, 320.7110, 030.1670.

Enhanced four-wave mixing (FWM) processes have been experimentally demonstrated recently in multilevel atomic systems with induced atomic coherence.[1–5] Under electromagnetically induced transparency (EIT)[6,7] conditions, not only can the third-order nonlinear susceptibilities can be resonantly enhanced but also the generated FWM signals can be allowed to transmit through the atomic medium with little absorption. Recently, efficient six-wave mixing (SWM) has also been observed in a four-level closed-cycle N-type rubidium atomic system[8] and doubly excited autoionizing Rydberg states of Ba atoms.[9] Contrary to the case of solid or liquid media (in which FWM and SWM signals can be generated at the same time),[10,11] only either FWM processes or SWM processes were experimentally generated in typical closed-cycle multilevel atomic systems done previously,[1–5,8,9] depending on the arrangements of lasers and number of energy levels involved.

In this Letter, we describe our experimental observation of efficient FWM process assisted by opening an EIT window and enhanced by optical pumping, as shown in Fig. 1(a). Destructive interference between three photons (two coupling and one probe) and the generated signal photon (or three-photon EIT) was measured in the FWM signals. More importantly, we demonstrate co-existing FWM and SWM processes in one system by adding two pumping beams in an adjacent atomic transition in the system, as shown in Fig. 1(b), and show interference between these two nonlinear wave-mixing signals.

The two relevant experimental systems are shown in Figs. 1(a) and 1(b). Five energy levels from ^{87}Rb atoms (in vapor cell) are involved in the experimental schemes. In the first experiment [Fig. 1(a)], energy levels of $|0\rangle$ $(5s_{1/2}, F=2)$, $|1\rangle$ $(5p_{3/2})$, and $|2\rangle$ $(5d_{3/2})$ form a cascade three-level atomic system. With coupling beam E_2 (or E_2') (connecting transition $|1\rangle$ to $|2\rangle$)

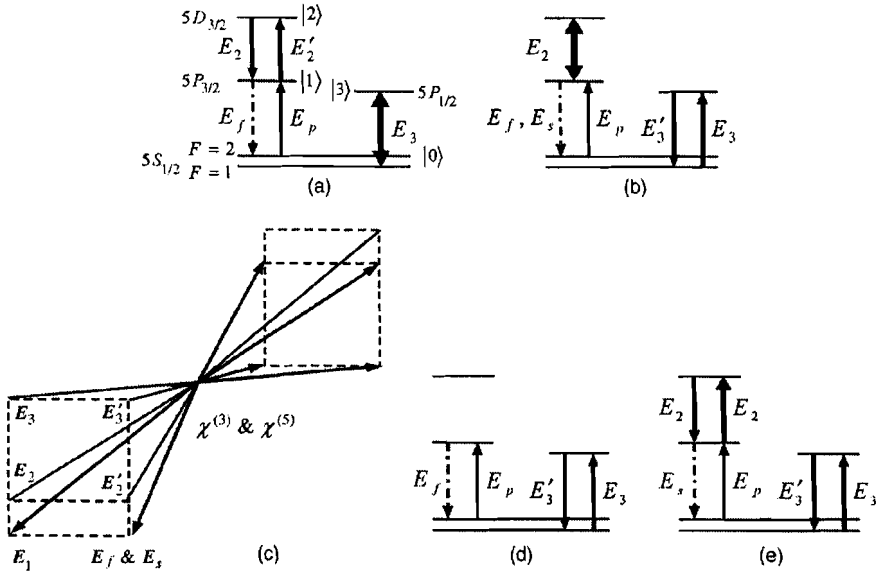

Fig. 1. (a) Five-level atomic system for the EIT- and optical pumping-assisted FWM process. (b) Five-level atomic system for generating co-existing FWM and SWM processes. (c) Three-dimensional beam geometry used in the experiment. (d) and (e) Typical FWM and SWM processes, respectively. The dashed–dotted lines ($\boldsymbol{E}_f$ and $\boldsymbol{E}_s$) in (d) and (e) are the generated FWM and SWM signals, respectively.

0146-9592/07/091120-3/$15.00

Generalized dressed and doubly-dressed multi-wave mixing

Yanpeng Zhang [1,2*] and Min Xiao [1]**

[1] *Department of Physics, University of Arkansas, Fayetteville, Arkansas 72701, USA*
[2] *Key Laboratory for Physical Electronics and Devices of the Ministry of Education, Xi'an Jiaotong University, Xi'an 710049, China*
* *ypzhang@mail.xjtu.edu.cn;* ** *mxiao@uark.edu*

Abstract: We present a theoretical treatment for generalized dressed and doubly-dressed multi-wave mixing processes. Co-existing four-wave mixing (FWM), six-wave mixing (SWM) and eight-wave mixing processes have been considered in a closed-cycle five-level system. Due to constructive interference of the secondarily-dressed and primarily-dressed excitation pathways, the FWM and SWM signals are greatly enhanced. The dually enhanced FWM channels are opened simultaneously. The dressing fields provide the energy for such large enhancement.

OCIS codes: (190.4380) Nonlinear optics, four-wave mixing; (270.4180) Multiphoton processes; (300.2570) Four-wave mixing; (320.7110) Ultrafast nonlinear optics; (030.1670) Coherent optical effects.

References and links

1. P. R. Hemmer, D. P. Katz, J. Donoghue, M. Cronin-Golomb, M. S. Shahriar, and P. Kumar, "Efficient low-intensity optical phase conjugation based on coherent population trapping in sodium," Opt. Lett. **20**, 982-984 (1995).
2. Y. Li and M. Xiao, "Enhancement of nondegenerate four-wave mixing based on electromagnetically induced transparency in rubidium atoms," Opt. Lett. **21**, 1064-1066 (1996).
3. B. Lu, W.H. Burkett, and M. Xiao, "Nondegenerate four-wave mixing in a double-L system under the influence of coherent population trapping," Opt. Lett. **23**, 804-806 (1998).
4. V. A. Sautenkov, A. S. Zibrov, L. Hollberg, G. R. Welch, M. D. Lukin, Y. Rostovtsev, E. S. Fry, and M. O. Scully, "Ultraslow group velocity and enhanced nonlinear optical effects in a coherently driven hot atomic gas," Phys. Rev. Lett. **82**, 5229-5232 (1999).
5. D. A. Braje, V. Balic, S. Goda, G. Y. Yin, and S. E. Harris, "Frequency mixing using electromagnetically induced transparency in cold atoms," Phys. Rev. Lett. **93**, 183601 (2004).
6. Y. P. Zhang, A. W. Brown, and M. Xiao, "Observation of interference between four-wave mixing and six-wave mixing," Opt. Lett. **32**, 1120-1122 (2007).
7. Y. P. Zhang and M. Xiao, "Enhancement of six-wave mixing by atomic coherence in a four-level inverted-Y system," Appl. Phys. Lett. **90**, 111104 (2007).
8. H. Kang, G. Hernandez, and Y. F. Zhu, "Slow-light six-wave mixing at low light intensities," Phys. Rev. Lett. **93**, 073601(2004).
9. Z. C. Zuo, J. Sun, X. Liu, Q. Jiang, G. S. Fu, L. A. Wu, and P. M. Fu, "Generalized n-photon resonant $2n$-wave mixing in an $(n+1)$-level system with phase-conjugate geometry," Phys. Rev. Lett. **97**, 193904 (2006).
10. H. Ma and C. B. de Araujo, "Interference between third- and fifth-order polarization in semiconductor doped glasses," Phys. Rev. Lett. **71**, 3649-3652 (1993).
11. D. J. Ulness, J. C. Kirkwood, and A. C. Albrecht, "Competitive events in fifth order time resolved coherent Raman scattering:Direct versus sequential processes," J. Chem. Phys. **108**, 3897-3902 (1998).
12. R. W. Boyd, *Nonlinear Optics* (Academic Press, New York, 1992).
13. S. E. Harris, "Electromagnetically induced transparency," Phys. Today **50** (7), 36 (1997).
14. J. Gea-Banacloche, Y. Li, S. Jin, and M. Xiao, "Electromagnetically induced transparency in ladder-type inhomogeneously broadened media: theory and experiment," Phys. Rev. A **51**, 576-584 (1995).
15. M. D. Lukin, S. F. Yelin, M. Fleischhauer, and M. O. Scully, "Quantum interference effects induced by interacting dark resonances," Phys. Rev. A **60**, 3225-3228 (1999).
16. M. Yan, E. G. Rickey, and Y. F. Zhu, "Observation of doubly dressed states in cold atoms," Phys. Rev. A **64**, 013412 (2001).

#79873 - $15.00 USD Received 7 Feb 2007; revised 13 May 2007; accepted 14 May 2007; published 29 May 2007

Opening Four-Wave Mixing and Six-Wave Mixing Channels via Dual Electromagnetically Induced Transparency Windows

Yanpeng Zhang,* Andy W. Brown, and Min Xiao†

Department of Physics, University of Arkansas, Fayetteville, Arkansas 72701, USA

(Received 25 November 2006; published 18 September 2007)

Highly efficient four-wave mixing (FWM) and six-wave mixing (SWM) processes can coexist in a four-level Y-type atomic system due to atomic coherence. The simultaneously opened dual electromagnetically induced transparency windows in this four-level atomic system allow observation of these two nonlinear optical processes at the same time, which enables detailed studies of the interplay between the FWM and SWM processes. Three-photon and five-photon destructive interferences are also observed.

DOI: 10.1103/PhysRevLett.99.123603 PACS numbers: 42.50.Gy, 32.80.Qk, 42.65.−k

Enhanced four-wave mixing (FWM) processes due to atomic coherence have been experimentally demonstrated in several multilevel atomic systems [1–5]. The keys to such enhanced nonlinear optical processes include the enhanced nonlinear susceptibility due to the induced atomic coherence and slowed laser beam propagation in the atomic medium, as well as greatly reduced linear absorption of the generated optical field due to electromagnetically induced transparency (EIT) [6,7]. Recently, the generation of six-wave mixing (SWM) has been reported in a closed-cycle N-type system in a cold atomic sample [8]. On the other hand, two-photon and three-photon destructive interferences have also been studied in various four-level Y-type [9], N-type [10], and double-Λ-type [2,5] atomic systems. These multiphoton interferences and light-induced atomic coherence are very important in nonlinear wave-mixing processes and might be used to open certain nonlinear optical processes in multilevel atomic systems that are otherwise closed due to high absorption [11]. Recently, there has been some theoretical interest in generating efficient $\chi^{(5)}$ processes in multilevel atomic systems for 3-qubit quantum computation [12] and liquid light condensate [13].

In this Letter, we report our experimental demonstration of generating highly efficient FWM and SWM processes simultaneously in an open-cycle Y-type atomic system, in which the dual-EIT windows are used to transmit the generated FWM and SWM signals, respectively. Several features in this work are distinctly different and advantageous over the previously reported SWM processes [8,14]. First, FWM and SWM processes can be observed simultaneously in this open-cycle Y-type system, which is not the case in the closed-cycle N-type system [8]. Such coexistence of FWM and SWM processes allows us to investigate the interplay between these two interesting nonlinear optical effects, and to obtain the beat signal between them to get the $\chi^{(5)}$ coefficient. Second, the generated FWM and SWM signals fall into two separate EIT windows in this four-level dual-EIT system, so the linear absorptions for the generated FWM and SWM signals are both greatly suppressed. By individually controlling (or tuning) the EIT windows, the generated FWM and SWM signals can be clearly separated and distinguished or pulled together (by frequency detunings) to observe interferences between them. Third, since the amplitude of the FWM signal can be controlled by the coupling beam (via dressed states), the relative strengths of the FWM and SWM can be adjusted easily. So, the SWM signal can be made to be in the same order as the FWM signal. Fourth, multiphoton destructive interference effects for both FWM (three-photon interference) and SWM (five-photon interference) are clearly observed in the experiment. Although double-resonance [9] and triple-resonance [10,15] EIT spectroscopies have been reported previously by detecting fluorescence, the current method is a coherent phenomenon. Finally, by designing the propagation directions of the (pump, coupling, and probe) laser beams, we can achieve Doppler-free configurations [7] for all the EIT subsystems in this Y-type atomic system. This makes the FWM and SWM processes very efficient even with relatively weak cw laser beams in an atomic vapor cell.

To the best of our knowledge, such a phenomenon of coexisting FWM and SWM channels via dual-EIT windows in multilevel atomic systems has not been reported, either experimentally or theoretically, in the literature. This specially designed experimental scheme to simultaneously generate different nonlinear wave-mixing processes opens a new research frontier in manipulating higher-order nonlinear optical processes with induced atomic coherence and quantum interference.

For a simple four-level Y-type atomic system as shown in Fig. 1(b), if two strong laser beams drive the two upper transitions ($|1\rangle$ to $|2\rangle$ and $|1\rangle$ to $|3\rangle$, respectively) and a weak laser beam probes the lower transition ($|0\rangle$ to $|1\rangle$), two ladder-type EIT subsystems will form and two EIT windows appear [9]. Depending on the frequency detunings of the two coupling beams, these two EIT windows can either overlap or be separated in frequency on the probe beam transmission signal. Now, if two pump fields, E_3 (ω_3, $\mathbf{k}_3$, and Rabi frequency G_3) and E_3' (ω_3, $\mathbf{k}_3'$, and Rabi frequency G_3'), drive the upper transition $|1\rangle$ to $|3\rangle$ and one strong field, E_2 (ω_2, $\mathbf{k}_2$, and Rabi frequency G_2),

Enhancement of six-wave mixing by atomic coherence in a four-level inverted Y system

Yanpeng Zhang[a] and Min Xiao[b]
Department of Physics, University of Arkansas, Fayetteville, Arkansas 72701

(Received 11 January 2007; accepted 12 February 2007; published online 12 March 2007)

The authors have considered the coexisting dressed four-wave mixing (FWM) and six-wave mixing (SWM) in an open four-level inverted Y configuration. The authors also report an experimental observation of optical pumping-assisted FWM and electromagnetically induced transparency (EIT)-assisted SWM. The efficient SWM can be selected by EIT window and controlled by the coupling as well as dressed field detuning and power. Due to EIT and optical pumping assistance, the enhanced SWM signal is more than ten times lager than the coexisting FWM signal. © *2007 American Institute of Physics*. [DOI: 10.1063/1.2713868]

Efficient higher-order multiwave mixing effects have been studied recently.[1–7] Under electromagnetically induced transparency (EIT) conditions,[8] not only the four-wave mixing (FWM) can be resonantly enhanced but also the generated FWM signals can be allowed to transmit through the atomic medium with little absorption.[1–5] The six-wave mixing (SWM) has also been observed in a closed-cycle four-level cold atom[6] and doubly excited autoionizing Rydberg states.[7] The nonlinear signal decreases by several orders of magnitude with an increase in the order of nonlinearity of the interaction.[9] On the contrary to the solid or liquid media (in which FWM and SWM signals can be generated at the same time),[10] only either FWM processes or SWM processes were experimentally generated in typical closed-cycle multilevel atomic systems previously,[1–7] depending on the arrangements of lasers and number of energy levels involved. There have also been some theoretical interests to generate efficient coexisting $\chi^{(3)}$ and $\chi^{(5)}$ nonlinear processes in multilevel atomic systems.[11]

In this letter, we consider the interplay between the coexisting FWM and SWM processes and demonstrate such coexistence in one atomic system by employing a specially designed experimental scheme [Fig. 1(a)]. More importantly, we can optimize the SWM process via opened EIT window and optical pumping from an additional hyperfine energy level ($|3\rangle$). Investigations of such intermixing and interplay between different types of nonlinear wave-mixing processes will help us to understand and optimize the generated high-order nonlinear optical signals.

The cw laser beams are aligned spatially in the pattern, as shown in Fig. 1(a), with four beams (E_2, E_2', E_3, and E_3') propagating through the atomic medium in the same direction with small angles ($\sim 0.3°$) between them in a square-box pattern. For a four-level inverted Y-type atomic system, as shown in Figs. 1(b)–1(g), if three strong laser beams (with either E_2' or E_3' beam blocked) drive the two transitions ($|1\rangle$ to $|2\rangle$ and $|1\rangle$ to $|3\rangle$) and a weak laser beam (propagating in the opposite direction) probes the transition ($|0\rangle$ to $|1\rangle$), these configurations satisfy the two-photon Doppler-free condition for the $|0\rangle$–$|1\rangle$–$|2\rangle$ ladder-type EIT subsystem (it is not the case for the $|0\rangle$–$|1\rangle$–$|3\rangle$ Λ-type EIT subsystem).[12] If two coupling fields E_3 (ω_3, $\mathbf{k}_3$, and Rabi frequency G_3) and E_3' (ω_3, $\mathbf{k}_3'$, and Rabi frequency G_3') drive the upper transition $|1\rangle$ to $|3\rangle$ and one strong dressing field E_2 (ω_2, $\mathbf{k}_2$, and Rabi frequency G_2) drives the transition $|1\rangle$ to $|2\rangle$, as shown in Fig. 1(b), there will be coexistent FWM and SWM processes that generate signal fields at frequency ω_1. First, without the strong dressing field E_2, a simple FWM process (the probe beam E_1 and two coupling fields E_3 and E_3') will generate signal field $\boldsymbol{E}_F$ at frequency ω_1 via the perturbation chain ($F1$) $\rho_{00}^{(0)} \rightarrow \rho_{10}^{(1)} \rightarrow \rho_{30}^{(2)} \rightarrow \rho_{10}^{(3)}$. When the dressing field E_2 is on, it will dress the energy level $|1\rangle$ to create dressed states $|+\rangle$ and $|-\rangle$ [Fig. 1(c)], which have the dressed FWM chains $\rho_{00}^{(0)} \rightarrow \rho_{\pm 0}^{(1)} \rightarrow \rho_{30}^{(2)} \rightarrow \rho_{\pm 0}^{(3)}$ in dressed-state picture. The constructive and destructive interferences between the "+" and "−" FWM channels result in the enhancement and suppression of the FWM signal, respectively.[13] Other than the dressed FWM processes, there are two possible SWM processes, as shown in Figs. 1(f) and 1(g), in which two photons from E_2 and one photon each from E_3 and E_3' participate in the SWM processes to generate $\boldsymbol{E}_S$ with different Liouville pathways [($S1$) $\rho_{00}^{(0)} \rightarrow \rho_{10}^{(1)} \rightarrow \rho_{20}^{(2)} \rightarrow \rho_{10}^{(3)} \rightarrow \rho_{30}^{(4)} \rightarrow \rho_{10}^{(5)}$ and ($S2$) $\rho_{00}^{(0)} \rightarrow \rho_{10}^{(1)} \rightarrow \rho_{30}^{(2)} \rightarrow \rho_{10}^{(3)} \rightarrow \rho_{20}^{(4)} \rightarrow \rho_{10}^{(5)}$]. These FWM and SWM processes can exist at the same time and can be phase-matched to travel in the same direction. On the other hand, when two coupling fields E_2 and E_2' (ω_2, $\mathbf{k}_2'$, and Rabi frequency G_2') are used to drive the transition $|1\rangle$ to $|2\rangle$ and one strong dressing field E_3 drives the transition $|1\rangle$ to $|3\rangle$, as shown in Figs. 1(d) and 1(e), there will be one FWM [($F2$) $\rho_{00}^{(0)} \rightarrow \rho_{10}^{(1)} \rightarrow \rho_{20}^{(2)} \rightarrow \rho_{10}^{(3)}$] and two SWM [($S1$) and ($S2$)] processes.

To quantitatively understand such phenomenon of interplay between coexisting FWM and SWM processes, we need to use perturbation chain expresses involving all the third-order and fifth-order nonlinear wave-mixing processes for arbitrary field strengths of E_2, E_2', E_3, and E_3'. When both E_2 and E_2' are blocked, the simple FWM via Liouville pathway ($F1$) gives $\rho_{F1}^{(3)} = -iG_a e^{i\mathbf{k}_{F1}\cdot\mathbf{r}}/d_1^2 d_2$, where $\mathbf{k}_{F1} = \mathbf{k}_1 + \mathbf{k}_3 - \mathbf{k}_3'$, $G_a = G_1 G_3 (G_3')^*$, $d_1 = \Gamma_{10} + i\Delta_1$, and $d_2 = \Gamma_{30} + i(\Delta_1 - \Delta_3)$ with $\Delta_i = \Omega_i - \omega_i$. Γ_{ij} is the transverse relaxation rate between states $|i\rangle$ and $|j\rangle$. Next, when the dressing field E_2 is turned on, there exist two physical mechanisms of interest. First, the above main FWM process ($F1$) will be dressed and a pertur-

[a]Electronic mail: ypzhang@mail.xjtu.edu.cn
[b]Electronic mail: mxiao@uark.edu

Available online at www.sciencedirect.com
ScienceDirect
Journal of Crystal Growth 301–302 (2007) 101–104
JOURNAL OF CRYSTAL GROWTH
www.elsevier.com/locate/jcrysgro

Electrical and optical studies of GaMnAs/GaAs(0 0 1) thin films grown by molecular beam epitaxy

J.F. Xu*, S.W. Liu, Min Xiao, P.M. Thibado

Department of Physics, University of Arkansas, Fayetteville, Arkansas 72701, AR, USA

Available online 2 January 2007

Abstract

GaMnAs/GaAs films were grown via molecular beam epitaxy using both low and high substrate temperatures. The films were investigated using Hall effect and photoluminescence (PL) measurements from 8 to 300 K. The carrier concentrations in the samples grown at a low substrate temperature are greater than those in the samples grown at a high substrate temperature. The PL spectra show a GaAs exciton peak, a peak involving a carbon acceptor, a substitutional Mn acceptor-related peak and an optical phonon-related peak.

PACS: 82.80.Pv; 75.50.pp; 61.82.Fk

Keywords: A1. Photoluminescence; B1. GaMnAs; B2. Semiconducting material

1. Introduction

Recently, the p-type dilute magnetic semiconductor (DMS) Mn-doped GaAs (GaMnAs) has been attracting much attention. GaMnAs can be described qualitatively as a random alloy in which Mn substitutes at Ga sites and takes the dual role of acceptor and local magnetic moment. The combination of ferromagnetism with the versatile semiconducting properties makes it promising for future spintronics applications. In addition, GaMnAs can be grown using several techniques, including molecular beam epitaxy (MBE) [1,2], liquid phase epitaxy (LPE) [3] and ion implantation [4,5]. The realization of spintronic devices requires a substantial increase in the ferromagnetic transition temperature (T_c) as the highest in GaMnAs is around 100 K. Because of the low solubility of Mn in GaAs, it is thought that most Mn ions form in the DMS as defects, such as interstitials. These defects compensate substitutional Mn acceptors (Mn_{Ga}) and, in turn, lead to a suppression of the ferromagnetic transition temperature [6]. It has been demonstrated that T_c exceeding 150 K can be achieved by low-temperature annealing in films thinner than ~60 nm [7,8]. Post-growth annealing is thought to enable Mn interstitials to diffuse to the surface thereby maximizing the concentration of uncompensated Mn_{Ga} and thus T_c. These results show this material is highly sensitive to the growth and post-growth conditions. A small change in alloying compositions or microstructures can induce significantly different physical properties. Thus, it is important to study the electrical and optical properties in the GaMnAs system as a function of growth parameters.

In this paper, we discuss DMS GaMnAs thin films that were grown at high and low substrate temperatures using MBE. These samples were investigated using Hall effect and PL measurement from 8 to 300 K. Carrier concentration and Hall mobility were evaluated, and the energy of the Mn acceptor level was determined from the photoluminescence (PL) data.

2. Experimental details

Samples were prepared in an ultrahigh vacuum (~2×10^{-10} Torr) MBE growth chamber (Riber 32) that includes Ga and Mn effusion cells together with a two-zone As valved-cracker cell. The MBE chamber is also equipped with a reflection high-energy electron diffraction (RHEED) system. Commercially available, "epi-ready," semi-insulating 2″ diameter GaAs(0 0 1)$\pm$0.1° wafers were cleaved into

*Corresponding author. Tel.: +1 479 575 6178.
E-mail address: jxu@uark.edu (J.F. Xu).

0022-0248/$ - see front matter © 2006 Elsevier B.V. All rights reserved.
doi:10.1016/j.jcrysgro.2006.11.049

Optimization of a Dual Pumped L-Band Erbium-Doped Fiber Amplifier by Genetic Algorithm

Cheng Cheng and Min Xiao, *Fellow, OSA*

***Abstract*—A dual pumped L-band erbium-doped fiber amplifier (DPLB-EDFA) is investigated by solving the optical propagation equation that takes into account radial effects of the fiber and the rate equation in a steady-state two-level model with a weakly guided approximation. Applying an inversing method and a genetic algorithm, the DPLB-EDFA is optimized for dual pumped wavelengths and directions, fiber lengths, as well as radial distributions of the erbium concentration and core refractive index. There is evidence to show that the optimal pumping wavelengths of the DPLB-EDFA are different in two different pumping schemes. The optimized DPLB-EDFA is characterized by a gain peak wavelength of 1600 nm, a gain peak of ~34 dB, a bandwidth of 30–37 nm, and a noise figure of 3.5–3.7 dB. Such characteristics are superior as compared with those using conventional 1480-nm pumps with step indexes and radial-uniform erbium concentrations.**

***Index Terms*—Dual pump, erbium-doped fiber amplifier (EDFA), genetic algorithm, L-band, radial effects.**

I. Introduction

As KEY components in wavelength-division-multiplexing (WDM) systems in optical telecommunication, erbium-doped fiber amplifiers (EDFAs) have received great attention over the past ten years. Conventional band (C-band) EDFAs are characterized by operation at the ~1550-nm wavelength region, an ~30-dB gain, a 20–25-nm bandwidth, and an ~4-dB noise figure. In recent years, developments of the EDFAs have stretched toward L-band and S-band from C-band while achieving high gains and low noise figures. There were many papers reported in this direction. For example, Lu *et al.* [1] recently reported a novel structure for ultrawide-band gain-flattened amplifier by combining two pieces of C- and L-band dual-core erbium-doped fibers. This novel amplifier has a flat gain of 15 dB over a wavelength range of 105 nm (1515–1620 nm). The gain variation for the C-band (1515–1555 nm) and L-band (1562–1620 nm) flat-gain regions is 1.3 and 1.5 dB, respectively. The noise figure varies from 4.5 to 4.8 dB over the entire bandwidth. Choi *et al.* [2] investigated a new pump wavelength of 1540-nm band for the L-band EDFA using a pump wavelength source of 1540-nm band from a small single-channel input signal to high-power WDM signals. It was shown that the small-signal gain of the 1545-nm pump among the 1540-nm band is 2.25 times higher compared with that of the conventional 1480-nm pump. Moreover, this improvement in gain is not limited by the pumping direction. They suggested that a broadband pump source, as well as a single wavelength pump, can be used as a 1540-nm band pump. In addition, the 1545-nm bidirectionally pumped EDFA is applied as a second stage amplifier. It was also shown that no noise figure degradation is observed compared with the case of the 1480-nm pump. For thulium-doped tellurite fiber amplifiers (TDTFAs), there were also dual pump schemes reported. For example, Taylor *et al.* [3] demonstrated gain in the S-band of a TDTFA using dual pump and bidirectional pump schemes. Two pump schemes were employed, namely 1) 795/1064 nm and 2) 1047/1550 nm. The gain profile is broader than that achieved in a fluoride fiber and overlaps with the C-band of the EDFA. A fiber-to-fiber gain of 11 dB and an internal gain of 35 dB are reached in these systems. Ng *et al.* [4] and Gomes *et al.* [5] also adopted dual pump schemes in TDTFAs, in which an improvement in gain by a factor of 2 is achieved using a 795- and 1064-nm dual pump scheme. Gain in tellurite fibers extends to longer wavelength than in fluorides, which shows improved overlap with the C-band EDFA.

However, all the methods used in the aforementioned papers can be ascribed as a "direct method," i.e., to obtain a direct solution by the given pumping wavelengths or schemes. Obviously, there is a limitation to such designed EDFAs because the pumping wavelengths or schemes adopted in advance are not always best suited for the desired performances. Moreover, it is impossible to try all pumping wavelengths or schemes to determine which is optimal by such "direct method." Therefore, as an attempt, it is interesting to determine optimal pumping wavelengths or schemes of the EDFAs by global optimization methods and, further, to optimize the EDFAs.

In this paper, by applying an inversing method and a genetic algorithm to implement global searches, we investigate the dual pumped [including dual-wavelength dual-forward (DF) directional and bidirectional pumped (B-pumped)] L-band EDFA (DPLB-EDFA) under the steady-state condition and a weakly guided approximation. Performances of the DPLB-EDFA are described by solving the optical propagation equation that takes

Manuscript received August 31, 2005. This work was supported by the Foundation for the Author of National Excellent Doctoral Dissertation of China under Grant 200433 and the Zhejiang Provincial Natural Science Foundation of China under Grant 602098.

C. Cheng is with the Department of Applied Physics, Zhejiang University of Technology, Xiaoheshan, Hangzhou 310023, China (e-mail: chengch@zjut.edu.cn).

M. Xiao is with the Department of Physics, University of Arkansas, Fayetteville, AR 72701 USA (e-mail: mxiao@uark.edu).

Color versions of all figures are available online at http://ieeexplore.ieee.org.
Digital Object Identifier 10.1109/JLT.2006.881476

Appl. Phys. B 82, 443–447 (2006)
DOI: 10.1007/s00340-005-2060-6

Applied Physics B
Lasers and Optics

S.W. LIU[1]
J. XU[1]
D. GUZUN[1]
G.J. SALAMO[1]
C.L. CHEN[2]
Y. LIN[2,*]
MIN XIAO[1,✉]

Nonlinear optical absorption and refraction of epitaxial $Ba_{0.6}Sr_{0.4}TiO_3$ thin films on (001) MgO substrates

[1] Department of Physics, University of Arkansas, Fayetteville, Arkansas 72701, USA
[2] The Texas Center for Superconductivity and Department of Physics, University of Houston, Texas 77204, USA

Received: 25 August 2005
Published online: 17 December 2005 • © Springer-Verlag 2005

ABSTRACT Highly epitaxial $Ba_{0.6}Sr_{0.4}TiO_3$ (BST) ferroelectric thin films were fabricated on (001) MgO substrates by pulsed laser deposition. The nonlinear optical absorption coefficients (β) and refraction indices (γ) of the BST thin films on (001) MgO substrates were investigated using the single beam Z-scan technique with femtosecond laser pulses at the wavelengths of 790 nm and 395 nm, respectively, at room temperature. The nonlinear absorption coefficients of BST thin films were measured to be ~ 0.087 cm/GW and ~ 0.77 cm/GW at 790 nm and 395 nm, respectively. The nonlinear refraction indices of BST thin films exhibit a strong dispersion from a positive value of 6.1×10^{-5} cm^2/GW at 790 nm to a negative value of -4.0×10^{-5} cm^2/GW at 395 nm near band gap. The dispersion of γ is roughly consistent with Sheik-Bahae's theory for the bound electronic nonlinear refraction resulting from the two-photon resonance. These results show that the BST film is a promising material as a candidate for nonlinear optical applications.

PACS 42.70.Mp; 78.20.-e; 81.05.-t

1 Introduction

Dielectric $Ba_{1-x}Sr_xTiO_3$ (BST) thin films have been considered to be an important material for use in tunable microwave devices such as tunable phase shifters, filters, oscillators, and antennas because of its high dielectric constant, relatively low dielectric loss tangent, and large electric field tunability [1–3]. BST thin films exhibit a large microwave tunability even up to 23.7 GHz [3], a feature that motivates the study of the nonlinear dielectric properties in optical frequency range. Recently, electro-optic (E-O) characterizations of BST films reveal an E-O coefficient with a very large saturation value of the field-induced birefringence at the wavelength of 632.8 nm [4]. Optical second-harmonic generation (SHG) has also been observed in the NIR (near infra-red) wavelength range using a high peak power Q-switched Nd-YAG laser at 1.06 μm [5] and a mode-locked Ti:Sapphire laser at 760 nm [6, 7]. Even more recently, the nonlinear optical absorption and refraction of the polycrystalline $Ba_{0.7}Sr_{0.3}TiO_3$ film on quartz substrate have been measured [8]. However, less effort has been taken to study the third-order nonlinearity of epitaxial BST thin films. The quantitative measurements of both nonlinear refraction index and adsorption coefficient of high quality epitaxial BST thin films have not been reported.

Several kinds of ferroelectric oxide thin films have already been investigated as the promising candidates for applications in nonlinear optics such as $SrBi_2Ta_2O_9$ [9], $BiMnO_3$ [10], $Bi_2Nd_2Ti_3O_{12}$ [11], PLT30 [12], $(Pb, La)(Zr, Ti)O_3$ [13], $PbZr_xTi_{1-x}O_3$ [14], $BaTiO_3$ [15], Ce:$BaTiO_3$ [15, 16], and Fe:$BaTiO_3$ [17]. $Ba_{0.6}Sr_{0.4}TiO_3$, a ferroelectric solid solution of $BaTiO_3$ and $SrTiO_3$, is nominally in its paraelectic state at room temperature. $Ba_{0.6}Sr_{0.4}TiO_3$ thin films are highly transparent from near ultraviolet to infrared. The Curie temperature of (Ba, Sr)TiO_3 may be continuously tailored by selecting different mole content ratio of Ba and Sr. This versatile property enhances the potential applications of (Ba, Sr)TiO_3 in different temperature environments. Compared to lead-contained ferroelectrics where lead is a volatile constituent and poisonous, (Ba, Sr)TiO_3 is non-volatile and easy to be fabricated. Moreover, (Ba, Sr)TiO_3 thin films are compatible with various microwave devices, which are beneficial to the future integration of optoelectronics with microwave electronics.

2 Experimental details

Dielectric $Ba_{0.6}Sr_{0.4}TiO_3$ thin films were grown by using pulsed laser ablation by a KrF excimer laser with a wavelength of 248 nm. An energy density of ~ 2.5 J/cm^2 and a repetition rate of $5 \sim 10$ Hz were used for the film deposition. A stoichiometric BST (60:40) target with a density of 95% was used. Since the Z-scan technique is sensitive to crystalline defects, surface imperfections, and inhomogeneities, single-crystal double-side polished (001) cubic MgO substrates were selected for the epitaxial growth of BST thin films. Such substrates maintain excellent crystalline quality and are still highly transparent even when they are heated for more than one hour at the deposition temperature (higher than 820 °C) in a low oxygen-pressure chamber environment ($200 \sim 300$ mTorr). The crystalline quality and epitaxial behavior of the as-grown BST thin films were characterized

✉ Fax: 479-5754580, E-mail: mxiao@uark.edu
*Moved to: Superconductivity Technology Center, Los Alamos National Laboratory, Los Alamos, New Mexico 87545, USA

Modified two-photon absorption and dispersion of ultrafast third-order polarization beats via twin noisy driving fields

Yanpeng Zhang,[1,2,*] Chenli Gan,[1] and Min Xiao[1,†]
[1]*Department of Physics, University of Arkansas, Fayetteville, Arkansas 72701, USA*
[2]*Department of Electronic Science and Technology, Xi'an Jiaotong University, Xi'an 710049, China*
(Received 7 January 2006; published 1 May 2006)

We investigate the color-locked twin-noisy-field correlation effects in third-order nonlinear absorption and dispersion of ultrafast polarization beats. We demonstrate a phase-sensitive method for studying the two-photon nondegenerate four-wave mixing (NDFWM) due to atomic coherence in a multilevel system. The reference signal is another one-photon degenerate four-wave-mixing signal, which propagates along the same optical path as the NDFWM signal. This method is used for studying the phase dispersion of the third-order susceptibility and for the optical heterodyne detection of the NDFWM signal. The third-order nonlinear respouse can be controlled and modified through the color-locked correlation of twin noisy fields.

DOI: 10.1103/PhysRevA.73.053801 PACS number(s): 42.65.Sf, 42.65.Re, 32.80.Qk

I. INTRODUCTION

Recently, studies of nonlinear optical effects in multilevel atomic systems have received renewed interest due to the greatly enhanced nonlinearity and, at the same time, reduced linear absorption caused by light-induced atomic coherence among the energy levels [1–3]. By carefully choosing the atomic level configurations and laser fields, the efficiencies of wave mixing can be greatly increased at optimal atomic coherence conditions. Through directly measuring the nonlinear optical coefficients in multilevel atomic systems [4], one can see that the nonlinearity depends sensitively on various experimental parameters. Large enhancement of the nonlinear index in four-level atomic systems was also demonstrated [5]. In order to optimize certain nonlinear optical processes, it is beneficial to have exact knowledge of the nonlinear coefficients and their dependences on various experimental parameters. However, due to residual linear absorption and dispersion of the probe and signal beams, it is usually difficult to measure the nonlinear coefficients, especially both the real and imaginary parts under the same conditions. One of the early experiments to measure the Kerr nonlinear coefficient in a three-level atomic system used an optical cavity to eliminate the linear contributions [4], which directly gives the nonlinear refractive index n_2.

In this paper we present a type of phase-sensitive detection for the third-order complex susceptibility in a multilevel gas medium. We study two-photon nondegenerate four-wave mixing (NDFWM) in attosecond polarization beats induced by the third-order susceptibility. One can adjust the relative phase between the local oscillator field of one-photon degenerate four-wave mixing (DFWM) and the two-photon NDFWM signal by changing the relative time delay (τ) between two pump beams of DFWM and NDFWM through a Michelson interferometer. As the τ-dependent phase difference approaches $2n\pi$ or $(2n+1/2)\pi$, the attosecond polarization beat signal evolves into the nonlinear dispersion or absorption of two-photon NDFWM separately. Here the reference beam is another one-photon DFWM signal, which is introduced by adding an additional frequency component to the pump beams of the NDFWM scheme. The NDFWM signal beam and the DFWM reference beam then interfere directly at the detector. Our method is based on attosecond polarization interference between two FWM processes in a purely homogeneously broadened [6,7] or Doppler-broadened three-level ladder-type system [8–10].

This method is a good way to measure the third-order susceptibility directly. Alternative methods (in the purely homogeneously broadened and the extremely Doppler-broadened media, respectively) are used to study the nonlinear responses of the three-level ladder-type system. We proceed in the standard manner by calculating the expression for the density-matrix element (third-order response functions $\rho_{10}^{(3)}$), finding the complex susceptibility, and finally breaking it down into real and imaginary parts to obtain the desired results. The modified third-order absorption and dispersion can be controlled coherently by noisy-light color-locking bandwidth, frequency detuning, and time delay. Another advantage of our system is the use of a two-photon Doppler-free counterpropagation configuration [9,10] that allows us to observe these interesting effects in a long atomic vapor cell.

II. LIOUVILLE PATHWAYS

Nonlinear optical properties of an atomic medium can be controlled and modified through the color-locked correlation of twin noisy driving fields. A simply physical explanation of this process in a three-level ladder-type atomic system can be given in the bare-state picture. The polarization interference of two excitation paths $|0\rangle\rightarrow|1\rangle\rightarrow|0\rangle\rightarrow|1\rangle$ (one-photon DFWM) and $|0\rangle\rightarrow|1\rangle\rightarrow|2\rangle\rightarrow|1\rangle$ (two-photon NDFWM) leads to a third-order attosecond polarization beat (ASPB) phenomenon [7,8,10]. This polarization beat is based on the interference at the detector between FWM signals which originate from macroscopic polarizations excited simulta-

*Email address: ypzhang@mail.xjtu.edu.cn
†Email address: mxiao@uark.edu

Controlled polarization rotation of an optical field in multi-Zeeman-sublevel atoms

Shujing Li,[1] Bo Wang,[1] Xudong Yang,[1] Yanxu Han,[1] Hai Wang,[1,*] Min Xiao,[1,2] and K. C. Peng[1]
[1]*The State Key Laboratory of Quantum Optics and Quantum Optics Devices, Institute of Opto-Electronics, Shanxi University, Taiyuan, 030006, People's Republic of China*
[2]*Department of Physics, University of Arkansas, Fayetteville, Arkansas 72701, USA*
(Received 9 June 2006; published 27 September 2006)

We investigate, both theoretically and experimentally, the phenomenon of polarization rotation of a weak, linearly polarized optical (probe) field in an atomic system with multiple three-level electromagnetically induced transparency (EIT) subsystems. The polarization rotation angle can be controlled by a circularly polarized coupling beam, which breaks the symmetry in number of EIT subsystems seen by the left and right circularly polarized components of the weak probe beam. A large polarization rotation angle (up to 45°) has been achieved with a coupling beam power of only 15 mW. Detailed theoretical analyses including different transition probabilities in different transitions and Doppler-broadening are presented and the results are in good agreements with the experimentally measured results.

DOI: 10.1103/PhysRevA.74.033821 PACS number(s): 42.50.Gy, 33.55.Ad, 42.25.Ja

I. INTRODUCTION

The polarization rotation of an optical field or chirality can be caused by the intrinsic helicity of the molecules in the medium or introduced by external electric, magnetic, and optical fields. By introducing asymmetry in the index of refraction for the left and right circularly polarized components of a linearly polarized optical beam when propagating through the medium, the original linear polarization direction will be rotated. Many schemes have been demonstrated in inducing such chirality in various atomic and molecular systems. The most studied phenomenon in such induced polarization rotation is the magneto-optical effect. An external magnetic field can induce linear or nonlinear magneto-optical effects by introducing frequency shifts among various Zeeman sublevels in atomic vapors [1,2], which have led to the development of sensitive magnetometry and nonlinear magneto-optical tomography. Optical fields can also be used to introduce asymmetries in different energy levels, such to change the indices of refraction for the left and right circularly polarized optical components of the probe field. Induced polarization rotations by optical pumping of ground-state Zeeman sublevels with a nonresonant light field [3] and by resonant two-photon dispersion in a three-level cascade atomic system [4] were experimentally demonstrated more than 30 years ago. In recent years after demonstrations of the phenomenon of electromagnetically induced transparency (EIT) (especially with low power diode lasers) [5–7], there were renewed interests and new schemes to achieve polarization rotation of an optical beam controlled by another stronger (coupling or controlling) laser beam based on atomic coherence in multilevel EIT systems. Optical birefringence for a linearly polarized probe beam was experimentally demonstrated in a three-level cascade EIT system by making use of atomic coherence with a cw, circularly polarized coupling beam [8], which was later improved to have a lower absorption loss and larger achievable polarization rotation angle at a relatively lower coupling power [9]. Similar schemes to achieve polarization rotation were also reported recently in different atomic systems [10,11]. In these schemes, the asymmetry is introduced by connecting one circularly polarized component (say σ^+) of the linearly polarized probe beam to the circularly polarized coupling beam (σ^-) through one degenerate middle level ($m=+1$), which forms a cascade EIT system with less absorption, and leaving another circularly polarized probe component (σ^-) to be highly absorbed (not connected to the coupling beam). Such schemes suffer from strong circular dichroism and therefore still require high coupling beam power (in the order of 10^4 W/cm^2) [9] to achieve a large polarization rotation angle. A more detailed theoretical study was recently presented to reduce optical absorption in inducing polarization rotation of the above system [12]. Also, there were several schemes proposed to control and enhance magneto-optical polarization rotation of a laser beam by employing another laser beam [13,14]. One of such effects, electromagnetically induced magnetochiral anisotropy in a resonant medium, was recently demonstrated experimentally [15].

Another system to achieve optical polarization rotation of a linearly polarized weak (probe) light beam controlled by a strong, circularly polarized coupling laser beam was reported recently [16]. The polarization rotation is mainly induced by the asymmetry in the number of Λ-type EIT subsystems seen by the left and right circularly polarized components of the probe beam with the circularly polarized coupling beam. In this paper, we present detailed theoretical calculations with careful considerations for contributions of different Clebsch-Gordan (CG) coefficients for all involved atomic transitions, Stark shifts, and Doppler-broadening due to atomic motion in the vapor cell. We show that the essential contribution for the polarization rotation comes from the asymmetry in the number of EIT subsystems in such multi-Zeeman-sublevel atomic systems, with secondary contribution from different CG coefficients for various atomic transitions between different Zeeman sublevels. Such detailed studies are necessary to fully

*Corresponding author. E-mail address: wanghai@sxu.edu.cn

Multi-dark-state resonances in cold multi-Zeeman-sublevel atoms

Bo Wang, Yanxu Han, Jintao Xiao, Xudong Yang, Changde Xie, and Hai Wang

The State Key Laboratory of Quantum Optics and Quantum Optics Devices, Institute of Opto-Electronics, Shanxi University, Taiyuan 030006, China

Min Xiao

The State Key Laboratory of Quantum Optics and Quantum Optics Devices, Institute of Opto-Electronics, Shanxi University, Taiyuan 030006, China, and Department of Physics, University of Arkansas, Fayetteville, Arkansas 72701

Received August 14, 2006; revised September 26, 2006; accepted September 26, 2006; posted September 28, 2006 (Doc. ID 74036); published November 22, 2006

We present our experimental and theoretical studies of multi-dark-state resonances (MDSRs) generated in a unique cold rubidium atomic system with only one coupling laser beam. Such MDSRs are caused by different transition strengths of the strong coupling beam connecting different Zeeman sublevels. Controlling the transparency windows in such an electromagnetically induced transparency system can have potential applications in multiwavelength optical communication and quantum information processing. © 2006 Optical Society of America

OCIS codes: 270.1670, 020.1670, 020.6580.

Since the early demonstrations of the electromagnetically induced transparency (EIT) phenomenon in various three-level atomic systems,[1–3] many new EIT-related phenomena have been discovered and studied.[4] One such interesting effect is dual-EIT or dual dark-state resonances studied in two coupled three-level EIT systems[5–9] or by perturbing one of the lower states in the three-level EIT systems (by using one additional optical or microwave field connecting to the fourth auxiliary energy level).[10–13] In those dual EIT systems, two transparency windows are created that can be used to allow transmissions of two probe beams simultaneously at two different wavelengths. The typical conditions for observing such dual dark-state resonances are four energy levels and three optical (or two optical and one microwave) fields. Although the two-photon Doppler-free condition allows the use of continuous-wave, low-power diode lasers to eliminate the first-order Doppler effect and makes it possible to observe EIT with relatively low coupling power,[3] the use of cold atoms can further reduce the power requirement for the coupling beam and allow narrow EIT windows.[14,15] The dual dark-state phenomenon was also observed in cold atoms by perturbing the lower state for the coupling transition in a three-level Λ-type system with a microwave field.[11] Also, the effects of degenerate Zeeman sublevels and various polarization configurations on EIT were studied in detail in a vapor cell or in cold atomic samples.[16–19]

In this Letter, we propose and experimentally demonstrate a new scheme to generate multi-dark-state resonances in a three-level (with multi-Zeeman sublevels) atomic system with only two laser fields. First, let us consider two atomic systems in ^{87}Rb atoms, as shown in Fig. 1. In Fig. 1(a), the linearly polarized coupling beam E_c (frequency ω_c) drives transition $5S_{1/2}$, $F=2$ to $5P_{1/2}$, $F'=1$. Since the transition strengths between different Zeeman levels are very close,[20] the Rabi frequencies (defined as $\Omega_{cij}=\mu_{ij}E_c/\hbar$, where μ_{ij} is the transition dipole moment with i,j denoting Zeeman sublevels) for different coupling transitions are almost equal. The linearly polarized probe beam will have a simple single-peak EIT as was studied extensively before.[15] However, when one chooses the up energy level to be $F'=2$ instead of $F'=1$, as shown in Fig. 1(b), the situation changes dramatically. Due to the large differences in

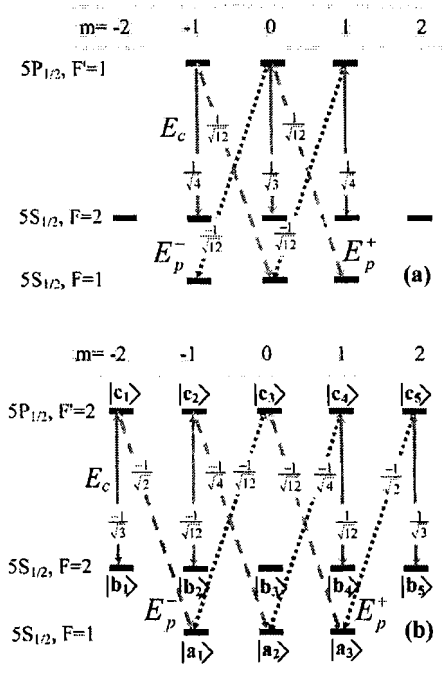

Fig. 1. (Color online) Λ-type EIT subsystems formed by linearly polarized probe and coupling fields (the polarizations of these two beams are perpendicular to each other) in $D1$ line of ^{87}Rb atoms. (a) Upper energy level is $5P_{1/2}$, $F'=1$; (b) Upper energy level is $5P_{1/2}$, $F'=2$.

0146-9592/06/243647-3/$15.00

Available online at www.sciencedirect.com
ScienceDirect
Physics Letters A 359 (2006) 390–395
PHYSICS LETTERS A
www.elsevier.com/locate/pla

Cavity-QED-based unconventional geometric phase gates with bichromatic field modes

Amitabh Joshi *, Min Xiao

Department of Physics, University of Arkansas, Fayetteville, AR 72701, USA

Received 7 February 2006; received in revised form 19 June 2006; accepted 25 June 2006

Available online 7 July 2006

Communicated by P.R. Holland

Abstract

Realization of two-qubit quantum phase gate is demonstrated using unconventional geometric phase in a cavity sustaining bichromatic field modes which are highly detuned from the atomic transition frequency. The two cavity modes are displaced simultaneously and thus acquire a geometric phase which can be used for realization of approximate phase gate operation.

PACS: 03.67.Lx; 42.65.-k; 42.50.Gy

1. Introduction

Quantum computers which could be exponentially faster [1] than their classical counterparts essentially work on the fundamental principles of quantum mechanics. To realize such a device on large scale operation with high fidelity, suppression of decoherence is of prime concern. The architect of built-in-fault-tolerant quantum gates requires avoiding of dynamical phases and utilization of decoherence free subspace [2] or the concept of geometric phases [3–11]. It is possible to realize universal quantum gates [3–9] through geometric phases when Hamiltonian describing qubits undergoes changes along suitable cycles in a control space. The quantum computation is called a geometric quantum computation if the phase associated with the gate operation is pure geometric one. When the logical gates in quantum computing are implemented through geometric phases then these gates provide fault-tolerant characteristics because the geometric phases depend only on some global geometric features and hence should be robust against dephasing. A geometric gate obtained by driving the qubits to undergo appropriate adiabatic evolution is called conventional geometric phase-gates [10,12]. On the other hand, evolution of the state generator (e.g., displacement operator for the coherent state) along the closed path conditional on the state of the qubits provides the so-called unconventional geometric phase gates [10,12]. Several proposals using NMR [5], superconducting circuits [7], trapped ions [9], and semiconductor nano structures [11], for the adiabatic geometric quantum computation were given. This was also generalized for the nonadiabatic case both theoretically [10, 12] and experimentally [13]. The universal quantum gates were proposed using nonadiabatic geometric phase [10] for Josephson junctions and for NMR systems. The gates categorized under conventional geometric quantum gates require certain extra operations in order to avoid dynamical phases that sometimes can bring additional errors. On the other hand, unconventional geometric quantum gates are independent of initial state of the system and can incorporate all advantages of conventional geometric gates and provide high fidelity. More specifically this is due to the fact that the unconventional geometric phase is a type of phase factor where the dynamic component is nonzero but proportional to geometric component so the total phase is dependent only on global geometric features [10]. The experimental realization of such gates has been reported in trapped ion system [13]. In a cavity QED

* Corresponding author.
E-mail address: ajoshi@uark.edu (A. Joshi).

0375-9601/$ – see front matter
doi:10.1016/j.physleta.2006.06.081

Enhanced dipole-dipole interaction of CdSe/CdS nanocrystal quantum dots inside a planar microcavity

Xiaoyong Wang[a] and Chih-Kang Shih
Department of Physics, The University of Texas at Austin, Austin, Texas 78712

Jianfeng Xu and Min Xiao
Department of Physics, University of Arkansas, Fayetteville, Arkansas 72701

(Received 13 April 2006; accepted 24 July 2006; published online 13 September 2006)

The energy transfer (ET) dynamics of closely packed CdSe/CdS nanocrystal quantum dots (NQDs) embedded in a planar microcavity were studied by using time-resolved photoluminescence measurements. An increase of ~20% was observed in the rates of ET from smaller to larger NQDs in the microcavity as compared with those measured in free space. This behavior was attributed to the enhanced dipole-dipole interactions between donor and acceptor NQDs at the spectral positions of the cavity modes. © *2006 American Institute of Physics*. [DOI: 10.1063/1.2352802]

Semiconductor nanocrystal quantum dots (NQDs) have attracted a lot of interest in recent years due to their relatively reproducible and controllable synthetic chemistry and strong size-dependent optoelectronic properties. When closely packed together in solid films, NQDs can interact with each other through dipole-dipole couplings so that such cooperative phenomenon as energy transfer[1–7] (ET) can occur and may prove useful in the quantum logic and computation schemes requiring communication between QDs.[8] It has been reported that the ET rate and consequently the coupling strength of NQDs can be increased by reducing the separation distance,[5] modifying the emission and absorption spectra,[4–6] and increasing the temperature[2] of the donor and acceptor NQDs. Another potential way of expediting the ET process of NQDs is to change their local optical environment by using microcavity structures. This kind of cavity-enhanced ET process has been previously observed in planar microcavities containing donor/acceptor pairs of dye/dye molecules,[9] polymer/polymer molecules,[10] and NQD/dye assemblies.[11] It has been suggested[2] that ET of closely packed NQDs embedded in microcavities could play very important roles in practical NQD-based optoelectronic devices such as lasers[12] and light-emitting diodes.[13] However, to the best of our knowledge, microcavity-enhanced ET between NQDs has not been reported. In this letter, we study the influence of a planar microcavity on the ET dynamics of closely packed CdSe/CdS core/shell NQDs through time-resolved photoluminescence (PL) measurements. We observed an increase of ~20% in the rates of ET from smaller to larger NQDs in the microcavity as compared with those measured in free space. This behavior can be attributed to the enhanced dipole-dipole interactions between donor and acceptor NQDs at the spectral positions of the cavity modes.

CdSe/CdS core/shell NQDs with an ~4.1 nm CdSe core diameter, a 3 ML CdS shell thickness, and an original quantum yield of ~0.5 in solution were used for the current study. The NQDs were mixed with poly(methylmethacrylate) (PMMA) in a toluene solution and drop cast onto a standard dielectric mirror with a reflectivity of 99.5% in the visible range. The average distance between two nearby NQDs is ~1.5 nm and the NQD filling fraction of the NQD/PMMA film is estimated to be ~8%. A PMMA thin film with a thickness of ~200 nm was then coated on top of the closely packed NQD solid film. Finally, an ~50 nm thick silver film was deposited as the top mirror of the cavity by the thermal evaporation technique. The complete microcavity structure with embedded NQDs is schematically shown in Fig. 1. For comparison, a reference sample was also fabricated with the same features as those of the microcavity one, except without the top silver mirror. The samples were excited with ~400 nm, picosecond pulses (repetition rate of 82 MHz) from a frequency-doubled Ti:sapphire laser. As shown in Fig. 1, the excitation laser with a power density of ~50 W/cm^2 was focused onto the sample surfaces at an incident angle of ~45° relative to the surface normal direction. PL of the samples was collected vertically from the sample surfaces by a microscope objective and sent through a 0.5 m spectrometer to a charge-coupled-device camera or a time-correlated single-photon counting system (~350 ps resolution) for the time-integrated or time-resolved PL measurements at room temperature. For the time-resolved PL measurements, the collected PL was spectrally selected by the spectrometer

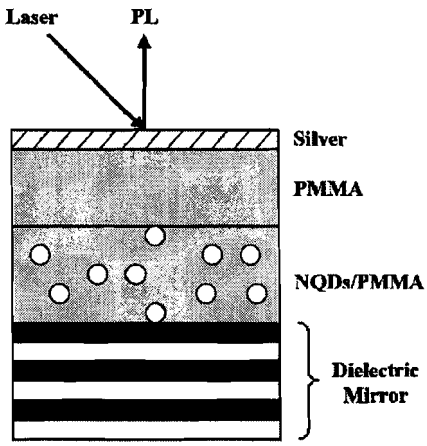

FIG. 1. Schematic diagram of the planar microcavity structure with embedded CdSe/CdS NQDs. The excitation laser beam was focused onto the sample surface at an incident angle of ~45° relative to the surface normal direction while the PL was collected vertically from the sample surface.

[a]Electronic mail: xywang@physics.utexas.edu

Matched ultraslow propagation of highly efficient four-wave mixing in a closely cycled double-ladder system

Yanpeng Zhang,* Andy W. Brown, and Min Xiao†
Department of Physics, University of Arkansas, Fayetteville, Arkansas 72701, USA
(Received 17 February 2006; revised manuscript received 29 September 2006; published 20 November 2006)

We present a fully time dependent, adiabatic solution, and steady-state analysis for the ultraslow propagation of the nondegenerate four-wave mixing (NDFWM) signal and the weak probe beam in a closely-cycled double-ladder system. Under appropriate (especially power balance) conditions, the two-mode probe and phase-matched NDFWM pulses, after a characteristic propagation length, evolve into a pair of amplitude and group velocity matched pulses. Double transparency for the probe and NDFWM beams can be achieved owing to an efficient one- and three-photon destructive interference involving the NDFWM beam and its back reaction to the probe beam. The forward and backward configurations are investigated in this double-ladder system, and their efficiencies are calculated and compared.

DOI: 10.1103/PhysRevA.74.053813 PACS number(s): 42.50.Gy, 32.80.-t, 42.65.Hw

I. INTRODUCTION

Efficiencies of nonlinear optical processes in multilevel atomic systems can be greatly enhanced through light-induced atomic coherence [1–5]. It is clear that the Kerr nonlinear coefficient can be greatly modified and enhanced near electromagnetically induced transparency (EIT) [6,7] resonance in three-level atomic systems [8]. In four-level atomic systems, more energy level configurations can be envisioned, and nonlinear optical processes can be optimized by suppressing linear absorption through EIT (destructive interference) and increasing the nonlinear optical coefficient through constructive interferences in three-photon processes [9–11].

In recent years, there have been many experimental demonstrations and theoretical calculations of enhancing different nonlinear optical processes in various four-level atomic systems. One of these interesting nonlinear optical processes is the nondegenerate four-wave mixing (NDFWM), which normally has high efficiency in closely-cycled multilevel systems such as double-Λ [3,4,12], four-level cascade [13], and double-ladder systems. The distinct features of the double-Λ systems are its symmetry in laser frequencies and near degeneracy between the probe beam and the generated signal beam. For a specially arranged laser beam configuration [two strong pump beams share one lower state, but connect to different excited states, as shown in Fig. 1(a)], both the probe beam and the generated signal beam can satisfy EIT condition simultaneously to minimize linear absorptions, and, at the same time, the NDFWM can have high efficiency. Recent studies have predicted 100% NDFWM efficiency in backward double-Λ configuration [14], but the forward NDFWM efficiency can only reach 25%. Since a near Doppler-free condition can be easily satisfied in such double-Λ system, a hot atomic vapor cell can be used for experimental demonstrations of the predicted effects. However, since the generated frequency is similar to the probe beam frequency (in the near degenerate case), no up-converted beam can be generated. On the other hand, recent theoretical studies on cascade four-level ladder system, as shown in Fig. 1(b), predicted high efficiency (75%) in forward NDFWM and generation of up-converted light beam. Due to the large difference in the generated signal frequency from the probe beam, near Doppler-free configuration is impossible to satisfy in this case, so experiments in this configuration cannot be done in atomic vapors.

Another important issue in such nonlinear optical processes is the pulse matching between the weak probe beam E_1 and the generated signal beam E_f. Since both the probe and signal beams are under EIT conditions, their group ve-

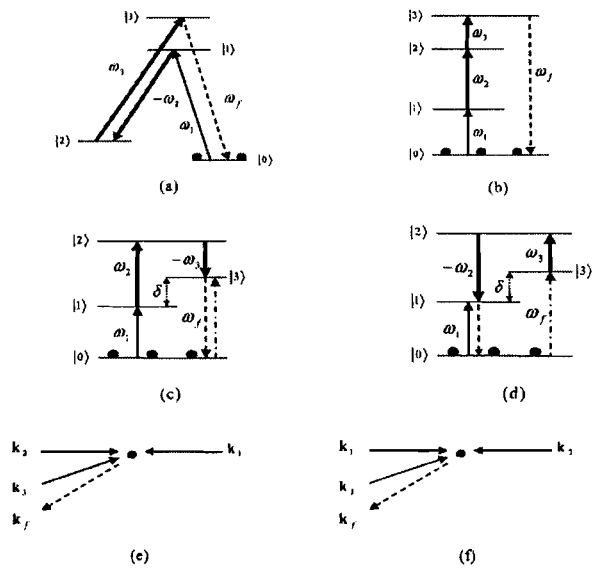

FIG. 1. The closely-cycled four-level systems: double-Λ (a) and four-level cascade (b) systems, double-ladder systems (c) and (d), where δ is the controllable detuning factor; The forward (e) and backward (f) NDFWM schemes. The solid arrows, dashed arrows, and dotted-dashed arrows represent the applied laser field, the emitted NDFWM signal, and the back-reaction of NDFWM, respectively.

*Email address: ypzhang@mail.xjtu.edu.cn
†Email address: mxiao@uark.edu

Optical switching in arrays of quantum dots with dipole-dipole interactions

J. Gea-Banacloche,* Mambwe Mumba, and Min Xiao†
Department of Physics, University of Arkansas, Fayetteville, Arkansas 72701, USA
(Received 6 June 2006; revised manuscript received 29 August 2006; published 26 October 2006)

We explore the possibility of using pairs of quantum dots coupled by the dipole-dipole interaction as effective three- or four-level systems whose transmission for an optical beam at some frequency may be switched on or off using a second optical beam (electromagnetically induced transparency). We conclude that the characteristic interaction strengths and decay rates should allow for a demonstration of this effect in molecular beam epitaxy-grown bilayer InAs/GaAs quantum dot structures.

DOI: 10.1103/PhysRevB.74.165330 PACS number(s): 78.67.Hc, 71.35.Gg, 42.50.Gy

I. INTRODUCTION

There has been recently much interest in the study of systems of pairs of coupled quantum dots,[1–7] where the coupling can be due to either tunneling or the electric dipole interaction between excitons. In quantum wells, it has been shown both theoretically and experimentally that the coupling resulting from tunneling can be used for optical switching,[8] via a mechanism similar to Fano interference. In this paper, we point out that for quantum dots coupled by the dipole interaction[2,9,10] one may obtain effective three- or four-level systems where the techniques of electromagnetically induced transparency (EIT) could also be used for optical switching (see Ref. 5 for a proposal of coherent population transfer, an effect closely related to EIT, in tunneling-coupled quantum dots, and Ref. 11 for a demonstration of EIT in a single quantum well via biexciton coherence; a theoretical treatment of EIT in a single quantum dot may be found in Ref. 12).

In the remainder of this Introduction we discuss the order of magnitude of the expected level splittings and the various level arrangements that may result. In the next section we develop a simple analytical model showing the basic features of the switching scheme, and in the section following that we compare this model with more complete numerical calculations.

The dipole moment of a dot of size a may be taken to be of the order of ea and the dipole-dipole interaction energy between two dots separated by a distance r is then of the order of $e^2a^2/4\pi\epsilon_0 r^3$. As an example, if $a=4$ nm and $r=20$ nm, this energy is of the order of 2.9 meV.

Two mechanisms for dipole-dipole coupling have been discussed in the literature (see Ref. 7 for more details). The first, Förster energy transfer, involves the exchange of a virtual photon between dots separated by a distance smaller than the wavelength of light. This can be represented by a term in the Hamiltonian of the form

$$V_F = \hbar d(|eg\rangle\langle ge| + |ge\rangle\langle eg|), \tag{1}$$

where $|eg\rangle$ ($|ge\rangle$) represents the state in which there is an exciton in the first (second) dot, and $\hbar d$ is a constant of the order of magnitude discussed in the previous paragraph.

The second mechanism involves a direct, static (Coulomb) interaction between the dipole moments of the excited dots, and can be represented by a term in the Hamiltonian of the form

$$V_D = \hbar d'|ee\rangle\langle ee|. \tag{2}$$

The result of this term is to make the energy of the biexciton state $|ee\rangle$ different from just the sum of the single exciton states $|eg\rangle$ and $|ge\rangle$.

As we shall show below, either term (1) or (2) can, under the appropriate circumstances, result in a level structure useful for optical switching. For clarity, we show this first analytically considering each term separately, and the simple (but not very realistic) situation in which the single exciton states are degenerate in the absence of the interaction. In a more realistic scenario, the two dots will have different sizes and the states $|eg\rangle$ and $|ge\rangle$ will not be degenerate even in the absence of the dipole-dipole interaction, but here again the addition of either term (1) or (2) results in a level structure in which optical switching is possible. The main requirement in all these cases is that the strength of the coupling, d or d' (in frequency units) be larger than the level widths γ, as we shall see below analytically, and also numerically explore later.

II. BASIC HAMILTONIAN AND COUPLING APPROACHES

A. Switching for identical dots

We adopt the following basic Hamiltonian, involving the lowering operators $\sigma_i = |g_i\rangle\langle e_i|$, $i=a,b$, for each dot ($|g\rangle$ stands for the ground state and $|e\rangle$ for the excited state), their Hermitian conjugates $\sigma_i^\dagger$, and two external fields represented by the Rabi frequencies Ω_p (for "probe") and Ω_c (for "coupling"), in a suitable interaction picture:

$$H = \frac{\hbar}{2}(\Omega_p e^{-i\Delta_p t} + \Omega_c e^{-i\Delta_c t})(\sigma_a^\dagger + \sigma_b^\dagger) + \text{H.c.} + \hbar d(\sigma_a\sigma_b^\dagger + \sigma_a^\dagger\sigma_b) + \hbar d'|ee\rangle\langle ee|. \tag{3}$$

Here the two dots have been assumed to be identical and to couple identically to the two fields, an assumption that will be relaxed later on. The detunings are therefore defined relative to the energy $\hbar\omega_0$ of the single exciton state(s): $\Delta_p = \omega_p - \omega_0$, $\Delta_c = \omega_c - \omega_0$.

Stochastic resonance in atomic optical bistability

Amitabh Joshi* and Min Xiao†
Department of Physics, University of Arkansas, Fayetteville, Arkansas 72701, USA
(Received 14 December 2005; revised manuscript received 1 March 2006; published 28 July 2006)

Stochastic resonance (SR) is experimentally demonstrated in an atomic optical bistable system consisting of three-level atoms in Λ-type configuration confined in an optical ring cavity. The optical bistable system with enhanced Kerr nonlinearity due to atomic coherence is driven by a periodic signal and a Gaussian white noise source with variable amplitude, and displays an improved output signal-to-noise ratio, a characteristic signature of SR. The measured results match qualitatively with the theoretical predictions of the generic model for the SR phenomenon.

DOI: 10.1103/PhysRevA.74.013817 PACS number(s): 42.65.Pc, 02.50.Ey, 42.50.Gy, 05.40.−a

Stochastic resonance (SR) is a quite general phenomenon appearing in climatic cycles, electronic and magnetic systems, optical systems, and biological and neuronal systems [1,2]. The essence of such interesting SR phenomena in various systems is its seemingly counterintuitive nature, i.e., adding a certain amount of noise to the input of a system can actually increase the output signal-to-noise ratio (SNR) for a signal passing through the nonlinear medium and the optimal improvement occurs at a certain noise strength. Such behavior reveals the basic nature of SR, i.e., noise can induce a resonance like effect in multistate nonlinear systems. In the past two decades, such SR effects were observed in many systems, including a simple electronic circuit, the Schmidt trigger [3], the semiconductor diode laser [4], the bidirectional ring dye laser [5], thermally induced optical bistability in semiconductors [6], and neurophysiological systems [7,8].

The generic model describing the SR phenomenon is given by [1]

$$\dot{x}(t) = -V'(x) + A_0\cos(\Omega t + \phi) + \zeta(t), \tag{1}$$

where $V(x)$ is the reflection-symmetric potential

$$V(x) = -\frac{a}{2}x^2 + \frac{b}{4}x^4. \tag{2}$$

In Eq. (1), A_0 represents the signal amplitude, Ω is the signal frequency, and ϕ is a simple phase factor. $\zeta(t)$ denotes a zero-mean Gaussian white noise with correlation function $\langle\zeta(t)\zeta(0)\rangle = 2D\delta(t)$, where D characterizes the noise amplitude. For an appropriately chosen set of parameters of a and b, the system has a double-well structure describing a standard two-state system. Equation (1) without the noise term is an overdamped, driven anharmonic oscillator with third-order nonlinearity. When a periodic signal is added to the system together with a source of noise, the SNR of the output shows a maximum at a certain noise strength D. This resonance like feature in the SNR as a function of D gives the signature of the SR phenomenon [1,2]. Under specific conditions, the output SNR can exceed the input SNR, which can be very useful in certain applications.

The system with two-level atoms inside an optical resonator can be modeled very well with a double-well potential in certain parametric regions having the well-known atomic optical bistability (AOB) [9]. Although SR behavior has been expected and theoretically studied in simple AOB systems [10], the effect has not been, to the best of our knowledge, observed experimentally in such ideal passive two-state systems. One of the main reasons for it could be the lack of controllability in the potential barrier (width and height) of the double-well potential in two-level AOB systems. In this paper, we present our experimental studies of SR in an atomic bistable system with three-level Λ-type atoms (which exhibit electromagnetically induced transparency) inside an optical ring cavity [11]. Due to the atomic coherence induced by the laser beams in the three-level atomic system, the Kerr nonlinearity of the atomic medium is greatly enhanced [12], which helps to boost the SR effect in this system at lower optical powers. Also, with an additional coupling laser beam, the bistable curve (therefore the potential barrier of the double well) can easily be controlled [11] and optimized for observing such interesting SR phenomena in this AOB system. Both the modulated signal and broadband noise are added onto the cavity input field. To avoid the issue of mechanical stability of the system, we choose to work with a periodic sinusoidal signal of moderate amplitude which has also been well discussed for SR in the literature [13,14].

The experimental setup is outlined in Fig. 1. The energy levels of the D_1 line of ^{87}Rb atoms are employed to form the required three-level system in Λ-type configuration [11] (Fig. 1 bubble). The optical ring cavity consists of three mirrors, two of which (M_1 and M_2) have about 1% and 3% transmissivities, respectively, while the third one (M_3) is almost a perfect reflector and is mounted on a piezoelectric transducer (PZT) in order to tune the cavity length. To provide magnetic shielding, the rubidium vapor cell is wrapped in μ-metal foil and then with a heating tape for controlling the atomic density. The probe laser beam [driving the transition $5S_{1/2}(F=1)\rightarrow 5P_{1/2}(F'=2)$] circulates inside the ring cavity as the cavity field while the coupling beam [driving the transition $5S_{1/2}(F=2)\rightarrow 5P_{1/2}(F'=2)$] is misaligned from the cavity axis slightly (by about a 2° angle) so it does not circulate in the cavity. The coupling and probe lasers are both extended-cavity diode lasers, frequency locked to their respective reference cavities [15]. To set and monitor the frequency detunings of the laser beams from their respective atomic transitions a saturated atomic spectroscopy setup is

*Email address: ajoshi@uark.edu
†Email: address: mxiao@uark.edu

PHYSICAL REVIEW A 73, 051801(R) (2006)

Controlling the polarization rotation of an optical field via asymmetry in electromagnetically induced transparency

Bo Wang,[1] Shujing Li,[1] Jie Ma,[1] Hai Wang,[1,*] K. C. Peng,[1] and Min Xiao[1,2]
[1]*The State Key Laboratory of Quantum Optics and Quantum Optics Devices, Institute of Opto-Electronics, Shanxi University, Taiyuan 030006, People's Republic of China*
[2]*Department of Physics, University of Arkansas, Fayetteville, Arkansas 72701, USA*
(Received 11 November 2005; revised manuscript received 10 March 2006; published 3 May 2006)

We propose and experimentally demonstrate a mechanism to achieve coherent control of the polarization rotation of an optical field in a multilevel electromagnetically induced transparency (EIT) system in rubidium atoms. By choosing a properly polarized coupling field and transition energy levels, the symmetry of the atomic medium to the propagation of two orthogonal polarization components of a weak linearly polarized probe field can be broken, which leads to a coherently controlled rotation of the probe field polarization. This mechanism of coherently controlled optical polarization rotation makes use of asymmetry in EIT subsystems for the two circular polarization components of the probe beam with a contribution from different transition strengths (due to different Clebsh-Gordan coefficients) in this multilevel atomic system.

DOI: 10.1103/PhysRevA.73.051801 PACS number(s): 42.50.Gy, 33.55.Ad, 42.25.Ja

A linearly polarized light beam will experience a polarization rotation when passing through a chiral medium. The chirality of the medium can be caused by either the intrinsic helicity of the molecules in the medium (called optical activity) or induced by external electrical or magnetic fields. For example, when a magnetic field is applied along the direction of the light beam propagation in an atomic medium, the asymmetry in Zeeman level splittings of the atoms will produce a polarization rotation for the linearly polarized light beam, which is the well-known Faraday effect. Optical fields can also induce chirality in an atomic medium through optical pumping [1], resonant two-photon dispersion [2], magneto-optical effects [3,4], self-induced birefringence [5], etc. In the past few years, several groups had experimentally demonstrated optical birefringence by using a circularly polarized laser beam to change the polarization rotation of a weak linearly polarized probe beam in multilevel ladder-type atomic systems [6–8]. In these experiments, the asymmetry for the two circularly polarized components (σ^+ and σ^-) of the probe beam, therefore the optical birefringence, is generated by the circularly polarized coupling laser beam in the ladder configuration connecting to only one of the two probe circular polarization components. In this situation, strong circular dichroism always exists, which is the major limitation of such experimental systems. Also, control and enhancement of magneto-optical polarization rotation of a laser beam by another coupling laser beam [9] and electromagnetically induced magnetochiral anisotropy in a resonant medium [10] have been proposed, and the latter effect was experimentally demonstrated recently [11].

In this paper, we propose and experimentally demonstrate a system to achieve large optical polarization rotation (up to 45°) of a linearly polarized probe beam controlled by a coupling laser beam under the condition of electromagnetically induced transparency (EIT) in a Λ-type configuration [12,13]. The relevant atomic levels of ^{87}Rb atoms are shown in Fig. 1. We denote Zeeman sublevels of $5S_{1/2}$, $F=1$ as $|a_i\rangle$ ($i=1,2,3$ for $m=-1,0,+1$), of $5S_{1/2}$, $F=2$ as $|b_j\rangle$ ($j=1-5$ for $m=-2,-1,0,+1,+2$), and of $5P_{1/2}$, $F'=2$ as $|c_k\rangle$ ($k=1-5$ for $m=-2,-1,0,+1,+2$), respectively. When both the probe and coupling laser beams are linearly polarized, this system is completely symmetric to the two circular polarization components of the probe beam for realizing EIT as demonstrated in Ref. [13]. We choose the coupling beam (with frequency ω_c) to be a left-circularly polarized (σ^-) beam driving the $|b_{j+1}\rangle$ to $|c_j\rangle$ transitions. The probe beam (with frequency ω_p) is a linearly polarized laser beam consisting of two circularly polarized components σ^- and σ^+, which are near resonant with transitions between levels $|a_i\rangle$ and $|c_k\rangle$. We can clearly see that the left-circularly polarized coupling beam (E_c^-) and the left-circularly polarized probe beam (E_p^-) form three simple Λ-type EIT systems, while E_c^- and the right-circularly polarized probe beam (E_p^+) form only two simple Λ-type EIT systems. This asymmetry in the EIT subsystems for the two circular probe beam components is the key for causing the chirality in this special atomic system. The major advantages of this scheme, compared to the previously demonstrated schemes [6–8], include relative low

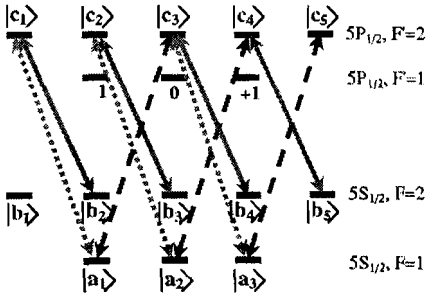

FIG. 1. (Color online) Relevant energy diagram of the D1 line in a ^{87}Rb atom. Solid lines: transitions for the left-circularly polarized coupling beam; dotted lines: transitions for the left-circularly polarized probe beam; dashed lines: transitions for the right-circularly polarized probe beam

*Corresponding author; e-mail address: wanghai@sxu.edu.cn

Three-qubit quantum-gate operation in a cavity QED system

Amitabh Joshi* and Min Xiao†
Department of Physics, University of Arkansas, Fayetteville, Arkansas 72701, USA
(Received 21 June 2006; published 13 November 2006)

A scheme is proposed to obtain three-qubit gates, such as quantum-phase gate and C^2-NOT gate operations, in a cavity QED system where highly detuned cavity-field modes interact with a four-level system in an inverted-Y configuration. The influence of the Stark shift is also included in such proposed gate operations. Since only the metastable lower levels are involved in the gate operations, the gates are not affected by the atomic decay rates. The potential application of such gates to realize Grover's algorithm is also discussed.

DOI: 10.1103/PhysRevA.74.052318 PACS number(s): 03.67.Lx, 42.65.−k, 42.50.Gy

I. INTRODUCTION

In the last decade, considerable progress has been made in quantum computing, which relies on the quantum-information processing, quantum-computing networking, etc., using various physical systems [1]. It is well known that a quantum-computing network can be partitioned into a sequence of one-qubit rotation and two-qubit gates [2]. There are a large number of theoretical proposals for two-qubit gate operations and some experiments have been carried out to implement CNOT (controlled-NOT) gates or controlled phase gates in ion trap [3], cavity-QED system [4], NMR [5], quantum dots [6], and superconducting charge qubits [7].

Multiqubit-controlled quantum gates are very useful in the construction of quantum-computing networks, implementing quantum-error-correction protocols and quantum algorithms. Important steps in the direction of realizing multiqubit gates have been recently made in several physical schemes. There are proposals to implement three-qubit Toffoli gates with neutral atoms in an optical lattice [8] and hybrid atom-photon qubit via a cavity-QED system [9]. In another interesting work the implementation of a multiqubit unitary gate using adiabatic passage with a single-mode optical cavity has been proposed [10]. Experimental realization of a controlled phase gate in a three-qubit NMR system was reported [11]. Very recently, a n-qubit-controlled phase gate with superconducting quantum-interference devices coupled to a resonator was also proposed [12].

In this work we propose a way to realize a three-qubit-controlled phase gate and a C^2-NOT (controlled-NOT gates with two controlling bits) gate in a cavity-QED system where a four-level atom in inverted-Y configuration interacts with three cavity-field modes. The cavity modes are considered to be highly detuned from the corresponding one-photon transitions. The Stark shifts are incorporated in this model. This system can be used to realize a number of three-qubit logic operations such as controlled quantum-phase gate and C^2-NOT gate. In this scheme, the gate operation takes place in the lower states of the system and hence the effect of decoherence due to radiative damping is minimized in this system.

*Email address: ajoshi@uark.edu
†Email address: mxiao@uark.edu

The rest of the paper is organized as follows. In Sec. II, we give the physical model with a theoretical description where a four-level system in inverted-Y configuration interacts with the three quantized cavity-field modes. Section III is devoted to a description of the implementations of a three-qubit quantum-phase gate and C^2-NOT gate. The application of these three-qubit quantum gates to Grover's algorithm is discussed in Sec. IV. Some concluding remarks are given in Sec. V.

II. MODEL

We consider a closed four-level atomic system in inverted-Y configuration, as shown in Fig. 1, which can be easily realized in a rubidium atom [13]. Essentially, this is a double-electromagnetically induced transparency (double-EIT) system [14] and many interesting results have been predicted for this system, such as vacuum Rabi splitting [15] and generalized dark-state polariton [16], etc. Levels $|g\rangle$, $|e\rangle$, and $|d\rangle$ form a three-level ladder-type configuration and levels $|l\rangle$, $|e\rangle$, and $|g\rangle$ form a three-level Λ-type configuration. So, the composite system consists of two subsystems, i.e., one ladder-type three-level system, and another Λ-type three-level system and hence exhibits double-EIT characteristics [14]. The transitions $|g\rangle$ to $|e\rangle$, $|l\rangle$ to $|e\rangle$, and $|e\rangle$ to $|d\rangle$ interact

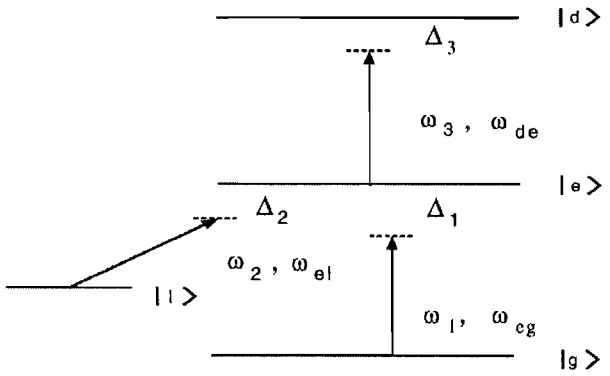

FIG. 1. Schematic diagram of a four-level atomic system in inverted-Y configuration. Here, ω_1, ω_2, and ω_3 are frequencies of probe, coupling, and pumping fields, respectively. The parameters Δ_1, Δ_2, and Δ_3 are corresponding frequency detuning of these field frequencies from the respective atomic transition frequencies.

Chaos in an Electromagnetically Induced Transparent Medium Inside an Optical Cavity

Wenge Yang, Amitabh Joshi, and Min Xiao*

Department of Physics, University of Arkansas, Fayetteville, Arkansas 72701, USA

(Received 22 March 2005; published 25 August 2005)

We theoretically predict and experimentally demonstrate chaotic behaviors in a system comprising of three-level atoms inside an optical ring cavity. This electromagnetically induced transparency (EIT) system is driven to chaos through period-doubling route by reducing the frequency detuning of the coupling laser beam. The chaos occurs in a different parametric regime as previously predicted and is believed to be caused by the enhanced dispersion and nonlinearity due to induced atomic coherence in such EIT system.

DOI: 10.1103/PhysRevLett.95.093902 PACS numbers: 42.65.Sf, 42.50.Gy

Dynamic behaviors, such as instability and chaos, in atomic optical bistability (AOB) systems were studied extensively more than 20 years ago [1]. Although dynamic instability and chaos were both theoretically predicted to exist in two-level AOB systems [2], and despite that dynamic instability was experimentally observed in many two-level atomic and molecular systems [1,3], the predicted chaotic behaviors and routes to chaos have not really been observed in AOB systems, except in a degenerate atomic system with strong radiation trapping [4]. One of the reasons for not observing such predicted period doubling to chaos in AOB systems was attributed to washing out of such behavior by the longitudinal and radial variations of electric field in the cavity [5]. On the other hand, chaotic behaviors were experimentally investigated and well studied in various laser systems [1,6] and in a hybrid optical bistable system [7] many years ago. In recent years, chaotic behaviors were shown to be controllable by employing various feedback mechanisms [8].

Chaos is one of the most fascinating phenomena in nature and therefore, understanding it not only has fundamental interests, but also will have great impact for applications, such as encryption in communications [9] and maintaining normal cardiac function [10]. In this Letter, we present our experimental and theoretical investigations of this "old problem," i.e., chaos in an AOB system. By using three-level atoms with electromagnetically induced transparency (EIT) inside an optical ring cavity [11], we show that chaos can be reached via period-doubling route in certain parametric regime. By controlling one experimental parameter, such as frequency detuning of the coupling laser in the EIT, the cavity output field can be driven from self-pulsing to period doubling, and then to chaos. We believe that the enhanced linear and nonlinear dispersions around EIT resonance in such a three-level atomic system [12] are the key reasons for such observed chaotic behavior, as for the case predicted in a three-level optically pumped laser system [13]. Such mechanism of generating chaos is absent in two-level AOB systems. A theoretical model with coupled density-matrix equations for a three-level EIT system, together with field equation [14], can be used to study such chaotic behavior and the simulated results match quite well with the experimentally observed phenomenon of route to chaos through period doubling. This model is beyond the usual Lorentz model used to study chaos in two-level atomic systems and lasers, but is still under single-mode mean-field approximation. The ability of manipulating chaotic behavior with an additional coupling field is very important in understanding the route to chaos and eventually in controlling such chaotic behavior in this system.

We consider a system with N three-level Λ-type atoms inside an optical ring cavity as shown in the bubble of Fig. 1. A coupling laser of frequency ω_c near the ω_{23} resonance couples levels $|2\rangle$ and $|3\rangle$, while a probe beam with frequency ω_p near the ω_{21} resonance couples levels $|2\rangle$ and $|1\rangle$. The equations of motion controlling the density-matrix elements and the cavity field under rotating-wave approximation are [14]:

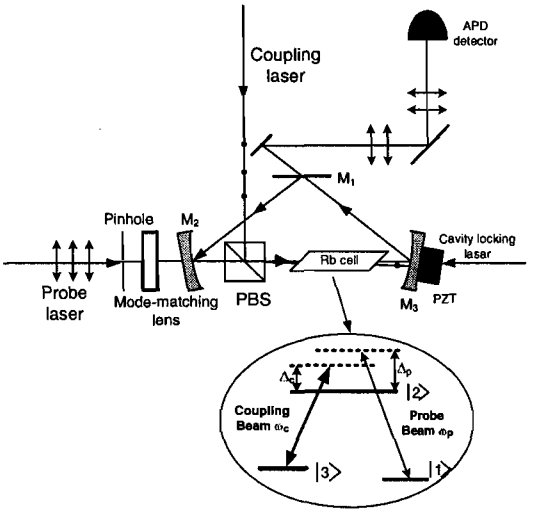

FIG. 1. Experimental setup. PBS, polarizing cubic beam splitters; $M1$–$M3$, cavity mirrors; APD, avalanche photodiode detector; PZT, piezo-electric transducer. Bubble: a three-level Λ-type atomic system.

Controlled release of stored optical pulses in an atomic ensemble into two separate photonic channels

Bo Wang,[1] Shujing Li,[1] Haibin Wu,[1] Hong Chang,[1] Hai Wang,[1,*] and Min Xiao[1,2]
[1]*The State Key Laboratory of Quantum Optics and Quantum Optics Devices, Institute of Opto-Electronics, Shanxi University, Taiyuan, 030006, People's Republic of China*
[2]*Department of physics, University of Arkansas, Fayetteville, Arkansas 72701, USA*
(Received 24 January 2005; published 4 October 2005)

We report an experiment in which optical pulses stored in an atomic system can be controllably released into two different photonic channels. By controllably turning on the retrieve control pulses at either 795 or 780 nm to read the stored optical pulses in a four-level double Λ-type atomic medium, we can obtain the released probe pulse at 795 or 780 nm, respectively. These readout pulses can be further separated spatially and directed into different optical propagation channels through a grating. Such controlled release of stored optical pulses may extend the capabilities of the quantum information storage technique, and can have applications in multichannel all-optical switching, all-optical routing, quantum information processing, and image storage systems.

DOI: 10.1103/PhysRevA.72.043801 PACS number(s): 42.50.Gy, 03.67.Hk

In the past few years, storing and releasing photon states in an atomic ensemble by using the effect of electromagnetically induced transparency (EIT) [1] have been proposed theoretically [2] and demonstrated experimentally [3,4]. Subsequent experimental works, such as transporting and time reversing light via atomic coherence [5], observing phase coherence of stored photonic information [6], atomic memory for correlated photon states [7,8], and storing light of arbitrary polarization in atoms [9], have been carried out in the laboratories. Some interesting theoretical schemes, such as the storage and retrieval of light pulses at moderate powers [10], manipulating the retrieval of stored light pulses [11], storing of a pair of pulses of light [12], controlled light storage in a double lambda system [13], and dividing photon memory into two channels in four-level double-EIT systems [14], have also been proposed. These researches have provided good understanding of the physical mechanisms for light storage in coherent atomic assembles.

The light storage experiments were generally carried out in three-level Λ-type atomic systems coupled by two laser beams. As the control light is adiabatically turned off when the probe pulse is in the atomic medium under EIT condition, the state of the probe pulse is mapped into purely atomic spin coherence between the pair of ground states [3,4]. Such photon storage mechanism allows one to transfer optical information between light fields at two different wavelengths by using a four-level double Λ-type atomic system as a storage medium [5,13]. Here, we report an experiment in which we can controllably release the stored light pulse in the atomic medium into the desired one of the two photonic channels in a four-level double Λ-type system, as shown in Fig. 1(a), in a rubidium atomic vapor cell filled with Ne buffer gas.

The present work can be understood qualitatively by considering a four-level double Λ-type configuration of atomic system [as shown in Fig. 1(a)] coupled by a probe field

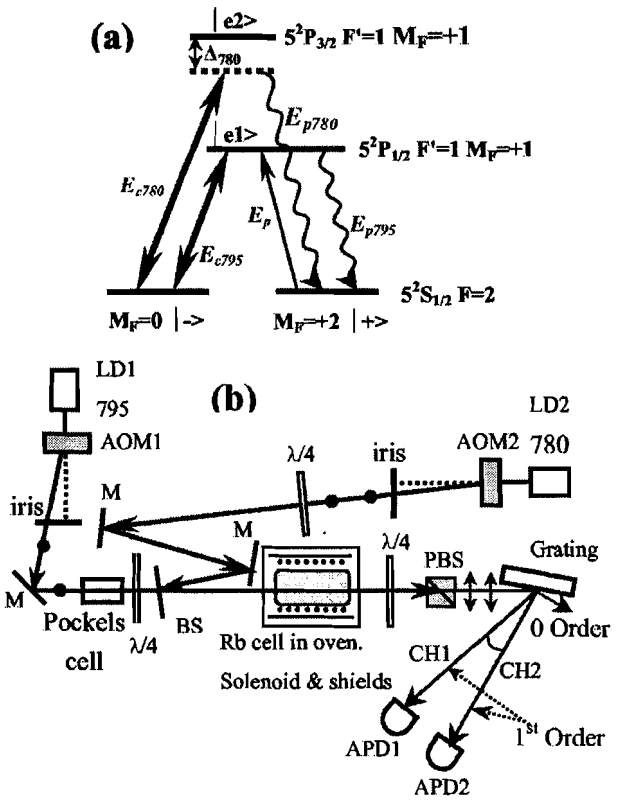

FIG. 1. (Color online) (a) Diagram of the four-level double Λ-type system in ^{87}Rb atom. E_p: the input probe laser; E_{p795} and E_{p780}: the revived probe photons at 795 and 780 nm, respectively; E_{c780} and E_{c795}: the control lasers at 795 and 780 nm, respectively. (b) Schematic of the experimental setup. LD1 and LD2 are extended-cavity diode lasers working at 795 and 780 nm, respectively; AOM1 and AOM2: acousto-optical modulators; M: high reflective mirror; BS: beam splitter; λ/4: quarter-wave plate; PBS: polarizing beam splitter; APD1 and APD2: avalanche photodiode detectors.

*Email address: wanghai@sxu.edu.cn

APPLIED PHYSICS LETTERS 86, 063102 (2005)

Interdot carrier transfer in asymmetric bilayer InAs/GaAs quantum dot structures

Yu. I. Mazur,[a] Zh. M. Wang, G. G. Tarasov,[b] Min Xiao, and G. J. Salamo
Department of Physics, University of Arkansas, Fayetteville, Arkansas 72701

J. W. Tomm and V. Talalaev
Max-Born-Institut für Nichtlineare Optik und Kurzzeitspektroskopie, Max-Born-Strasse 2A, 12489 Berlin, Germany

H. Kissel
Ferdinand-Braun-Institut für Höchstfrequenztechnik, Albert-Einstein-Strasse 11, 12489 Berlin, Germany

(Received 17 September 2004; accepted 7 December 2004; published online 1 February 2005)

Transient photoluminescence from a series of asymmetric InAs quantum-dot bilayers with a GaAs barrier layer thickness varying from 30 to 60 monolayers between the quantum-dot planes is investigated. The interdot carrier transfer process is analyzed. In the framework of a three-level system, interdot carrier transfer times between 200 and 2500 ps are derived and compared with similar data from the literature. Within the semiclassical Wentzel–Kramers–Brillouin approximation, the observed "transfer time-barrier thickness-relation" supports nonresonant tunneling as the microscopic carrier transfer mechanism. © *2005 American Institute of Physics*. [DOI: 10.1063/1.1861980]

Semiconductor quantum dots (QDs) are a promising material for various optoelectronic applications.[1] For many practical purposes, such as semiconductor lasers and infrared detectors, three-dimensional QD arrays are needed in order to achieve significant interaction between the optical field and carriers confined within the QDs.[2] As a result, both lateral *transport* of nonequilibrium carriers within one layer of QDs as well as vertical transport between QD layers is expected to play a significant role in device performance. In previous studies, we have addressed *lateral* carrier transfer, i.e., the transport of carriers within one QD plane. For this purpose we studied QD structures with a bimodal size distribution and monitored their transient population, in particular the population of larger-sized dots by carriers from smaller-sized QDs, by means of time-resolved photoluminescence (PL).[3,4]

The present study is devoted to the *vertical* transfer of carriers, i.e., the transport of carriers between two neighboring QD layers along the growth direction. That is, in analogy to our previous work on lateral transport, we report on the transient population of a structure consisting of two QD layers separated by a spacer layer, similar to the structure used in Refs. 5 and 6. By using different InAs deposition rates, growth temperatures, or annealing times for the specific layers, vertically stacked QD layers with differently sized dots, but uniform size distribution in each layer, have been achieved.[7–13] In this case, the spacer thickness between the QD layers represents a very important parameter. In this letter, the population of larger-sized dots (LQD) affected by carriers from smaller-sized dots (SQD) is monitored and transient PL is used as the main tool for the visualization of this inter-QD carrier transfer. In particular, the investigation of a series of asymmetric QD bilayers with barriers of different thicknesses separating the QD layers allows the identification of the nature of the interdot carrier transfer process as nonresonant tunneling.

The samples studied here are grown using a solid-source molecular beam epitaxy system coupled to an ultrahigh vacuum scanning tunneling microscope (STM). The structures consist of two InAs layers grown on a GaAs(001) substrate, followed by a 0.5 μm GaAs buffer layer. 10 min of annealing at 580 °C provides a nearly defect-free atomically flat surface. The seed, or first QD layer, is fabricated by depositing 1.8 monolayers (ML) of InAs with a growth rate of 0.1 ML/s under an As_4 partial pressure of 8×10^{-6} Torr at a substrate temperature of 500 °C. GaAs spacer layer (d_{sp}) of 30, 40, 50, or 60 ML was deposited on top of the seed QD layer for each sample, respectively. The second QD layer is then added by deposition of 2.4 ML InAs followed by a 150 ML GaAs cap layer. Structural characterizations are accomplished by plan-view STM and cross-sectional transmission electron microscopy (XTEM). In the seed layer we find a size distribution of (4 ± 1.5) nm for the height, (20 ± 3) nm for the width, and a dot density of about 4.5×10^{10} cm^{-2}. The QD density in the second layer changes over the range of $(2.5–4)\times10^{10}$ cm^{-2} depending on the value of d_{sp}. The QDs in the second layer are found to have nearly twice the volume of the seed QDs (for $d_{sp}=30$ ML). This is due to additional deposition as well as to the influence of the strain field from the seed layer.[5,10,11] Thus, we obtain two vertically correlated QD layers with different sized dots in each layer. Such a system has been called an "asymmetric QD pair" (AQDP) in analogy with extensive work on an *asymmetric* double quantum-well (ADQW) system.[5] Naturally, the number of QDs in the seed layer participating in the creation of AQDPs must be strongly dependent on the d_{sp}. Our XTEM statistical analysis proves this dependence of the AQDP fraction (the correlation degree α) on the d_{sp} value: α=0.95, 0.70, 0.50, and 0.10 for the d_{sp}=30, 40, 50, and 60 ML, respectively. A single layer 1.8 ML QD sample is fabricated as well and analyzed as a reference.

[a]Electronic mail: ymazur@uark.edu
[b]On leave from Institute of Semiconductor Physics, National Acad. of Sci. of Ukraine, prospect Nauki 45, 03028 Kiev, Ukraine.

Dynamical hysteresis in a three-level atomic system

Amitabh Joshi, Wenge Yang, and Min Xiao

Department of Physics, University of Arkansas, Fayetteville, Arkansas 72701

Received October 4, 2004

We have experimentally investigated dynamical hysteresis behavior by changing the sweeping frequency of the cavity input field in the optical bistability of rubidium atoms (in a three-level Λ-type configuration) inside an optical cavity. The shape, width (or area), and direction of the hysteresis cycle are sensitive functions of the sweeping frequency for such an optical bistable system. © 2005 Optical Society of America

OCIS codes: 270.0270, 270.1670, 190.1450.

Hysteresis cycles (HCs) exist in magnetic, optical, electronic, mechanical, chemical, and biological systems. This phenomenon not only is of fundamental and mathematical interest but also can be important in some applications such as all-optical switches and memory devices. Optical bistability (OB) has been studied extensively in two-level alkali atoms within optical resonators.[1,2] OB was further explored in three-level atomic systems, in which multistable and unstable behaviors were observed.[3,4] For OB in an input–output field intensity plot for atomic or semiconductor systems, the HC is observed normally when the cavity input field is scanned adiabatically.[5,6] The HC can have a nonzero area even within the limit of zero sweeping rate of the input field; we then say that such a system exhibits a static HC. When the amplitude of the cavity input field is varied slowly but not quite adiabatically, with a sweeping frequency Ω, the shape and area of the HC can have significant changes, which yield a dynamical HC.[7,8] Such a dynamical HC is due to the nonadiabatic variation of the input field, which causes a delay in transition to the upper state of the HC. The extra area (known as a dynamical hysteresis area) acquired in the hysteresis loop is due to the instability of the system. The static hysteresis features of OB have been well established, but dynamical hysteresis is still a field of continuing investigation because of some unresolved issues. Dynamical hysteresis is important in several physical situations. For example, in magnetic and optical switching devices, areas of such HCs provide power dissipation by repetitive switching at a frequency Ω. It has been shown by a one-dimensional theory of dynamical hysteresis in experiments with bistable semiconductor lasers[7,9] that the shift of switching points and the area of the HC scale as two-thirds power of the switching frequency. Recently a dynamical HC was demonstrated in warm Rb vapor by use of resonantly enhanced Raman generation without an optical cavity.[10] Here we experimentally investigate the dynamical HC of an OB system that comprises rubidium atomic vapor in a three-level Λ-type configuration contained inside an optical ring cavity with a much wider range of sweeping frequency (Ω). This experimental system exhibits electromagnetically induced transparency (EIT) and can have enhanced nonlinearity even at low light intensities.[11]

Analytical calculations of the dynamical HC by use of a switched bistable system have been reported in the literature.[7,8] Such a system is described by a particle in a quartic double-well potential with a periodic driving force whose dynamical equation is given by

$$\frac{dx}{dt} = ax - bx^3 + G(t), \tag{1}$$

where a and b are constants and control parameter $G(t)=E\sin(\Omega t)$. Also, E is chosen to be large enough that the system is repeatedly going past the turning points. A physical justification of Eq. (1) has been provided by the longitudinal mode bistability of a semiconductor laser in terms of quartic potential.[12] Another physical justification of Eq. (1) has been given for a nonlinear polarization model that describes dispersive bistability.[13] Parameters a and b are identified as cavity frequency detuning and third-order nonlinear dispersion parameters, respectively.[13] In the EIT system considered here the third-order nonlinear dispersion or parameter b is given by the following expression[11]:

$$b = \mathrm{Re}\left[\frac{-iN|\mu_{21}|^4}{3\hbar^3}\frac{F+F^*}{(2\gamma+\gamma_{21})F|F|^2}\right], \tag{2}$$

where $\gamma=(\gamma_{21}+\gamma_{23}+\gamma_{31})/2$. γ_{21} and γ_{23} are the spontaneous decay rates of excited state $|2\rangle$ to ground states $|1\rangle$ and $|3\rangle$, respectively; γ_{31} is the nonradiative decay rate between the two ground states [Fig. 1(a)]; N is the atomic number density; μ_{21} is the transition matrix element between states $|1\rangle$ and $|2\rangle$; $F=\gamma-i\Delta_P+(|\Omega_C|^2/4)/[\gamma_{31}-i(\Delta_P-\Delta_C)]$; Ω_C is the Rabi frequency associated with the coupling laser field; and $\Delta_P=\omega_P-\omega_{12}$ and $\Delta_C=\omega_C-\omega_{32}$ are the probe and the coupling laser frequency detunings, respectively. According to Ref. 7, the area of the dynamical HC obeys the scaling law $A(\Omega)-A(0)\propto\Omega^{2/3}$ within the limit of $\Omega\to 0$, where $A(0)$ is the area of the static hysteresis loop. This prediction fits well the experimental measurements of the bistable semiconductor laser system.[9] In Ref. 8 a general scaling law for the area of a dynamical HC is given for small Ω as $A(\Omega)\sim\Omega^{\beta}$, such that the exponent $\beta\to 1$ as $\Omega\to 0$ but otherwise $\beta<1$. The

0146-9592/05/080905-3/$15.00

Journal of Modern Optics
Vol. 52, No. 16, 10 November 2005, 2365–2371

Taylor & Francis
Taylor & Francis Group

Frequency detuning and power dependence of reflection from an electromagnetically induced absorption grating

ANDY W. BROWN and MIN XIAO*
Department of Physics, University of Arkansas,
Fayetteville, Arkansas 72701, USA

(*Received 15 February 2005; in final form 31 March 2005*)

When the strong-coupling laser beam is replaced by a standing wave under conditions of electromagnetically induced transparency (EIT) in a three-level atomic vapour, an electromagnetically induced absorption grating is formed. The weak probe beam in this EIT system is partially reflected by this absorption grating under certain conditions. The dependences of reflection signals on frequency detuning and coupling laser power are presented.

1. Introduction

An electromagnetically induced absorption grating (EIG) [1] is created in a three-level system when a weak probe beam and a strong-coupling standing wave satisfy the conditions for electromagnetically induced transparency (EIT) [2, 3]. The probe beam is partially reflected owing to spatially modulated absorption regions, where transparency occurs at the peaks of the standing-wave field and absorption is high at the nodes. The EIG transmission behaviour is also significantly different from that of the typical EIT configuration [4, 5]. For example, when the coupling standing wave is detuned from resonance, the transmission behaviour as a function of probe detuning resembles the superposition of the transmission resulting from the separate forward- and backward-propagating components of the standing wave. However, the transmission is significantly reduced at probe resonance for certain three-level systems when the coupling standing wave is on resonance, in contrast with the typical EIT situation where the probe field interacts with one travelling-wave coupling field [2].

While the transmission behaviour of a weak probe beam in a three-level atomic vapour system under the influence of a strong laser standing wave was studied theoretically many years ago [5], reflection was not investigated at that time. Diffraction of the probe laser beam due to EIG was theoretically predicted [1] and then experimentally demonstrated [6, 7] in cold three-level atomic systems. It has been demonstrated that EIG in a three-level EIT system can be used in the

*Corresponding author. Email: mxiao@uark.edu

Journal of Modern Optics
ISSN 0950–0340 print/ISSN 1362–3044 online © 2005 Taylor & Francis
http://www.tandf.co.uk/journals
DOI: 10.1080/09500340500275314

NANO LETTERS

2005
Vol. 5, No. 10
1873−1877

Photoluminescence Intermittency of InGaAs/GaAs Quantum Dots Confined in a Planar Microcavity

X. Y. Wang,[†] W. Q. Ma,[‡] J. Y. Zhang,[‡] G. J. Salamo,[‡] Min Xiao,[‡] and C. K. Shih*,[†]

Department of Physics, The University of Texas at Austin, Austin, Texas 78712, and Department of Physics, University of Arkansas, Fayetteville, Arkansas 72701

Received June 2, 2005; Revised Manuscript Received August 9, 2005

ABSTRACT

Photoluminescence intermittency, or "blinking", was observed in semiconductor InGaAs/GaAs quantum dots (QDs) inside a planar microcavity. Most of the blinking QDs were found around defect sites such as dislocation lines naturally formed in the GaAs barrier layers, and the carrier traps responsible for blinking had an excitation threshold of ~1.53 eV. The blinking properties of epitaxial QDs and colloidal nanocrystal QDs were also compared by performing laser intensity dependent measurements and statistics of the "on" and "off" time distributions.

Semiconductor quantum dots (QDs) have attracted a lot of interest recently for both their fundamental physics and potential applications ranging from quantum information science to optoelectronic devices. The spontaneous emission of QDs can be greatly affected by their local environment. For example, photoluminescence (PL) intermittency, or "blinking", has been universally observed in colloidal nanocrystal QDs (NQDs) and is attributed to the ionization and neutralization processes sequentially happening under the influence of trapped carriers.[1] Compared with colloidal NQDs, epitaxially grown semiconductor QDs using molecular beam epitaxy (MBE) or metalorganic vapor phase epitaxy (MOVPE) are robust against blinking due to their more ideal interfaces with surrounding materials. So far, from the limited reports in the literature, most of the blinking properties of epitaxial QDs, such as the necessary presence of nearby carrier traps,[2−4] have been consistent with the models established for colloidal NQDs. However, blinking studies of epitaxial QDs have also made some new discoveries that are helping to set up a unifying picture for the blinking mechanisms of both colloidal NQDs and epitaxial QDs. In colloidal NQDs, it is still debated whether the carrier traps are located on the NQD surface or in the surrounding matrix. It was recently shown in epitaxial InP/GaInP QDs that in many cases blinking QDs were near artificial scratches on the sample surface,[3] thus directly specifying the physical locations of those carrier traps.

In this paper, we report optical studies of the blinking behaviors of epitaxial InGaAs/GaAs QDs inside a planar microcavity where the density of *observable* QDs was greatly reduced by the coupling between the QDs and the cavity modes. Most of the blinking QDs were observed to be around defect sites such as dislocation lines naturally formed in the GaAs barrier layers during the sample growth process, while the carrier traps responsible for blinking have energy levels below ~1.53 eV. Laser intensity dependent measurements and statistics of the "on" and "off" time distributions were also performed to compare the blinking properties of epitaxial QDs and colloidal NQDs.

The microcavity sample containing InGaAs/GaAs QDs was fabricated using MBE on a semi-insulating GaAs (100) substrate (see Figure 1a). After the native oxide was desorbed at 580 °C in an As atmosphere, the temperature was increased to 600 °C for the growth of a 5000 Å GaAs buffer layer. This was followed by the bottom distributed Bragg reflector (DBR) consisting of an 18-period AlAs (770 Å)/GaAs (644 Å) multilayer structure. Another GaAs layer of 5383 Å was then grown, and the temperature was reduced to 540 °C in 2 min for the subsequent growth of GaAs(200 Å)/$In_{0.35}Ga_{0.65}As$(30 Å)/GaAs(170 Å)/$In_{0.35}Ga_{0.65}As$(30 Å)/GaAs-(170 Å)/$In_{0.35}Ga_{0.65}As$(30 Å)/GaAs (6228 Å) and the top DBR consisting of an 11-period AlAs(770 Å)/GaAs(644 Å) multilayer structure. During the growth of the three $In_{0.35}Ga_{0.65}As$ (30 Å) QD layers, after every deposition of an $In_{0.35}Ga_{0.65}As$ layer, 3 monolayers (MLs) of GaAs were deposited without interruption to suppress the In segregation. Then after 10 s of interruption, the rest of the GaAs layer was grown. For the whole structure, an As_4/Ga beam equivalent pressure ratio of 15 was maintained and the growth rate of both GaAs and AlAs was 1 ML/s. For comparison, a reference sample was also grown using the same procedures as described above except without the top and bottom DBRs.

* Corresponding author: shih@physics.utexas.edu.
[†] The University of Texas at Austin.
[‡] University of Arkansas.

10.1021/nl051026x CCC: $30.25
Published on Web 09/02/2005

Available online at www.sciencedirect.com
SCIENCE DIRECT®
Optics Communications 254 (2005) 215–222
OPTICS COMMUNICATIONS
www.elsevier.com/locate/optcom

Optimization of an erbium-doped fiber amplifier with radial effects

Cheng Cheng [a,b,*], Min Xiao [b]

[a] Department of Applied Physics, Zhejiang University of Technology, Xiaoheshan, Hangzhou 310023, China
[b] Department of Physics, University of Arkansas, AR 72701, USA

Received 30 December 2004; received in revised form 13 April 2005; accepted 25 May 2005

Abstract

Applying an inversing method and a genetic algorithm, two radial distributions, i.e., a core graded-index and erbium-doped concentration, are optimized for an erbium-doped fiber amplifier (EDFA) in a two-level model under single-mode condition and weakly guided approximations. There is evidence to show that the core graded-index has obvious influence on the gain bandwidth of the EDFA, and similarly, the radial distribution of the erbium concentration has effect on the bandwidth, while no effect on the gain. As an example, we provide an optimized single-fiber EDFA with the graded-index and the erbium concentration distribution, which is characterized with a 33.5 dB gain, a 30 nm bandwidth, and a noise figure of 3.55 dB. The broader bandwidth is one of the outstanding advantages over current single-fiber EDFAs with uniform radial distributions.

PACS: 42.60.Da; 42.55.Wd

Keywords: Erbium-doped fiber amplifier; Radial effect; Optimization; Gain; Bandwidth

1. Introduction

Erbium-doped fiber amplifiers (EDFAs), as key components in wavelength division multiplexing (WDM) systems in optical telecommunication, have received great attention over the past 10 years. The rapid growth and the future commercial importance of multi-wavelength optical networking create strong incentives for the development of EDFAs with higher gain and broader bandwidth. Many interesting research results were reported in recent years. For example, Chernyak and Qian [1] established modeling high-concentration L-band EDFA at high optical powers based

* Corresponding author. Tel.: +86 571 8529 0305/0306; fax: +86 571 8539 3550.
E-mail address: chengch@zjut.edu.cn (C. Cheng).

0030-4018/$ - see front matter © 2005 Elsevier B.V. All rights reserved.
doi:10.1016/j.optcom.2005.05.049

All-optical switching and routing based on an electromagnetically induced absorption grating

Andy W. Brown and Min Xiao

Department of Physics, University of Arkansas, Fayetteville, Arkansas 72701

Received November 4, 2004

An electromagnetically induced absorption grating is formed in a three-level atomic vapor under the condition of electromagnetically induced transparency in which the strong coupling beam is replaced by a standing wave. The transmission and reflection behaviors of the weak probe beam are greatly modified at certain frequencies near the two-photon resonance. An all-optical two-port signal router–all-optical switch is demonstrated. © 2005 Optical Society of America

OCIS codes: 020.1670, 060.1810, 020.5580, 050.2770.

An electromagnetically induced absorption grating (EIG) can form when a weak probe beam coupled to one atomic transition interacts with a strong standing wave that is coupled to another atomic transition in a three-level atomic system.[1] Diffraction of the probe laser beam owing to an EIG was experimentally demonstrated in cold three-level atomic systems.[2,3] Recently it was demonstrated that such an EIG in a three-level electromagnetically induced transparency[4,5] (EIT) system can be used to store probe pulses in a vapor of rubidium atoms.[6] The EIG is formed by spatially modulated absorption regions that are due to EIT (reduced absorption at the peaks of the standing-wave field and high absorption at the nodes) in a three-level atomic medium, which modifies both the transmission and the reflection properties of the probe beam. Actually, the transmission behavior of a weak probe beam under the influence of a strong standing-wave field in a three-level atomic vapor system was studied theoretically long before EIT phenomena became popular.[7] This EIG is quite different from the usual four-wave mixing grating, which depends on the third-order Kerr nonlinear index of refraction.[8,9]

In this Letter we report our experimental investigations of the EIG effect in a three-level Λ-type atomic system in a vapor cell. The reflection and transmission behaviors of the signal (probe) beam are studied with particular attention to their dependence on laser frequency detunings. By making use of the special transmission and reflection properties of the EIG we demonstrate, in principle, a scheme for achieving an all-optical two-port signal router–all-optical switch in such a three-level EIT system, which is an important element in quantum networking with atomic ensemble systems.[10]

Our experimental system is shown in Fig. 1. The atomic medium is a vapor of natural rubidium. The D_1 line of ^{87}Rb at 795 nm is used; here the probe beam couples ground state $|1\rangle$ $(5^2S_{1/2}, F=1)$ to excited state $|2\rangle$ $(5^2P_{1/2}, F'=2)$ with frequency ω_p and detuning $\Delta_p=\omega_p-\omega_{21}$. The coupling laser beam (copropagating for an EIT or a standing wave for an EIG) interacts with the transition between level $|3\rangle$ $(5^2S_{1/2}, F=2)$ and level $|2\rangle$ with frequency ω_c and detuning $\Delta_c=\omega_c-\omega_{23}$. The $|1\rangle \leftrightarrow |3\rangle$ transition between the hyperfine levels of the ground state is dipole forbidden but has a dephasing rate γ_{31} owing to collisions and transient time effects.

The probe beam has a power of 100 μW and a diameter of ~0.6 mm inside the vapor cell. The coupling beams are composed of two oppositely propagating beams (copropagating and counterpropagating beams relative to the probe beam propagation) with identical frequency that overlaps the probe beam inside the vapor cell. A standing wave is formed when both coupling beams are present. Each coupling beam has a power of 4 mW, and the two beams have similar diameters of ~1.2 mm. Both coupling beams have the same linear polarization, which is orthogonal to the probe beam polarization. Laser frequency detunings are monitored with a saturation absorption spectroscopy setup along with Fabry–Perot cavities. The coupling and probe lasers are diode lasers with grating feedback, and each has a (half) linewidth of approximately 250 kHz. The rubidium vapor cell is 7.5 cm in length and is wrapped in μ metal to eliminate external magnetic fields. The

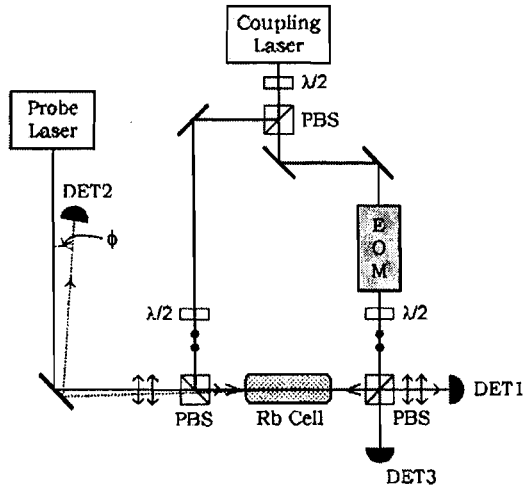

Fig. 1. Simplified schematic of the experimental setup: DET1–DET3, photodetectors; EOM, electro-optic modulator; PBSs, polarizing beam splitters; $\lambda/2$s, half-wave plates.

0146-9592/05/070699-3/$15.00

Semiconductors, Vol. 39, No. 1, 2005, pp. 127–131. Translated from Fizika i Tekhnika Poluprovodnikov, Vol. 39, No. 1, 2005, pp. 140–144.

AMORPHOUS, VITREOUS, AND POROUS SEMICONDUCTORS

Resonant Raman Scattering and Atomic Force Microscopy of InGaAs/GaAs Multilayer Nanostructures with Quantum Dots

M. Ya. Valakh*^, V. V. Strelchuk*, A. F. Kolomys*, Yu. I. Mazur, Z. M. Wang**, M. Xiao**, and G. J. Salamo****

**Institute of Semiconductor Physics, National Academy of Sciences of Ukraine, Kiev, 03028 Ukraine*

^e-mail: valakh@isp.kiev.ua

***University of Arkansas, Department of Physics, 72701 Arkansas, USA*

Submitted June 1, 2004; accepted for publication June 16, 2004

Abstract—The transition from two-dimensional (2D) pseudomorphic growth to the three-dimensional (3D) (nanoisland) growth in $In_xGa_{1-x}As$/GaAs multilayer structures grown by molecular-beam epitaxy was investigated by atomic force microscopy, photoluminescence, and Raman scattering. The nominal In content x in $In_xGa_{1-x}As$ was varied from 0.20 to 0.50. The thicknesses of the deposited $In_xGa_{1-x}As$ and GaAs layers were 14 and 70 monolayers, respectively. It is shown that, at these thicknesses, the 2D–3D transition occurs at $x \geq 0.27$. It is ascertained that the formation of quantum dots (nanoislands) does not follow the classical Stranski–Krastanov mechanism but is significantly modified by the processes of vertical segregation of In atoms and interdiffusion of Ga atoms. As a result, the $In_xGa_{1-x}As$ layer can be modeled by a 2D layer with a low In content ($x < 0.20$), which undergoes a transition into a thin layer containing nanoislands enriched with In ($x > 0.60$). For multilayer $In_xGa_{1-x}As$ structures, lateral alignment of quantum dots into chains oriented along the $[\bar{1}10]$ direction can be implemented and the homogeneity of the sizes of quantum dots can be improved. © *2005 Pleiades Publishing, Inc.*

1. INTRODUCTION

An important line of development of fundamental and applied solid-state physics is investigating the processes of self-assembled formation of semiconductor quantum dots (QD) upon molecular-beam growth of strained heterostructures. It is believed that this process follows the Stranski–Krastanov mechanism; i.e., when the thickness of a deposited layer attains some critical thickness, elastic strain relaxation occurs with the formation of three-dimensional (3D) nanoislands (QDs) on a thin (several monolayers) two-dimensional (2D) wetting layer.

Most attention has been paid to InAs QDs, which are formed as a result of the 2D–3D transition under epitaxial growth of strained InAs/GaAs heterostructures. Some recent results indicate that the initiation and the growth of InAs QDs cannot be described in terms of the classical Stranski–Krastanov mechanism. It was indicated that these processes may be affected by the vertical segregation of In atoms and interdiffusion of Ga atoms [1]. For $In_xGa_{1-x}As$ QDs formed in a GaAs matrix, the situation is even more complicated due to the simultaneous deposition of cations of two types. In addition, despite the fact that arrays with high densities ($\sim 10^{11}$ cm^{-2}) of $In_xGa_{1-x}As$ QDs have been obtained, the spread of sizes and shapes of QDs hinder their wide application in practice. The use of multilayer structures makes it possible to solve in general the problem of vertical alignment of QDs along the growth direction and improve the homogeneity of their sizes [2, 3], but lateral alignment (in the interface plane) is still a problem [4–6]. In the case of multilayer nanoisland structures $In_xGa_{1-x}As$/GaAs, the alignment critically depends on the surface elastic anisotropy of the matrix material [7] and the crystallographic orientation of the surface [8]. Previously, we showed for a multilayer system that, with the use of growth interruption upon deposition of a separating GaAs layer, lateral alignment of QDs into a line can be implemented with an increasing number of layers. The QD parameters and the features of their spatial alignment are controlled by the epitaxial growth conditions.

In this study, we investigated the formation and optical properties of QDs in $In_xGa_{1-x}As$ multilayer structures by methods of atomic force microscopy, resonant Raman scattering, and photoluminescence. It is shown that laterally ordered QD arrays can be formed in such structures upon deposition of $In_{0.5}Ga_{0.5}As$ solid solution onto a (100) plane.

2. EXPERIMENTAL

$In_xGa_{1-x}As$/GaAs multilayer structures with quantum wells (QWs) and QDs were grown on semi-insulating GaAs(100) substrates by molecular-beam epitaxy. After removal of the oxide layer from the surface, a buffer GaAs layer 0.5 μm thick was grown at a rate of one monolayer (ML) per second. All samples were grown at a constant As vapor pressure (10^{-5} Torr).

1063-7826/05/3901-0127$26.00 © 2005 Pleiades Publishing, Inc.

Photoluminescence from colloidal CdS–CdSe–CdS quantum wells

Jianfeng Xu

Department of Physics, University of Arkansas, Fayetteville, Arkansas 72701

David Battaglia and Xiaogang Peng

Department of Chemistry and Biochemistry, University of Arkansas, Fayetteville, Arkansas 72701

Min Xiao

Department of Physics, University of Arkansas, Fayetteville, Arkansas 72701

Received September 16, 2004; revised manuscript received December 14, 2004; accepted December 15, 2004

We report investigations of CdS–CdSe–CdS (core–well–shell) nanostructures by photoluminescence (PL) spectroscopy at temperatures between 77 and 300 K. PL intensity measurements show a transition from a pump-rate-limited regime at low excitation intensity to the range determined by a spontaneous emission lifetime at a high excitation limit. PL intensity changes as a function of temperature. Also, the temperature dependences of the PL linewidth and PL peak energy are all determined experimentally. The PL linewidth is narrower for thicker quantum wells and becomes broader when the temperature increases owing to longitudinal-optical (LO) phonon scattering. The LO phonon scattering strength is around 30 meV, which is independent of the well thickness, and is much smaller than the value for bulk CdSe. © 2005 Optical Society of America

OCIS codes: 160.2540, 300.6280.

Colloidal semiconductor nanocrystals (NCs) with at least one dimension within the nanometer scale (i.e., 1–10 nm) exhibit unique optical properties arising from quantum confinement of carriers.[1] Quantum confinement leads to the formation of discrete, blueshifted absorption bands, as well as enhanced emission efficiency, nonlinearity, and redshifted Raman spectra.[2] In such NCs, especially for small quantum dots (QDs), a large percentage of atoms are located at the surface, so imperfections on the surface of NCs, such as unsaturated atoms with dangling bonds, can lead to trap states, which often hinder radiative charge-carrier recombination. For obtaining strong excitonic emission and long-term optical stability, the surface of such colloidal NCs is usually passivated by inorganic materials with a larger bandgap. For example, one can significantly improve the efficiency of photoluminescence (PL) by growing a shell of CdS or ZnS around the CdSe QD core.[3,4] Because the CdS or ZnS shell has a wider bandgap than the CdSe core, such a structure forms an ideal isolated zero-dimensional QD system. The overcoating with CdS or ZnS results in the saturation of CdSe surface dangling bonds, which suggests that surface native defects, such as selenium or cadmium vacancies, can be efficiently eliminated by epitaxial growth of the shell.

As an extension of the above simple core–shell QD structure, one can form a quantum-well (QW) structure by sandwiching low-bandgap CdSe layers between a high-bandgap CdS core and an outside shell.[5] This CdS–CdSe–CdS system, with a QW thickness between 1 and 5 CdSe monolayers (ML) (1 ML≈0.7 nm), was synthesized by a modified successive ion-layer adsorption and reaction method.[4] For all the samples used in the experiments, the CdS core diameter is 3.7 nm, and the outside shell layer of CdS is 4 ML. In this study the optical properties of this unique CdS–CdSe–CdS QW structure with different well thicknesses are characterized by PL spectroscopy. The PL spectra were obtained by use of a conventional far-field optical microscopic technique and were excited by the 514.5-nm line of an Ar^+ laser. The laser beam focuses onto the samples (deposited on Si wafers) by a high-magnification microscope objective ($50\times$, N.A. = 0.55). The laser spot size on the sample is approximately 26 μm in diameter. Luminescence was collected by the same objective, directly projected into the spectrometer, and then detected by a liquid-nitrogen-cooled charged-coupled device (CCD). For temperature-dependent measurements, the samples were mounted inside a micro-objective cryostat with a controllable temperature between 77 K and room temperature.

Figure 1 presents the evolution of the optical properties of CdSe QWs with thicknesses from 1 to 5 ML at room temperature. The absorption spectrum shifts to the lower-energy side with the increase of the QW's thickness. The PL peak position was strongly dependent on the thickness of the QW and was shifted from 2.23 eV for the 1-ML CdSe QW to 1.89 eV for the 5-ML CdSe QW, in agreement with the theoretical calculation.[6] The inset in Fig. 1 shows the dependences of the PL peak position and PL quantum yield (QY) on the thickness of the QW measured

0740-3224/05/051112-5/$15.00

APPLIED PHYSICS LETTERS 87, 043107 (2005)

Exciton radiative recombination in spherical CdS/CdSe/CdS quantum-well nanostructures

Jianfeng Xu and Min Xiao[a)]
Department of Physics, University of Arkansas, Fayetteville, Arkansas 72701

David Battaglia and Xiaogang Peng
Department of Chemistry and Biochemistry, University of Arkansas, Fayetteville, Arkansas 72701

(Received 1 February 2005; accepted 13 June 2005; published online 19 July 2005)

Photoluminescence (PL) and lifetimes of colloidal CdS/CdSe/CdS (core/well/shell) quantum-well (QW) nanostructures are investigated for different well thicknesses in the temperature range of 77–300 K. When the temperature increases, the PL intensity decreases continuously and PL peak shifts to lower energy side. The PL lifetimes for the 1–3 monolayer (ML) CdSe QWs increase with temperature and radiative recombination dominates the decay processes. The radiative lifetimes basically increase linearly with temperature, which indicates the existence of free two-dimensional excitons. For the 4 ML CdSe QW sample, the lifetime does not increase with temperature, showing more nonradiative processes due to more defect formation within the thicker QWs. © *2005 American Institute of Physics*. [DOI: 10.1063/1.2001731]

The optical properties of planar two-dimensional (2D) semiconductor quantum wells (QWs) and zero-dimensional (0D) colloidal CdSe quantum dots (QDs) have been studied extensively[1,2] and their emission recombination processes are well understood.[3,4] Recently, a new spherical QW nanostructure, which includes one or more monolayers (ML) of CdSe (1.75 eV bulk bandgap) between a CdS (2.7 eV bulk bandgap) core and an outer CdS shell, has been synthesized.[5] Since the CdS core is only 3.7 nm in diameter and the well is very thin (1–4 ML of CdSe), such QW nanostructures could have very different recombination dynamics and optical properties from the typical 2D planar QW structure and the 0D QDs. The excitons in such QWs are mainly confined to the thin and spherical CdSe well, resulting in an improved photochemical stability and high quantum yield (QY). Analogous to planar QWs, the strong confinement of the charge carriers within the embedded CdSe region should lead to well-separated electronic states.

In this letter, we report our detailed optical studies of such unique spherical CdS/CdSe/CdS QW nanostructures, especially the temperature dependence of photoluminescence (PL) and lifetime of QWs with different thicknesses. The exciton lifetime measurements can help us to understand and determine different radiative and nonradiative recombination processes, which are very important for the potential applications of such colloidal QW nanostructures in optoelectronic devices and biophotonic labeling.

The QW structure is formed by growing low bandgap CdSe layers between a high band gap CdS core and an outside shell.[5] This CdS/CdSe/CdS QW system, with a well thickness between 1 and 4 CdSe ML (1 ML≈0.35 nm), was synthesized by a modified successive ion layer adsorption and reaction method[6] and the PL as well as Raman spectra were measured.[7] The CdSe layers have the wurtzite crystal structure, the same as that of CdS core and outside shell. Their QYs were measured by comparing the emission spectra against that of a laser dye having known QY. For all the samples used in the experiments, the CdS core diameter is 3.7 nm and the outside shell layer of CdS is 4 ML. The PL spectra were excited by the 514.5 nm line of a cw Argon ion laser and detected by a liquid-nitrogen-cooled charged coupled device camera. A frequency-doubled (400 nm), mode-locked (~1 ps) Ti:sapphire pulse laser and a time-correlated photon-counting system were used for the PL decay measurements.[4] Each sample for PL and PL decay measurements was prepared by spin-coating a clean fused silica coverslip with a solution of QWs in toluene followed by a 1 wt. % PMMA solution. The samples were mounted inside a micro-objective cryostat with a controllable temperature between 77 K and room temperature.

Figure 1(a) presents the PL spectra of CdSe QWs with thicknesses from 1 to 4 ML at room temperature. The PL peak position is strongly dependent on the thickness of the QWs and is shifted from 2.23 eV for the 1 ML CdSe QW to 1.93 eV for the 4 ML CdSe QW. In addition, the PL spectra

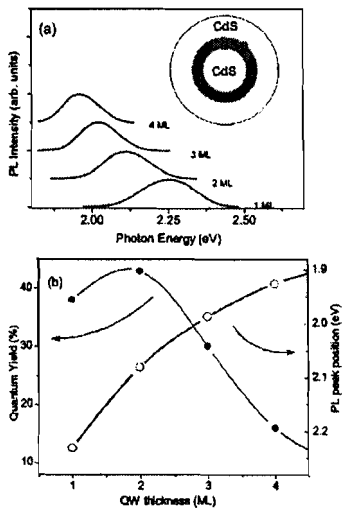

FIG. 1. (a) PL spectra of CdS/CdSe/CdS QW structure with various QW thicknesses. Inset: a schematic diagram of the QW structure. (b) PL QY and peak position as a function of CdSe QW thickness, respectively.

a)Electronic mail: mxiao@uark.edu

Lasing action in colloidal CdS/CdSe/CdS quantum wells

Jianfeng Xu and Min Xiao[a)]
Department of Physics, University of Arkansas, Fayetteville, Arkansas 72701

(Received 5 July 2005; accepted 1 September 2005; published online 20 October 2005)

Lasing action is observed in random medium of colloidal CdS/CdSe/CdS quantum wells (QWs) at 77 K. Sharp lasing peaks appear over a broad spectral range as pumping power increases. The lasing threshold is around 3 W/cm^2, which is much lower than that of other random or nanocrystal laser systems. Such improvement in lasing threshold opens the door to practical applications of QW random laser. The characteristic cavity length is determined by the Fourier transform of the lasing spectrum. © *2005 American Institute of Physics*. [DOI: 10.1063/1.2119423]

Colloidal semiconductor nanocrystals, or quantum dots (QDs), are very attractive for light emitting applications, such as fluorescent tagging and lasing.[1,2] However, a main obstacle in the development of optical gain and stimulated emission in QDs is fast nonradiative decay processes due to Auger recombination.[2] A number of studies are currently performed on so called core-shell nanostructures, where electrons and holes are separated in cores or shells.[3] Such nanostructures were designed to reduce the Auger processes by minimizing carriers' wave function overlap. On the other hand, researchers[4] found that the nonradiative Auger recombination in nanocrystals is strongly affected by the change in the confinement regime. Suppressed nonradiative Auger recombination and increased absorption cross sections are observed in one-dimensional CdSe quantum rods compared to zero-dimensional QDs. Thus, CdSe quantum rods provide an improved gain performance compared to QDs. This motivates us to work on two-dimensional CdSe quantum wells (QWs) structure. Previous experimental works showed that light emission in such CdSe QWs can be saturated at low pump intensity[5] and has longer lifetime compared QDs.[6] That means QWs have large absorption cross section and suppressed nonradiative Auger process, therefore, we hope to find stronger gain and lower threshold lasing in such system.

It is well known that semiconductor QW lasers can operate with a much lower threshold current, much narrower laser linewidth, and higher efficiency than the bulk semiconductor lasers. Today the most efficient commercial diode lasers are made of multiple QWs. However, the fabrication processes of the planar QWs are complicated and the defects and strains formed within the QWs, which hinder their wide applications. On the other hand, colloidal QDs have the advantages of high emission quantum yield (QY) and easily tunable emission wavelengths. Recently, colloidal CdS/CdSe/CdS QW structures were fabricated by chemical synthesis,[7] and their light emission and emission dynamic properties were studied.[5,6] Berezovsky *et al.* have recently investigated the spin dynamics and quantum size levels in such systems and found the electron g factor varies as a function of quantum well width.[8] Such colloidal QW nanocrystals have a lower band gap layer (CdSe) sandwiched between a higher band gap core (CdS) and an outer CdS shell. The spherical QW nanostructure studied here combines the promising characteristics of both two-dimensional planar QW and zero-dimensional colloidal QD. In this letter, we show that such colloidal QWs can be used as a strong gain medium for observing lasing action, and the threshold pump intensity required to achieve such lasing action is much lower than that in other laser systems.[9–11]

The QW structure used in this work is one monolayer (ML) CdSe grown between the CdS core and an outer shell (4 ML thickness) synthesized by a successive ion layer adsorption and reaction technique with accurate control over the well width. Detail sample syntheses can be found in Ref. 7. For lasing action measurements, the samples were prepared by spin coating colloidal QW solution (toluene) onto a clean silicon wafer. Thin films (~200 nm thickness) are formed on silicon wafer. The sample was mounted inside a microcryostat with a controllable temperature between 77 K and room temperature. Photoluminescence (PL) spectrum of the QW sample was measured by using a frequency-doubled (400 nm), mode-locked (~1 ps) Ti:sapphire laser (repetition rate 82 MHz) as an excitation source. Optical pump was achieved by using a cylindrical lens to focus the laser beam into a stripe of 2 mm × 50 μm onto the sample (perpendicular to the sample surface). The emitted light was collected by the same lens and directly projected into a spectrometer, and then detected by a photomultiplier tube detector.

Figure 1 shows the absorption and PL spectra from the CdSe QWs in toluene at room temperature. The emission

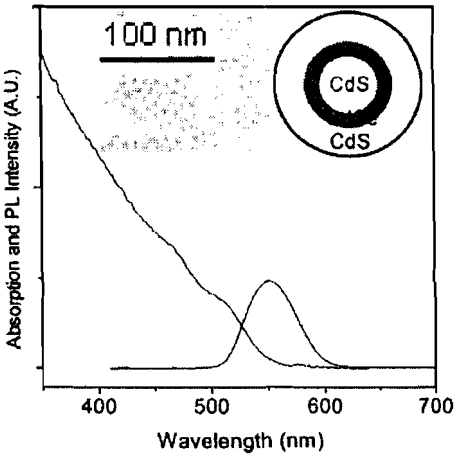

FIG. 1. Absorption and PL spectra from the CdS/CdSe/CdS QW solution (in toluene). Insets show a TEM image of the QW nanocrystals (left) and a schematic diagram of the QW structure (right).

a)Author to whom correspondence should be addressed; electronic mail: mxiao@uark.edu

Strong optical nonlinearity in strain-induced laterally ordered $In_{0.4}Ga_{0.6}As$ quantum wires on GaAs (311)A substrate

Yu. I. Mazur,[a] Zh. M. Wang, G. G. Tarasov,[b] H. Wen, V. Strelchuk,[b] D. Guzun, M. Xiao, and G. J. Salamo
Physics Department, University of Arkansas, Fayetteville, Arkansas 72701

T. D. Mishima, Guoda D. Lian, and M. B. Johnson
Center for Semiconductor Physics in Nanostructures, University of Oklahoma, Norman, Oklahoma 73019

(Received 1 February 2005; accepted 29 July 2005; published online 13 September 2005)

Strain-induced laterally ordered $In_{0.4}Ga_{0.6}As$ on (311)A GaAs template quantum wires have been fabricated and identified with cross-section transmission electron microscopy technique to be of average length ~ 1 μm, and on average width and height of 23 and 2 nm, respectively, under InGaAs coverage of six monolayers. The photoluminescence spectrum of a sample demonstrates unusually strong optical nonlinearity even at moderate excitation densities. The excitonic peak energy blueshifts by ~ 25 meV without essential contribution of the quantum wire excited states at elevating excitation density. Strong decrease of the polarization anisotropy and increase of the energy of excitonic photoluminescence are attributed to a combined action of the phase-space filling effects and the screening of the internal piezoelectric field by free carriers. © *2005 American Institute of Physics*. [DOI: 10.1063/1.2039999]

I. INTRODUCTION

Recently, self-assembled quantum wires (QWRs) of various shapes, sizes, densities, optical and electronic properties have been fabricated[1–5] promising further advances in optoelectronic devices (e.g., lasers[6] and modulators[7]). The two-dimensional (2D) confinement inherent to QWRs produces a singularity in the density of states (DOS).[8] The narrowing of the DOS leads to a lower excitation threshold for phase-space filling in QWRs,[9] thus enhancing nonlinear optical effects important for applications in optical communications.

One of the interesting optical features associated with strain-driven self-assembled QWRs is an intrinsic photoluminescence (PL) polarization anisotropy due to the complicated structure of the valence band at the center of the Brillouin zone.[10] The complex, nontetragonal strain deformation, developed due to the lattice mismatch, splits the degenerated valence band into a complicated subband structure,[11,12] resulting in both the polarization anisotropy[13] and lateral piezoelectric fields.[14] These fields could be important for optical nonlinearities due to screening of the field as well as the range of the field away from the strained layers. Indeed, it has been demonstrated in a series of (110) InAs/GaAs QWR structures that in high excitation density PL experiments produce a pronounced (up to 22 meV) blueshift of the PL lines, simultaneously with a clear reduction of the linewidth.[14] In these experiments, the observed blueshift and linewidth reduction were attributed to the screening of the internal piezoelectric fields by photogenerated carriers. In addition, the photoexcited carriers could also result in the screening and eventually bleaching of the exciton binding energy in QWRs. Enhancement of the optical nonlinearity has been revealed also in quasiplanar sidewall QWRs on GaAs (311)A substrate by means of continuous-wave PL.[15]

While screening would seem to explain the optical behavior of QWRs under high-density optical illumination, this is not the case due to the fact that there exist numerous contradictory observations of the PL peak energy behavior under high optical excitation density for strained QWR systems: from a sizable redshift ~ 10 meV,[16] virtually no shift[17,18] to a sizable blueshift [~ 25 meV (Ref. 19); 17 meV (Ref. 20)]. It is clear that different mechanisms can contribute to this behavior at high excitation density such as band filling, excitonic correlations, band-gap renormalization, and disorder. In fact, the nature of the PL peak shift and the polarization anisotropy properties in QWR systems are not yet well understood in spite of good potential for applications in low-threshold lasers and exotic light modulators.

In this study, we examine the nonlinear optical properties of strain-induced laterally ordered (SILO) $In_{0.4}Ga_{0.6}As$ QWRs on the GaAs (311)A substrate. The QWRs have been unambiguously identified with transmission electron microscopy (TEM) and PL measurements carried out at the moderate excitation optical densities. We demonstrate the existence of interesting excitation and temperature-dependent polarization anisotropy and a strong blueshift in the PL spectrum coming from the SILO QWRs that give evidence for strong nonlinear optical effects.

II. SAMPLES AND EXPERIMENTAL DETAILS

The QWR structures for this study were grown by molecular-beam epitaxy on a GaAs(311)A substrate. The GaAs wafer was first covered with a buffer layer of 0.5-μm thickness grown at 600 °C. For the (In,Ga)As deposition, the substrate temperature was reduced to 540 °C, the

[a]Electronic mail: ymazur@uark.edu
[b]On leave from Institute of Semiconductor Physics, National Academy of Sciences of Ukraine, Prospect Nauki 45, 03028 Kiev, Ukraine.

Eur. Phys. J. D **35**, 547–551 (2005)
DOI: 10.1140/epjd/e2005-00093-9

THE EUROPEAN
PHYSICAL JOURNAL D

Dark-state polaritons using spontaneously generated coherence

Amitabh Joshi[a] and Min Xiao

Department of Physics, University of Arkansas, Fayetteville, AR 72701, USA

Received 14 December 2004 / Received in final form 16 March 2005
Published online 14 June 2005 –

Abstract. A three-level atomic system in V-configuration (interacting with a single mode laser field) with parallel transition dipole moments exhibiting spontaneously generated coherence due to quantum interference of decaying channels is considered here for the purpose of storing light pulses. This system is equivalent to (with some restrictions) another three-level system in which ground state is coupled with one of the upper states but the upper states are coupled through a DC field and hence can be used to store electromagnetic pulse using the concept of dark-state-polariton.

PACS. 42.50.Gy Effects of atomic coherence on propagation, absorption, and amplification of light; electromagnetically induced transparency and absorption – 42.65.Tg Optical solitons; nonlinear guided waves – 42.50.Ct Quantum description of interaction of light and matter; related experiments

Recently, propagation of electromagnetic pulses and their storage have been extensively studied using a three-level atomic medium in Λ-type configuration [1]. The three-level atomic medium in Λ-type configuration irradiated by a strong coupling field on one of its transitions becomes transparent for a signal field (on another transition) due to electromagnetically induced transparency (EIT) [2]. Adiabatically turning off the coupling field allows signal field to be completely absorbed by the atomic medium. The phenomenon of EIT causes extraordinary change in dispersive properties of the atomic medium [3] which drastically alters the velocity of light pulses [4] and can store such pulses as induced atomic coherence or polarization in the medium [1]. In other words, by changing the coupling field slowly towards zero it is possible to store the signal pulse in the atomic medium and by reapplying (i.e., increasing) the coupling field in the same manner the stored signal field can be released back. This phenomenon of storing the optical pulse in an atomic ensemble has been discussed in terms of the 'dark state polaritons (DSP)' which describes entangled state of photon and atomic polarization [5]. Recently, experimental realizations of such DSP have been demonstrated [1].

A three-level atomic or molecular systems in V-configuration interacting with the vacuum field such that dipole moments of two transitions (from ground state to two upper states) being parallel or nearly parallel can control the spontaneous decay of two excited states due to spontaneously generated coherence (SGC) or quantum interference of decaying channels [6]. Many interesting features arising due to the SGC in a number of atomic and molecular schemes were reported in recent past which could find some very useful applications in laser spectroscopy and other areas of quantum optics. Some such interesting effects are quenching of spontaneous emission, ultra narrow spectral profiles, phase dependent population inversion, phase control of spontaneous emission, and controlling optical bistability to optical multistability behavior etc. [7–9]. We propose that this system can also be used for storing signal field and their retrieval (on demand), i.e., like a quantum field storage device by manipulating the degree of SGC in adiabatic manner. Though the three-level systems in V-configuration with parallel dipole moment exhibit many interesting effects but their practical realization is very difficult as the atomic or molecular systems in V-configuration normally posses dipole moments of two transitions perpendicular to each other. Some experimental efforts were made in past to generate SGC from such system [10] but could not reproduce consistent results [11]. Some related analysis for this kind of experiment was also provided [12].

Many other schemes were proposed to circumvent the experimental difficulties in obtaining the parallel dipole moments [13]. Very recently, another proposal has been given by Ficek and Swain [14] to obtain SGC from a three-level system in V-configuration without needing the parallel dipole moments. This scheme consists of a three-level system with perpendicular dipole moments for the transitions coupling the upper nearly degenerate levels with the ground level. One of the transitions is interacting with a laser field while the upper two levels are coupled by a DC field. It has been demonstrated that this system is equivalent to the usual three-level atomic system in V-configuration with parallel dipole moments of transitions. Such a system can be used for storing signal pulses in the atomic medium and can be manipulated for retrieval of pulses by adiabatically changing either decay

[a] e-mail: ajoshi@uark.edu

Controlling subluminal to superluminal behavior of group velocity with squeezed reservoir

Amitabh Joshi,[1,*] Shoukry S. Hassan,[2] and Min Xiao[1]
[1]*Department of Physics, University of Arkansas, Fayetteville, Arkansas 72701, USA*
[2]*Department of Mathematics, College of Science, University of Bahrain, P. O. Box 32038, Kingdom of Bahrain*
(Received 1 June 2005; published 30 November 2005)

We consider a three-level Λ-type atomic medium in an electromagnetically induced transparency configuration interacting with two independent broadband squeezed baths. We show that absorptive and dispersive properties of the medium can be controlled using squeezed bath parameters and coupling field strength such that the medium can have subluminal to superluminal group velocity for the probe pulse.

DOI: 10.1103/PhysRevA.72.055803 PACS number(s): 42.50.Gy, 42.50.Lc

Over the past 15 years, a great deal of attention has been devoted to studying the phenomena of electromagnetically induced transparency (EIT) and related topics [1–4]. This is because of the potential applications of EIT in lasing without inversion [5], high-efficiency nonlinear optical processes [6], efficient propagation of a laser beam through an optically thick medium [7], high-efficiency population transfer via a coherent adiabatic process [8], controlled optical bistability and multistability [9], slow light [10], and storage of optical pulses [11]. The phenomenon of EIT can be considered as an interrelated group of processes (e.g., the coherent population trapping, coherent adiabatic population transfer) that results from quantum mechanical coherence and interference in a multilevel system. EIT has been studied extensively and many significant experimental and other results were obtained for a system with three levels in a Λ configuration [1–4]. In all such studies of EIT, normal heat baths interacting with two transitions of Λ configuration are considered. Here, we investigate absorptive (dispersive) properties of the EIT medium as well as related effects such as subluminal and superluminal propagation of light, in an ensemble of three-level atoms in the Λ configuration interacting with two laser beams and two independent broadband squeezed baths [12]. The central frequency of one of the squeezed baths is near to one of the atomic transitions; whereas, that of the other bath is close to the other atomic transition. There are pairwise correlations between modes symmetrically placed around the central frequency of each of the two baths [12]. However, we assume that there is no correlation between the modes belonging to different baths. A recent work shows that a two-level atomic system, damped by a broadband squeezed vacuum and driven by a weak laser, exhibits a finite refractive index accompanied by zero absorption and can lead to the situation of superluminal group velocity [13]. Some other interesting works were also reported recently on the superluminal light propagation of probe pulses [14].

We consider a three-level atomic system in the Λ configuration (Fig. 1) with levels $|l\rangle$ $(l=1,2,3)$ having energies $E_1>E_2>E_3$. The amplitudes of the external driving fields are E_P (the probe field with frequency ω_P) and E_C (the coupling field with frequency ω_C) interacting with $|1\rangle$ to $|3\rangle$ and $|1\rangle$ to $|2\rangle$ transitions, respectively. The master equation for the density operator of this system under dipole and rotating-wave approximations is given by

$$\dot{\rho} = -i[H_{atom}+H_{int},\rho] - i[B_1(t)A_{13}+A_{31}B_1^{\dagger}(t),\rho] - i[B_2(t)A_{12}+A_{21}B_2^{\dagger}(t),\rho], \quad (1)$$

where

$$H_{atom}=\sum_{i=1}^{3}E_iA_{ii}, \quad H_{int}=d_1E_P(A_{31}+A_{13})+d_2E_C(A_{21}+A_{12}), \quad (2)$$

$A_{mn}=|m\rangle\langle n|$, $(m,n=1,2,3)$ are the atomic ladder operators and $B_i(i=1,2)$ are the bath operators; whereas, $d_1(d_2)$ is the dipole operator corresponding to the transition $|1\rangle$ to $|3\rangle$ ($|1\rangle$ to $|2\rangle$). The two squeezed baths are assumed to be independent and their modes are δ correlated, such that

$$\langle B_l(t)B_m^{\dagger}(t')\rangle = 2\gamma_l(n_l+1)\delta(t-t')\delta_{lm},$$

$$\langle B_l^{\dagger}(t)B_m(t')\rangle = 2\gamma_l n_l\delta(t-t')\delta_{lm},$$

$$\langle B_l(t)B_m(t')\rangle = 2\gamma_l m_l\delta(t-t')\delta_{lm}e^{-2i\Omega_l t},$$

$$\langle B_l^{\dagger}(t)B_m^{\dagger}(t')\rangle = 2\gamma_l m_l^{*}\delta(t-t')\delta_{lm}e^{2i\Omega_l t}, \quad (l,m=1,2), \quad (3)$$

in which $2\Omega_l$ is the frequency of the pump driving the lth bath, $2\gamma_l$, $(l=1,2)$ are the Einstein A coefficients for the transitions $|1\rangle$ to $|3\rangle$ and $|1\rangle$ to $|2\rangle$, respectively. The m_l's are the squeezing parameters ($m_l=|m_l|\exp(i\Phi_l)$, Φ_l is the phase of lth squeezed bath), such that $|m_l|^2\leq n_l(n_l+1)$, the equality sign holds in case of an ideal bath that yields a maximum degree of squeezing. In this work, we keep the equality sign for simplicity. Because of the δ correlation, the bath variables can be eliminated from Eq. (1) [12] resulting in the master equation

$$\partial\rho/\partial t = -i[H_0,\rho]+L_{therm}-L_{sqz}, \quad (4)$$

where

$$H_0=\alpha_P(A_{13}+A_{31})+\alpha_C(A_{12}+A_{21})+\Delta_P(A_{11}+A_{22})-\Delta_CA_{22},$$

*Corresponding author. Email address: ajoshi@uark.edu

Phase gate with a four-level inverted-Y system

Amitabh Joshi* and Min Xiao
Department of Physics, University of Arkansas, Fayetteville, Arkansas 72701, USA
(Received 3 June 2005; published 14 December 2005)

The four-level atomic system in an inverted-Y configuration is investigated for large Kerr nonlinearities. The cross-Kerr nonlinearity generated in such a system can produce a phase shift of order π and can be used for realizing polarization quantum phase gates.

DOI: 10.1103/PhysRevA.72.062319 PACS number(s): 03.67.Lx, 42.65.−k, 42.50.Gy

I. INTRODUCTION

An all-optical quantum computation has been proposed but a realization of two-qubit quantum gates, which are required for universal quantum computation, is not so straightforward due to lack of significant photon-photon interaction [1]. Many proposals have come up in recent years for efficiently implementing all-optical quantum computation. The linear optics quantum computation scheme is based on single-photon sources, passive linear optical devices, and detectors [2]. The scheme essentially uncovers the nonlinearities associated with the photodetection process and is basically a probabilistic scheme for implementing any quantum gate. Other schemes are based on the nonlinear responses of optical systems, i.e., making use of the optical nonlinearities to realize quantum phase gate operations. Under normal circumstances optical nonlinearities are too small to enhance the photon-photon interaction so the optical quantum gate operation cannot be efficiently implemented. The optical nonlinearity in atomic systems can be greatly enhanced in the presence of quantum interference in electromagnetically induced transparency (EIT) systems [3,4]. This enhancement is commonly observed in the weak probe laser beam in the presence of another strong coupling or driving laser beam(s) when these lasers are slightly off resonant from their respective transitions. The absorption, dispersion, and nonlinearity of the EIT systems are very sensitive to the probe, and coupling laser frequency detunings. This means that if exact two-photon resonance condition is disturbed in the typical three-level Λ-type system, the enhancement of nonlinearity could be observed [5]. Some other multilevel schemes have been investigated involving four and five levels in which enhancement of Kerr nonlinearities has been predicted, including the enhancement of self-phase modulation as well as cross-phase-modulation [6,7]. Schmidt and Imamoglu [6] used an EIT system of four levels in an N configuration and predicted dramatic improvement by several orders of magnitude in nonlinearities, as well as enhancement in cross-phase modulation in comparison with conventional three-level ladder system. The importance of cross-phase modulation is in implementing two-qubit all-optical quantum phase gates, where one qubit gets a phase shift dependent on the state of the other qubit. Cross-phase-modulation can occur in multilevel EIT systems when propagating pulses are allowed to interact for a considerably longer time by reducing their group velocities and also making these group velocities of the same order of magnitude, which was demonstrated in a tripod or adjacent Λ system [8]. Here we propose a phase-gating scheme using four-level atoms in an inverted-Y configuration [9]. Such a level scheme with a Λ system at its heart (or that can also be seen as an adjacent ladder system with a common middle level, as discussed in Sec. II), exhibiting double EIT (i.e., having double dark states [9]), is an alternate scheme to obtain enhanced nonlinearity and cross-phase-modulation by allowing the system to be tuned to its dark states, having EIT windows for each of the dark states to be narrow with a steep dispersion, enabling a significant reduction of group velocities as well as their matching due to symmetry of the system. In this way the EIT system in an inverted-Y configuration is different from the conventional three-level ladder scheme [6], and the latter does not give large nonlinearities and is limited by system parameters like detuning and the lifetime of the middle level. However, the EIT system in an N configuration of four levels [6] produces large nonlinearity and cross-phase modulation due to the simultaneous elimination of absorption loss. The inverted-Y configuration can easily be realized experimentally in rubidium atomic vapor and is very straightforward to implement. The two lower transitions are used for encoding the binary information in the polarization degree of freedom of the probe and signal pulses. The phase-gate mechanism operates on the cross-phase modulation effect between probe and signal fields. The electromagnetic fields are proposed as a possible environment for performing quantum logical operations. The atoms act as catalyzers of the logical operations. In the search of scalable quantum computing, the new methods of implementing QPG or CNOT gates are always desirable and has motivated us to do this work. Our purpose is first to explore the nonlinearities associated with such a kind of four-level system and their maneuverability using the atomic and laser parameters, and then finding the optimum conditions so that cross-phase-modulations of probe-signal fields become enhanced and can be used for a very efficient polarization phase gating for all-optical quantum computation purposes. The phase gate operation in multilevel systems in other configurations (adjacent Λ system, etc., which was different from the current work) has been demonstrated recently [7,8].

*Electronic address: ajoshi@uark.edu

